VOLUME 23 JULY, 1935 NUMBER 7

PROCEEDINGS
of
The Institute of Radio Engineers

Application Blank for Associate Membership on Page XIII

U OF I
LIBRARY

Institute of Radio Engineers Forthcoming Meetings

DETROIT SECTION
September 20, 1935

LOS ANGELES SECTION
September 17, 1935

NEW YORK MEETING
October 2, 1935

PHILADELPHIA SECTION
September 5, 1935

PITTSBURGH SECTION
October 15, 1935

WASHINGTON SECTION
September 9, 1935

INSTITUTE NEWS AND RADIO NOTES

Committee Work

Awards Committee

The Awards Committee met in the Institute office on May 1 and those present were L. M. Hull, chairman; Stuart Ballantine, Melville Eastham, Alfred N. Goldsmith, George Lewis, William Wilson, and H. P. Westman, secretary.

The committee prepared its recommendations in regard to the 1935 Institute Medal of Honor and the Morris Liebmann Memorial Prize. These were acted upon by the Board of Directors as reported in the June Proceedings.

Convention Papers Committee

Two meetings of the Convention Papers Committee were held. The first on April 22 in the Institute office was attended by William Wilson, chairman; George Lewis, Haraden Pratt, and H. P. Westman, secretary.

The second meeting was held on May 15 and was attended by William Wilson, chairman; Haraden Pratt, and H. P. Westman, secretary. At these meetings the papers submitted for presentation at our Tenth Annual Convention were reviewed and the program arranged.

New York Program Committee

The New York Program Committee met in the Institute office on April 12 and those present were George Lewis, chairman; H. H. Beverage, L. A. Hazeltine, R. A. Heising, J. K. Henney, Haraden Pratt, A. F. Van Dyck, and H. P. Westman, secretary.

Another meeting of the committee was held on May 23 and was attended by George Lewis, chairman; H. H. Beverage, L. A. Hazeltine, R. A. Heising, Haraden Pratt, A. F. Van Dyck, and H. P. Westman, secretary. At these meetings preparations were made for papers to be presented at Institute meetings up to and including that for November, 1935.

Nominations Committee

Melville Eastham, chairman; Stuart Ballantine, Alfred N. Goldsmith, L. M. Hull, George Lewis, E. W. Ritter (representing J. C. Warner), and H. P. Westman, secretary, attended a meeting of the Nominations Committee held in the Institute office on May 1. The committee's recommendations for candidates for election for President,

41732

Vice President, and Directors were prepared and submitted to the Board of Directors which acted on them at its meeting on May 1.

STANDARDIZATION—I.R.E.

Technical Committee on Electro-Acoustic Devices

A meeting of the Technical Committee on Electro-Acoustic Devices operating under the Standards Committee of the Institute was held on April 12 and attended by H. F. Olson, chairman; Sydney Bloomenthal, L. G. Bostwick, Knox McIlwain, Benjamin Olney, Hans Roder, V. E. Whitman, H. A. Zahl, and H. P. Westman, secretary.

Another meeting of this committee was held on May 17 and attended by H. F. Olson, chairman,; H. S. Knowles, Knox McIlwain, Hans Roder, H. A. Zahl, and H. P. Westman, secretary. The committee reviewed some proposed American tentative standards on acoustic terminology and adopted a number of items contained therein. Some additional definitions were prepared and a discussion was held on the desirability of establishing standard room tests of electro-acoustic devices.

Technical Committee on Electronics

The Technical Committee on Electronics of the Institute Standards Committee met on May 3 in the Institute office. Those present were B. J. Thompson, (representing B. E. Schackelford), acting chairman; E. A. Lederer, G. F. Metcalf, O. W. Pike, P. T. Weeks, and H. P. Westman, secretary. The committee reviewed the reports submitted by its various subcommittees and endeavored to prepare a schedule looking toward the completion of its work this fall.

Subcommittee on Electron Beam and Miscellaneous Tubes

This subcommittee met in the Institute office on May 2 and those present were G. F. Metcalf, chairman; A. B. DuMont, M. S. Glass, Ben Kievit, Jr., B. J. Thompson, and H. P. Westman, secretary.

Certain of the material prepared at previous meetings was reviewed and a number of new definitions on cathode-ray tubes were prepared.

Subcommittee on Gas-Filled Tubes

A meeting of the Subcommittee on Gas-Filled Tubes was held in the Institute office on May 3 and was attended by O. W. Pike, chairman; D. V. Edwards, H. E. Mendenhall, P. T. Weeks, and H. P. Westman, secretary.

Methods of testing gas or vapor rectifier tubes were prepared and some recommendations for graphical and letter symbols formulated.

Subcommittee on Large High Vacuum Tubes

This subcommittee met at Bell Telephone Laboratories on May 17 and those present were M. J. Kelly, chairman; R. D. Hall, R. W. Larson, E. E. Spitzer, and C. M. Wheeler.

The committee continued its preparation of material for submission to the Technical Committee on Electronics.

Subcommittee on Small High Vacuum Tubes

P. T. Weeks, chairman; M. Cawein, G. F. Metcalf, H. A. Pidgeon, E. W. Schafer, and H. P. Westman, secretary, attended the meeting of the Subcommittee on Small High Vacuum Tubes held in the Institute office on May 23. The committee reviewed the report which was prepared for submission to the Technical Committee on Electronics and made some modifications in it.

Sectional Committee on Radio—A.S.A.

A meeting of the Sectional Committee on Radio was held in the Institute office on June 3 and was attended by Alfred N. Goldsmith, chairman; Moe Asch, G. L. Beers, A. R. Belmont, J. Blanchard (representing William Wilson), A. H. Castor, Lloyd Espenschied, J. W. Fullmer (representing R. B. Shepard), J. W. McNair, Haraden Pratt, D. F. Schmidt, L. E. Whittemore, and H. P. Westman, secretary.

The meeting was devoted to a review of material submitted by several of the technical committees in reply to proposals prepared by the Dutch National Committee of the International Electrotechnical Commission which will be acted upon at a meeting of Committee 12 on Radio Communication of the International Electrotechnical Commission held in The Hague on June 18, 1935.

Technical Committee on Radio Recievers

A meeting of the Technical Committee on Radio Receivers was held in the Institute office on May 3 and those present were G. L. Beers, chairman; D. E. Foster, J. W. Fullmer, V. M. Graham, Gordon Thompson, and H. P. Westman, secretary. The committee's time was devoted to the preparation of an analysis of material submitted for a meeting of the International Electrotechnical Commission.

Several items were recommended for adoption as American standards.

Technical Committee on Transmitters and Antennas

The Technical Committee on Transmitters and Antennas met at the Institute office on May 7 and those present were Haraden Pratt,

chairman; H. A. Chinn, J. L. Finch, A. A. Oswald, and E. G. Ports. The committee reviewed material on safety standards and prepared a number of items for recommendation as American standards.

Technical Committee on Vacuum Tubes

This committee met in the Institute office on April 17 and those present were M. J. Kelly, chairman; K. N. Cummings, George Lewis, D. F. Schmidt, Gordon Thompson, and H. P. Westman, secretary.

The committee prepared a series of drawings for tube bases which will be recommended for acceptance as an American standard. In addition, it reviewed that portion of the proposed material submitted for American viewpoints prior to the meeting of the International Electrotechnical Commission at which it will be voted upon.

Institute Meetings

Atlanta Section

The February meeting of the Atlanta Section was held on the 28th at the Atlanta Athletic Club. I. H. Gerks, chairman, presided and introduced C. Owen. Mr. Owen presented John Candler of the General Radio Laboratories of Atlanta, Georgia, who spoke on "Grinding and Measuring Crystals for Transmitters." Several rough crystals and blanks were exhibited and the paper was discussed by Messrs. Bangs, Gerks, Holey, and Owen of the eighteen members and guests present. Nine attended the informal dinner which preceded the meeting.

On March 28, a meeting of the Atlanta Section was held at the Transmitting Station of WSB of the Atlanta Journal.

The members and guests assembled at the studios of WSB at the Biltmore Hotel and were taken from there to the transmitting station at Tucker, Georgia, where a buffet dinner was served. The evening was devoted to a series of inspection trips through the transmitting station which were conducted by C. F. Daugherty, chief engineer, and his staff. At the completion of the tours, all gathered in the conference room where a general discussion of the station was held. Twenty-nine members and guests were present.

Boston Section

A meeting of the Boston Section was held on March 15 at Harvard University with Chairman Chaffee presiding. One hundred and eighty members and guests were present and twenty attended the informal dinner which preceded the meeting.

G. W. Pierce, Rumford Professor of Physics of Harvard University, presented a "Demonstration of Supersonics." By the use of magnetostriction and piezo-electric oscillators, he demonstrated transmission and reception of various supersonic devices. The adaptability of this type of equipment to the study of supersonic sounds produced by nature was explained by numerous illustrations.

The second portion of the evening was devoted to a "Demonstration of a Mechanical Model of Electric Circuit" by E. L. Chaffee, Professor of Physics at Harvard University. With the aid of a mechanical model of an electric circuit, he illustrated the effect of varying the constants and coupling of electrical circuits. By photographing the movement of the pendulums excellent anologies of energy interchange between circuits have been obtained. It is possible to use this equipment to illustrate the drag-loop phenomenon commonly encountered in oscillators.

The April meeting of the Boston Section was held on the 22nd at Harvard University. Dr. Chaffee presided and the attendance was 140, of whom twenty were present at the informal dinner which preceded the meeting.

"Some Theoretical Considerations Relating to Vacuum Tube Design" was the subject of a paper presented by G. D. O'Neill, tube engineer of the Hygrade Sylvania Corporation. A summary of this paper appears in the June PROCEEDINGS in the convention program.

A second paper on "Some Mechanical Features of Tube Design" was presented by W. L. Krahl, division engineer of the Hygrade Sylvania Corporation. In it he described the mechanical features employed in receiving tubes for the purposes of controlling major characteristics, preventing undesired primary and secondary emission, enabling the tube to withstand shock and continued vibration, and eliminating noise.

The third paper in the series, presented by P. T. Weeks, chief engineer of Raytheon Manufacturing Company, was on "Gas Elimination from Vacuum Tubes." It was devoted primarily to this problem as viewed in the process of mass production of tubes.

BUFFALO-NIAGARA SECTION

A meeting of the Buffalo-Niagara Section was held on April 17 at the University of Buffalo. L. E. Hayslett, chairman, presided and fifty-six were present.

M. V. Horn of the engineering staff of WBEN presented a paper on "High Fidelity From a Broadcaster's Standpoint." By means of block diagrams he outlined the various units between the microphone

and radiating antenna and described the extent of the loss in fidelity due to each part. The disadvantages which would be experienced by the average broadcast listener using a low fidelity receiver if the broadcast station fidelity were increased were explained. A number of pieces of apparatus were used to illustrate the effects of distortion.

"Radio-Frequency Considerations in High Fidelity Receivers" was the subject of a paper presented by J. W. White, receiver engineer, Colonial Radio Corporation. The engineering and manufacturing problems met in improving the fidelity of broadcast receivers were described. This paper was devoted to radio-frequency portions of the receiver.

"Audio and Reproducing Systems for High Fidelity Receivers" was the subject of a third paper which was presented by G. C. Crom, engineer in charge of magnetic design, Colonial Radio Corporation. This paper described the audio-frequency amplifier and loud speaker problems met with in improving receiver fidelity. A general discussion of the papers was participated in by Messrs. Burbank, Crom, Hayslett, Hector, Horn, Wesselman, and White.

The May meeting of the Buffalo-Niagara Section was held on the 22nd at the University of Buffalo. R. J. Kingsley, vice chairman, presided and the attendance was fifty-six.

J. M. Stinchfield, engineer for RCA Radiotron, presented a paper on "Cathode-Ray Tubes and Their Circuit Applications." In it he explained how the usefulness of these tubes can be extended by suitable auxiliary apparatus. Various applications of the tubes were described as were sweep circuits and the requirements of other equipment for use with cathode-ray tubes.

Chicago Section

The Chicago Section met on April 26 in the R.C.A. Auditorium of the Merchandise Mart. Sixty were present and fifteen attended the informal dinner which preceded the meeting.

A paper on "Low Voltage Gaseous Conversion Tubes and Circuits" was presented by R. U. Clark, an engineer for the Magnevox Company of Fort Wayne, Indiana. He covered the history and theory of conversion tubes, the construction of cathode, grid, and plate for highest efficiency, stability, and power handling capacity; the gas used and the influence of operating conditions such as temperature and gas pressure, circuit requirements, frequency effects, and performance characteristics. The developments of 115-, 32-, and 6-volt converter tubes of high efficiency were described and their performance outlined. A 32-volt unit was demonstrated.

Cincinnati Section

A meeting of the Cincinnati Section was held on April 23 at Wright Field, Dayton, Ohio. It was presided over by Thomas Reeves, vice chairman. One hundred and thirty members and guests were present and seventy-five attended the informal dinner which preceded the meeting.

"Novel Trends in Aircraft Radio Design" was the subject of a paper presented by A. G. Messer, Captain, U. S. Signal Corps. He described and displayed the various types of aircraft equipment used by the Signal Corps since the inception of aircraft radio. Many interesting pieces from the Wright Field Museum were displayed. A complete exhibit of modern aircraft equipment was available for inspection and included all-wave receivers, blind flying apparatus, landing marker station equipment, beacon receivers and transmitters, and radio compasses.

After the presentation of the paper, members were permitted to examine the equipment, and the engineers who developed it were available to answer all inquiries.

An inspection trip to the hangars and laboratories of Wright Field was held during the afternoon and offered an opportunity to examine the gondola of the stratosphere balloon to be used by Captain Stevens on his next flight. About 100 participated in this inspection trip.

The May meeting of the Cincinnati Section was held on the 21st at the University of Cincinnati. Ninety-one were present and A. F. Knoblaugh, chairman, presided.

A paper on "Automatic Frequency Control" was presented by Charles Travis, engineer for RCA License Laboratory. This paper is summarized in the June Proceedings. It was discussed by Messrs. Kilgour, Masser, Osterbrock, Rockwell and others.

A special committee on radio publicity reported that four broadcasts on popular radio topics had been made by members of the Cincinnati Section over WKRC during the past month.

Cleveland Section

The March meeting of the Cleveland Section was held on the 28th at Case School of Applied Science. K. J. Banfer, chairman, presided and 136 were present. Nineteen attended the informal dinner which preceded the meeting.

"Modulation in Radio Transmitters" was the subject of a paper by W. L. Everitt, Professor of Electrical Engineering at Ohio State University. Professor Everitt reviewed the various types of modulation; nonlinear, linear, flux, and energy control. The fact that an oscillator

supplied with energy in "lumps" may distribute energy sinusoidally was demonstrated mechanically with a pendulum energized by a motor during part of its cycle. A commutator attached to the shaft about which the pendulum turned controlled the current to two movable brushes. By changing the angular relationship of the brushes, the duration of the motor operation was varied and the stroke of the pendulum increased or decreased.

The speaker subdivided modulation into two types; that brought about in the plate circuit of the final amplifier as one type and the other being modulation before the plate circuit of the final amplifier. The first type has an efficiency of about 65 per cent, the audio-frequency amplifier providing energy for the side bands. In the second type, the energy for the side bands is provided by an increase in efficiency during modulation. Causes of distortion in modulators were outlined and the necessity for a linear relationship between the tank current and the plate voltage was stressed.

The April meeting of the Cleveland Section was held on the 25th at Case School of Applied Science. Chairman Banfer presided and forty-three were present.

H. P. Boswau, chief engineer of the Lorain County Radio Corporation, presented a paper on "Relay Remote Control of Telephone and Radio Circuits." He described telephone relays and outlined various methods of delaying operation and release. He then enumerated the various systems of obtaining multiple control over a single pair of wires such as changing the polarity, magnitude, or frequency of the current. This led to a discussion of the telephone dial system and the types of relays used therein. This system is of the supervisory control type which includes train dispatching systems and remote control of electrical substations also. It is developed from the old hand lever train dispatching system. A demonstration of the Westinghouse supervisory control system and an explanation of its adaptation to industrial use concluded the paper.

Connecticut Valley

A paper on "Some Comments on Low Angle Vertical Radiation for Broadcasting" was presented by R. N. Harmon, radio engineer for Westinghouse Electric and Manufacturing Company, at the April 29 meeting of the Connecticut Valley Section at the Hotel Charles in Springfield, Massachusetts. J. A. Hutcheson, chairman, presided and the attendance was sixteen.

A brief outline of the history of broadcast antennas was presented.

A modified vertical radiator with unlimited height from an electrical standpoint was proposed. Its characteristics were calculated on the basis of a constant phase and amplitude of current throughout its length. A moderately close approach to these conditions was found possible in practice by rephasing currents at about 3/8-wave intervals with a condenser whose reactance just neutralized the inductive reactance at the point of insertion. Curves of results of experiments made at 980 kilocycles for antenna heights up to two wavelengths and with calculated data up to five wavelengths for constant power input were shown and the field intensity along the ground was proportional to the antenna height. Calculations of vertical radiation patterns indicate that the minor high lobes of radiation are smaller than for sinusoidal current distribution and is a factor which limits the nonfading range. Curves were shown to illustrate the nonfading range versus antenna height for several broadcast frequencies together with the range of soil conductivity generally encountered. It was pointed out from the results of these curves that the optimum antenna height for any given frequency and ground conductivity may be obtained.

The May meeting of the section was held at the Hotel Charles and presided over by Chairman Hutcheson. Thirty were present.

"Some Problems in Tube Manufacture" was the subject of a paper by P. T. Weeks, chief engineer of Raytheon Production Corporation. In it Dr. Weeks pointed out that the elimination of occluded gas developed during the process of manufacture was appreciably more difficult than the simple evacuation of air from a vacuum tube bulb. Manufacturing operations were described and methods were outlined for eliminating gas from the glass, plates, grids, cathodes, filaments, shields, and mica pieces used in vacuum tubes. Cleaning and firing are the principle modes of elimination. The exhaust operation from the initial pumping to the sealing off was described in detail.

A paper on "Outline of the Theory of Tube Design" was presented by G. D. O'Neill of the Hygrade Sylvania Corporation. This paper is practically identical with the paper "Some Theoretical Considerations Relating to Vacuum Tube Design" by the same author presented at Boston.

Detroit Section

A. B. Buchanan, chairman, presided at the April 19 meeting of the Detroit Section held at the Harper Hospital Amphitheater. The attendance was 600 and thirty-five were present at the informal dinner which preceded the meeting.

P. F. Morse, a doctor of medicine who is Director of the Harper Laboratories, outlined the work in the electronics field that has been done at Harper Hospital. He then introduced Kenneth Corrigan, a physicist, who spoke on "New Concepts of Physics as Related to Medical Research." Dr. Corrigan presented a picture of how the problems of medicine and physics are interrelated and discussed the uses of radio equipment in medical work. He then described the million-volt X-ray equipment which was inspected later.

Dr. Morse then introduced G. D. Coolidge who discussed the design and operation of apparatus for the measurement of skin temperature colorimetry and dielectric loss angle in the human body. Dr. Morse spoke briefly on the "Measurement of Nerve and Muscle Chronaxie by Condenser Discharges" and then introduced Dr. Leucutia who presented a paper on "The Use of High Voltage X-ray Equipment in the Treatment of Cancer." The paper, and particularly some of the slides and pictures of cancer cases and cures that Dr. Leucutia had, were exceptionally well received by the audience. The meeting ended with an inspection of the apparatus that had been discussed and of the laboratories of the hospital.

Philadelphia Section

The annual meeting of the Philadelphia Section was held on May 2 with E. D. Cook, chairman, presiding. One hundred and forty members and guests attended the meeting and ten were present at the informal dinner which preceded it.

A paper on "A Chronograph System" was presented by C. J. Young and Maurice Artzt, Engineering Department, RCA Manufacturing Company. The instrument described may be used to measure quickly the accuracy with which a watch or clock keeps time and determine how much will be gained or lost in a day. Its accuracy is within one second per day. A dot for each tick or sound from the watch under test is recorded along a series of lines traced across a paper tape two inches wide at a rate of sixty inches per second. The dots line up along the tape in straight columns and the drift of the column indicates whether the watch is running fast or slow. A variation of one part in a million may be recorded and measured quite closely in eight minutes. The tape travels at the rate of two inches per minute and is driven by a forty-watt motor whose speed is timed and controlled by a tuning fork which generates a sixty-cycle alternating current, accurate to within five parts in a million. The microphone for picking up the ticks of the watch may be either carbon or crystal but must not contain magnets which will affect the running of the watch. The micro-

phone output is amplified and operates the recording equipment which is practically the same as the facsimile receivers developed by the Radio Corporation of America.

"An Electromagnetic Gun Detector" was the subject of a paper presented by G. D. Luck of the engineering department, RCA Manufacturing Company. In it he described the principles underlying the development of a device for detecting the presence of metallic objects in a region to be protected. Uses made of the effect of metallic bodies on an alternating magnetic field and the desirability of using a high-frequency field for nonmetallic objects or a low-frequency field for magnetic objects was pointed out as well as the advantage of using the curvature of the field to detect objects in any orientation of the field. A mutual inductance balance is used as a detecting device, highly symmetrical construction and high reactive power in the field providing stability and freedom from interference. A balance indicator utilizing a cathode-ray oscillograph which gives separate indications of direction and magnitude of resistive and reactive unbalance was described. This device which is applicable to any impedance bridge or alternating-current potentiometer permits instinctive balancing by even an unskilled operator. Details of the design of a commercial device for detecting the presence of guns carried by prisoners or visitors was mentioned. The device was demonstrated, giving an alarm at the passage of a pistol, a large key, or a plate of brass through the detecting field.

In the election of officers for the forthcoming year, the following were named: Chairman, Knox McIlwain, of the University of Pennsylvania; Vice Chairman, Irving Wolff, RCA Manufacturing Company; and Secretary-Treasurer, R. L. Snyder.

Pittsburgh Section

A meeting of the Pittsburgh Section was held on April 16 at the Fort Pitt Hotel with C. K. Krause, chairman, presiding and thirty-five present.

A paper on "Fundamental Aspects of Radiation Theory" was presented by L. J. Peters, head of the magnetic and seismic sections, Gulf Research and Development Corporation. Dr. Peters started his discussion with the fundamental laws for electric and magnetic fields obtained from simple experiments and from these basic facts developed the electric and magnetic equations for a radiation field. It was shown that both the electric and magnetic components varied inversely as the distance from the antenna and are in time phase and space quadrature. He also explained the tipping or rotating of the force vector as

a function of earth resistance. Several drawings were used to illustrate electromagnetic radiations. The paper was discussed by Messrs. Gabler, Hammer, Krause, Noble, Parke, Scott, Sunnergren, Wyckoff and others.

The May meeting of the Pittsburgh Section was held on the 21st in Utility Hall. C. K. Krause, chairman, presided and twenty-four were in attendance.

J. A. Hutcheson, radio engineer for Westinghouse Electric and Manufacturing Company, presented a paper on "Requirements of High Quality Broadcast Transmission." He stated that experiments showed that for a given loudness to the ear or sound pressure per unit area, the lower frequencies would modulate a transmitter more deeply than the higher frequencies. Therefore, a transmitter capable of modulating 100 per cent at sixty cycles would modulate only about ten per cent on certain higher frequencies at the same sound intensity. Thus a station modulating between twenty and thirty per cent on these higher frequencies would overmodulate greatly on low frequencies. Low-frequency overmodulation causes the greatest amount of undesired distortion partly because the harmonics produced are in the audible range to which the ear is most sensitive, and partly because a definite time is required for a tone to excite the ear. Thus the low-frequency overmodulations last longer and the ear is excited long enough to give detectable response. Messrs. Best, Kozanowski, Krause, Mag, Noble, Place, Stevens, Sutherlin, Swedlund, Wyckoff and others participated in the discussion of the paper.

Rochester Section

The annual meeting of the Rochester Section was held on May 9 at the Sagamore Hotel and was presided over by H. J. Klumb, chairman.

A. F. Van Dyck, director of RCA License Laboratory, presented a paper on "Radio and its Possibilities." In it he sketched briefly the history of radio in all its important phases pointing out as he went along where the activity in the radio field affected our daily lives. He mentioned many things now in the development stage, such as electronic musical instruments, facsimile, television, and elaborated to some degree on the development of sound on film for home use such as the talking book, as well as the possible uses of pocket type portable transceivers.

At the election of officers, E. C. Karker of the Rochester Mechanics Institute was named chairman; L. A. DuBridge, Professor of Physics

at the University of Rochester, vice chairman; and H. A. Brown, Rochester Gas and Electric Company, secretary-treasurer.

Eighty members and guests attended the meeting and fourteen were present at the dinner which preceded it.

San Francisco Section

A joint meeting with the San Francisco Signal Corps Association was held on April 2 at the Hotel Bellevue. G. T. Royden, chairman of the Signal Corps Association, presided and the attendance was eighty-four. Forty-two were present at the informal dinner which preceded the meeting.

D. K. Lippincott, a patent attorney, presented a paper on "Television in Europe." In it he outlined the organization and operation of the television systems of Great Britain and Germany. Many interesting side lights were covered and the paper was discussed by several of those present.

Seattle Section

A meeting of the Seattle Section was held on May 3 at the University of Washington. E. D. Scott, vice chairman, presided and 115 were present.

A symposium on "Obscure Electrical Effects" was presented by a group of advanced students of the Department of Electrical Engineering of the University of Washington. The first speaker was L. Tibbals who discussed and demonstrated the magnetic reactions arising with parallel conductors carrying heavy currents. These phenomena were shown to lead in the limiting case to the "pinch effect" which was demonstrated with the aid of a mercury conductor carrying a current in the order of 1000 amperes.

The optical effects of short electrical waves were then demonstrated by G. W. Clothier and G. C. Larson. Polarization was shown with the aid of a diffraction grating and the reflecting properties of plane and parabolic surfaces were both demonstrated and discussed.

The Barkhausen effect was then demonstrated by G. K. Barger who showed how this phenomenon varied with a large number of magnetic materials including permalloy, coppernick, hypernick, and cobalt steel.

Toronto Section

On April 17 a meeting of the Toronto Section was held at the University of Toronto and F. J. Fox, vice chairman, presided. The attendance was sixty-three and twelve were present at the informal dinner which preceded the meeting.

A paper on "Cathode-Ray Tubes—Their Construction and Use" was presented by Dr. Kohl, research engineer for Rogers Radio Tube Company. In it Dr. Kohl covered the history of cathode-ray tubes and the cathode-ray effect going back as far as 1859. He explained briefly the electron theory and construction of the cathode-ray gun. Amplitude modulation of the beam, the effect of frequency on the deflecting plates, and the requirements of cathode-ray tubes for television purposes were discussed. The paper was discussed by Messrs. Bayley, Fox, and Hunt.

The annual meeting of the Toronto Section was held on May 15 at the University of Toronto with Vice Chairman Fox presiding. The attendance was eighty-four, twelve of whom were present at the dinner prior to the meeting.

Dr. Kohl presented the second part of his paper "Cathode-Ray Tubes—Their Construction and Use." In it he pointed out the chief differences between gas-filled and vacuum type cathode-ray tubes and outlined the various applications of each. Construction details of the vacuum type tube were covered. Details of the electron gun and the analogy between optical lens systems and the electron optical system of these tubes was discussed. Demonstrations were given of the focusing of the electron beam on the fluorescent screen. The line focus experiment in which the line focus is produced by a magnetic field was demonstrated as was the electron microscope. Its application to cathode coating problem research work and to problems dealing with crystal structure of metals was explained. The speaker showed how emission from the face of crystals and lack of emission from boundaries between crystals gave a clearly defined visual picture of crystal structure on the cathode face. The paper was discussed by Messrs. Bayley, Fox, Hackbusch, and Price.

In the election of officers, L. M. Price of The Radio Valve Company of Canada was named chairman; B. DeF. Bayley, University of Toronto, vice chairman; H. P. Knap, treasurer; R. Klingelhoeffer, International Resistance Company, recording secretary.

Washington Section

The Washington Section met on April 8 at the Potomac Electric Power Company auditorium with E. K. Jett, chairman, presiding. Twenty were present at the informal dinner which preceded the meeting and ninety-four attended the meeting.

W. G. Diehl of the RCA Manufacturing Company presented a paper on "Recent Developments in Cathode-Ray Oscillographs." Mr.

Diehl first presented the fundamental considerations in the design of cathode-ray tubes and equipment, particularly with regard to the adjustments provided for electrostatic focusing and other control of the beam. Apparatus was demonstrated showing the application of some recently developed cathode-ray equipment and the manner in which this equipment is used for various test purposes was described in detail. The paper was discussed by Drs. Taylor and Wheeler and others.

The May meeting of the section was held on the 13th in the Potomac Electric Power Company auditorium and Chairman Jett presided. Sixty were present and twenty-four attended the informal dinner which preceded the meeting.

"Recent Developments in Vacuum Tubes for Ultra-High Frequencies" was the subject of a paper by A. L. Samuel of Bell Telephone Laboratories. The speaker outlined the reasons why the conventional vacuum tube oscillator fails to operate at very high frequencies. Various steps which may be taken to increase the frequency range were discussed and illustrated by reference to specific tubes. It was concluded that the upper limiting frequency for the negative grid tube is set by practical limitations of tube structure. For higher frequencies recourse may be had to oscillators of the Barkhausen type and magnetron types. The characteristics of such oscillators were discussed, and the paper closed with some general remarks on the problem of amplification and on the future of the ultra-high-frequency field. Several in attendance participated in the discussion of the paper.

Personal Mention

W. E. Benham formerly with Marconi's Wireless Telegraph Company has joined the staff of Pye Radio, Ltd., Cambridge, England.

Previously with International Standard Electric Corporation in Brazil, J. C. Braggio has joined the radio engineering department of the International Telephone and Telegraph Corporation at Buenos Aires, Argentina.

Formerly with Television Laboratories, A. H. Brolly has become chief engineer for Farnsworth Television, Philadelphia, Pa.

T. R. Bunting has left the staff of R.C.A. Institutes to join the Signal Corp Aircraft Radio Laboratory at Dayton, Ohio.

W. G. Carson is now with National Union Radio Corporation, Newark, N. J., having formerly been with the Johnsonburg Radio Corporation.

F. C. Carter is now a member of the designs section of the Office of the Engineer in Chief of the British General Post Office in London, having previously been located at the Post Office Research Station.

J. M. Chapple has been transferred from Los Angeles to take charge of the Federal Communications Commission inspection office in Honolulu, Hawaii.

Previously with Aero-Electrical Equipment Company, E. N. Elford has become technical manager for Gambrells, Rowse and Snoaden, Ltd., London, England.

B. V. K. French formerly with United American Bosch Corporation has joined the staff of RCA License Laboratory of New York City.

J. C. G. Gilbert previously connected with Bakers Selhurst Radio is now a research engineer for Partridge and Mee, London, England.

G. C. Gross is now chief of the International Section of the Federal Communications Commission at Washington, D. C.

Formerly with the Post Office radio station at Rugby, J. F. Hartwright is now a member of the engineering staff of the British Broadcasting Corporation.

E. A. Hayes of the General Electric Company has been transferred from Schenectady to Bridgeport.

A. P. Huchberger previously with Sylvania Products Company has become assistant to the president of Stupakoff Laboratories.

K. W. Jarvis is now general manager of the Eastern Division of Meissner Manufacturing Company in New York, having formerly been with Zenith Radio Corporation.

R. J. Keogh formerly with Sears Roebuck and Company has joined the radio engineering staff of Colonial Radio Corporation, Buffalo.

Previously with Les Laboratoires Standard at Paris, S. G. Knight has joined Standard Telephones and Cables at London.

Bernard Marsden has left RCA Victor Company to become regional technical supervisor for Jam Handy Picture Service, Detroit, Mich.

F. M. McCarthy of Meissner Manufacturing Company has been transferred from Chicago to New York.

P. deF. McKeel is now with the Bureau of Air Commerce, Washington, D. C., having previously been with the Westinghouse Electric and Manufacturing Company at Chicopee Falls, Mass.

Formerly with Firth Brothers Party of Melbourne, G. J. Menon has become chief radio engineer for Airzone, Ltd., at Comperdown, New South Wales, Australia.

M. H. Mizell, Lieutenant, U. S. Marine Corp, has been transferred from Quantico, Va., to the American Legation at Peiping, China.

Proceedings of the Institute of Radio Engineers
Volume 23, Number 7 *July, 1935*

TECHNICAL PAPERS

A SINGLE SIDE-BAND SHORT-WAVE SYSTEM FOR TRANSATLANTIC TELEPHONY*

By

F. A. Polkinghorn and N. F. Schlaack

(Bell Telephone Laboratories, Inc., New York City)

Summary—*This paper describes the construction of a short-wave single side-band reduced-carrier system of radio transmission. It also reports the results of comparisons made between this system and an ordinary short-wave double side-band system between England and the United States. It was found that the single side-band system gave an equivalent improvement in radiated power over the double side-band system averaging eight decibels. This is in good agreement with the theoretical improvement to be expected.*

Introduction

THE single side-band suppressed-carrier method of transmission has been used to effect economies in the power capacity required, energy consumed, and space in the frequency spectrum on carrier telephone circuits for over fifteen years. On the basis of equal peak amplitudes in a transmitter a single side-band suppressed-carrier system gives a possible theoretical improvement of nine decibels in received signal-to-noise ratio over a double side-band and carrier system. Six decibels of this improvement is obtained by omitting the carrier and utilizing the entire available amplitude capacity of the transmitter for the side band. The other three decibels are obtained by reducing the band width of the receiver to only that required to pass one side band, thus reducing the noise energy at the receiver output by one half.

In order that speech may be transmitted without undue distortion over a single side-band system, it is necessary that the carrier frequency at the receiver be within about ± 20 cycles of the correct value. For the transmission of music a much higher precision is required. The practical construction of a single side-band radio system at frequencies of the order of 60 kilocycles, such as is used in the long-wave transatlantic telephone circuit, requires only a careful application of known technique to obtain the desired degree of stability of the oscillators. At the short-wave transatlantic radiotelephone frequencies of from

* Decimal classification: R412. Original manuscript received by the Institute, March 8, 1935.

5000 to 20,000 kilocycles, however, the very best crystal oscillators, such as are now used only for the very highest quality laboratory standards, would be required at both transmitter and receiver to obtain the degree of synchronization required.

The high degree of frequency stability required for single side-band suppressed-carrier transmissions can be dispensed with by transmitting a pilot frequency over the channel. For this purpose the carrier frequency serves as well as, if not better than, any other frequency since it is easily obtainable at the transmitter and is readily utilized at the receiver. If a single side-band transmitter is fully loaded by two equal side frequencies and a carrier of amplitude ten decibels below one of the side frequencies, the power in the carrier is only about five per cent of the power in the side frequencies. If the peak voltage in the transmitter is kept the same, each side frequency could be 1.3 decibels greater when no carrier is transmitted. Practically it was found that since distortion rather than peak voltage was the limiting factor, the presence of the carrier ten decibels down had no appreciable effect on the permissible side-band amplitude. By using a very narrow filter at the receiver to pass the carrier, the same carrier-to-noise ratio can be obtained with the reduced carrier as is ordinarily obtained with a common double side-band receiver receiving a carrier of full strength. After passing through this narrow filter the carrier may be used to synchronize automatically a local carrier, or by amplifying to a greater extent than the side band and recombining with the side band, it may be used for direct demodulation of the side band. When used in the latter manner it will be called "reconditioned carrier."

In 1928, after extensive tests of short-wave double side-band transmissions had been conducted[1] and while the short-wave transatlantic telephone channels between the United States and England were under construction, some preliminary trials of a short-wave single side-band system were made under the direction of R. A. Heising between Deal, New Jersey, and New Southgate, England, using a local carrier supply at the receiver. The local carrier was produced by beating the output of a variable-frequency tuned-circuit oscillator with that of a crystal oscillator. It was necessary to adjust the oscillator continuously in order to keep the oscillator frequency in the proper relation to the incoming side band.

[1] Reports of some of these tests were contained in the following articles: R. A. Heising, J. C. Schelleng, and G. C. Southworth, "Some measurements of short-wave transmission," Proc. I. R. E., vol. 14, pp. 613–649, October (1926); R. K. Potter, "Transmission characteristics of a short-wave telephone circuit," Proc. I. R. E., vol. 18, pp. 581–649; April, (1930); C. R. Burrows, "The propagation of short radio waves over the North Atlantic," Proc. I. R. E., vol. 19, pp. 1634–1660, September, (1931).

Notwithstanding the limitations of the equipment, encouraging results were obtained and the study of the problem was continued, although along a slightly different path. Receivers were built which were capable of separating the side bands and carrier of an ordinary double side-band and carrier transmission in such a manner that single side-band and other types of reception could be simulated. The carrier could be separately filtered and reconditioned so that even with considerable selective fading a satisfactory carrier was continuously available. Tests made with these receivers showed that the elimination of one side band at the receiver did not affect the intelligibility or quality of reception to any extent if allowance were made for the reduction in the received power.

Description of Apparatus

For the purpose of obtaining more complete quantitative information on the improvement to be realized from single side-band operation and a better understanding of the requirements of commercial single side-band equipment, apparatus was constructed for a trial of a short-wave single side-band system across the Atlantic. Transmitter input equipment was constructed which was capable of delivering a single side-band signal to the input of the water-cooled amplifiers used in the short-wave double side-band transmitters. This input equipment was sent to Rugby, England, and with the coöperation of the British Post Office installed in conjunction with one of the transatlantic transmitters. For comparison purposes the normal double side-band output of this same transmitter was used. A single side-band receiver having a number of novel features was also constructed and installed at the transatlantic receiving station at Netcong, New Jersey. During the latter part of 1933 and the early part of 1934 comparative tests of double and single side-band transmissions were conducted between the British Post Office Headquarters in London and the Bell Telephone Laboratories in New York City.

Transmitting Input Equipment

Fig. 1 shows a rear view of the transmitting input equipment. The equipment is mounted on three bays of panels in two welded steel cabinets, each panel being the width of the usual telephone relay rack panel. A schematic of the input equipment is shown in Fig. 2. The incoming speech is applied to the balanced modulator No. 1, to which is also applied voltage having a frequency of 125 kilocycles, obtained through a multivibrator from a 625-kilocycle crystal oscillator. The low-frequency filter following the first modulator is of the lattice type

of construction and uses quartz crystals as elements[2] in order to obtain the necessary attenuation to the carrier frequency and one side band

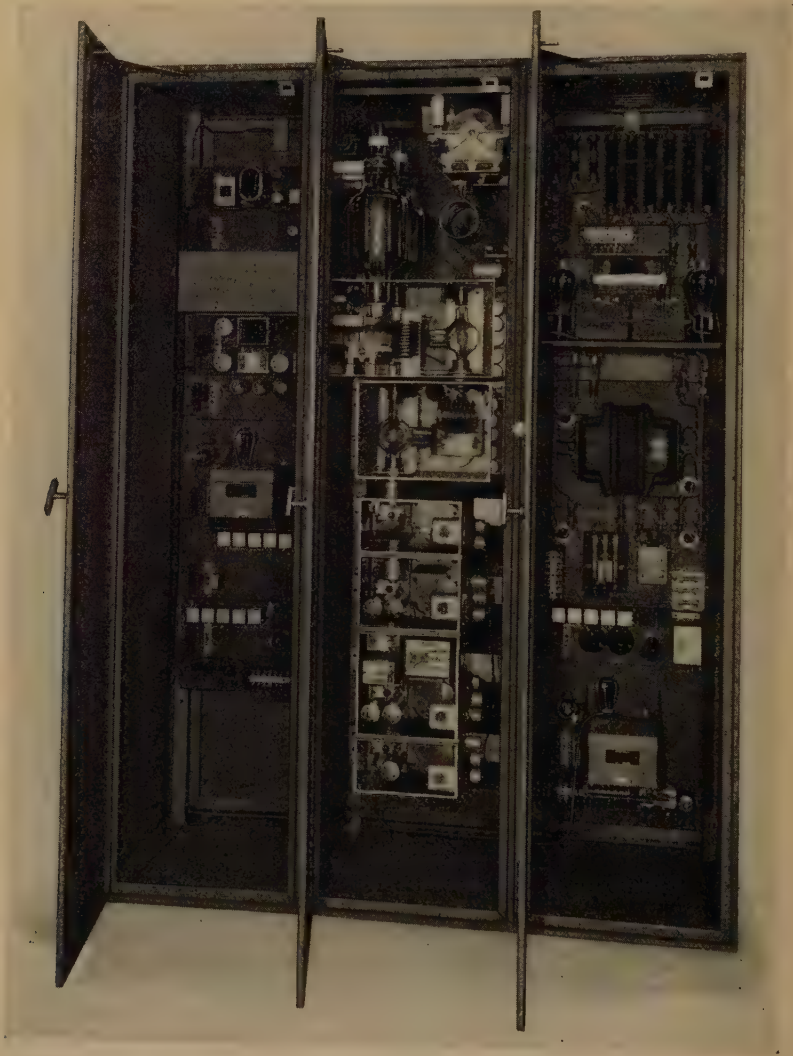

Fig. 1—Rear view of single side-band transmitting input equipment.

while passing the other side band. This filter passes frequencies from 125.1 to 130 kilocycles. The unwanted side band is suppressed from

[2] For information on the construction of such filters see W. P. Mason, "Electrical wave filters employing quartz crystals as elements," *Bell Sys. Tech. Jour.*, vol. 13, pp. 405–452; July, (1934).

forty to sixty decibels and the carrier is suppressed approximately twenty decibels in the modulator and about fifteen decibels more in the filter. In order to obtain a variable amplitude of carrier for experimental purposes, an arrangement was provided for by-passing a variable quantity of the carrier around the first modulator and low-frequency filter. The single side-band voltage obtained from the low-frequency filter, together with the reintroduced 125-kilocycle carrier, is impressed on the input of balanced modulator No. 2. A 2500-kilocycle carrier voltage, which is obtained from the 625-kilocycle crystal oscillator by means of a harmonic generator, is also supplied

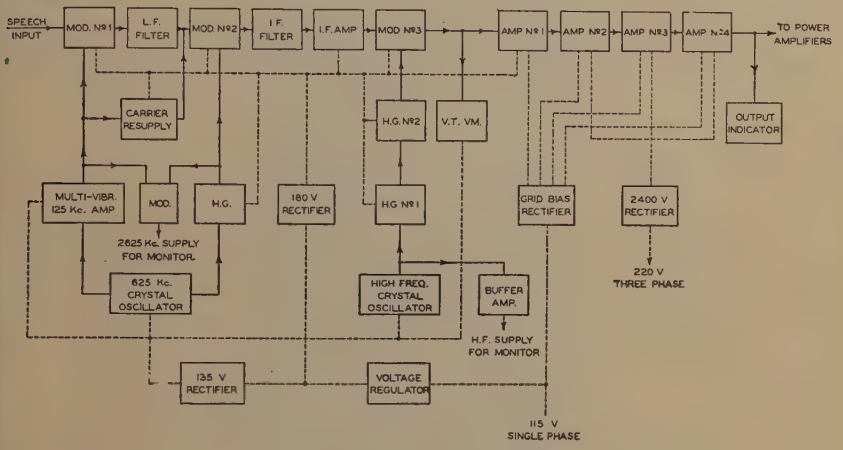

Fig. 2—Schematic of single side-band transmitting input equipment.

to the input of the second modulator. The intermediate-frequency filter which follows the second modulator passes the upper side band generated in the second demodulator (from 2625.1 to 2630 kilocycles) and suppresses the other side band and the carrier approximately fifty decibels. The single side band thus obtained is then amplified before it is impressed on the input of the third modulator. The circuits up to and including the intermediate amplifier are fixed and do not have to be adjusted in order to change the final output frequency of the equipment. The third modulator is of the unbalanced type and both the output of the intermediate-frequency amplifier and a third carrier are applied to its input. The third carrier is obtained from a high-frequency crystal oscillator through two harmonic generators in tandem. The frequency of the carrier applied to the third modulator depends on the output frequency desired and since either side band may be selected the carrier frequency must be 2625 kilocycles greater or less than the desired final output carrier frequency. In order to cover the range from

4700 to 21,000 kilocycles, the carrier must range from 7325 to 18,375 kilocycles. No filter is required in the output of the third modulator since the output tuned circuits are narrow enough to exclude the third carrier and the other side band, which are, respectively, 2625 and 5250 kilocycles away from the desired side band. The output circuit of the third modulator is the first point in the equipment where the final frequency to be transmitted is obtained. The output voltage of the third modulator is applied to the input of a series of four amplifiers in tandem, which serve to increase the amplitude of the single side band and the reduced carrier to a value which will excite to full capacity the power amplifiers of a regular double side-band transmitter. Receiving type screen-grid tubes are used in all but the multivibrator, crystal oscillator, and the final amplifiers. Amplifiers 2 and 3 consist of one 75-watt screen-grid tube each and amplifier 4 consists of two one-kilowatt screen-grid tubes in push-pull.

Transmitting Monitor

It is extremely important in operating the single side-band equipment to know that the distortion is within reasonable limits. With the ordinary double side-band type of transmission it is possible to simulate the receiving equipment with a very simple rectifier, thus allowing

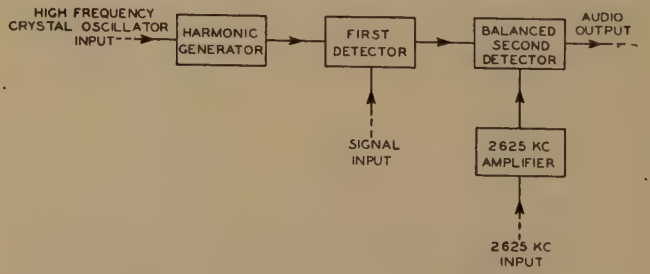

Fig. 3—Schematic of transmitting monitoring device.

local distortion tests to be made on the transmitter. With single side-band transmissions in which the carrier is either totally or partially suppressed such a simple receiver is not adequate, as the distortion produced in a simple rectifier would be excessive. It is necessary that a carrier of the right frequency and of an amplitude considerably greater than that of the side bands be present in the rectifier. After a study of the situation it was decided to build up the carrier for monitoring purposes from the same crystal oscillators used in the transmitter. The monitoring device, a schematic of which is shown in Fig. 3, consists of two detectors and a harmonic generator which take the high-frequency carrier and combine it with the signal to produce an inter-

mediate frequency, which is in turn beaten with the 2625 kilocycles derived from the low-frequency carrier crystal to obtain a demodulated voice frequency.

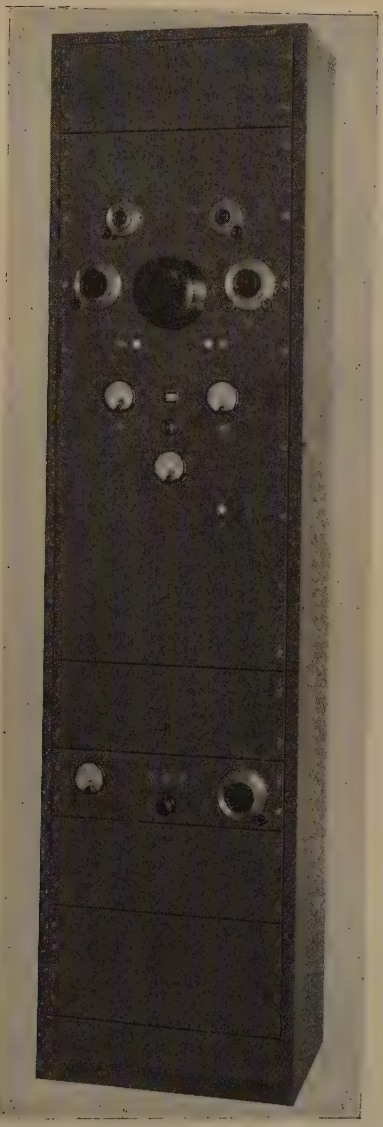

Fig. 4—Front view of single side-band receiver.

Receiver

The front view of the receiver is shown in Fig. 4. The receiver is mounted in a steel cabinet seven feet high and a standard telephone

bay in width. Fig. 5 shows a block schematic of the receiver. The receiver is of the usual double detection variety, having a high-frequency amplifier stage, a balanced first detector, a three-stage intermediate-frequency amplifier, and a balanced second detector. A branch circuit, taken from the grid of the third intermediate-frequency amplifier tube, contains a narrow crystal filter which passes

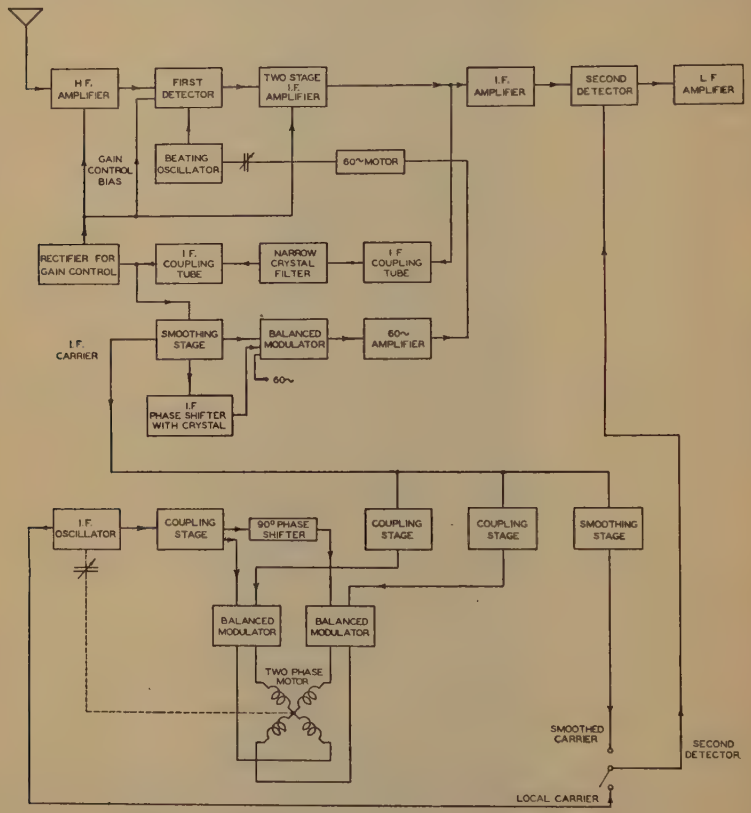

Fig. 5—Schematic of single side-band receiver.

the carrier, but not the side band. After passing through the filter the carrier is amplified and rectified by a linear rectifier, the rectified output giving automatic volume control action on the high-frequency tube, first detector, and first and second intermediate-frequency amplifiers. Another branch circuit passes the filtered carrier through an overloaded amplifier which reduces the fluctuations of carrier amplitude which may be present due to fading or modulation. This reconditioned carrier is then used for obtaining automatic frequency

control of the beating oscillator and synchronization of the local carrier oscillator, or it may be applied directly to the second detector for demodulation purposes.

By using an intermediate-frequency band of moderate width, an ordinary double detection receiver for double side-band operation may be built which will require tuning of the beating oscillator at very infrequent intervals, perhaps only two or three times a day. For receivers in which the carrier is to be separated from the side band by a narrow filter, a much higher degree of frequency stability is required in both the transmitter and the receiving beating oscillator if frequent or almost continuous tuning is to be avoided. Rather than endeavor to obtain the high-frequency stability required, it was decided to arrange that the incoming carrier automatically tune the beating oscillator of

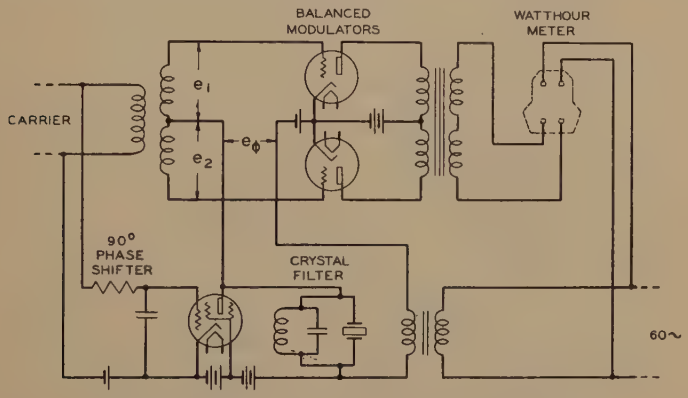

Fig. 6—Schematic of automatic tuning device.

the receiver in such a manner that the carrier at intermediate frequency would always pass through the narrow crystal filter in a satisfactory manner. The manner in which this is accomplished is shown in Fig. 6. The reconditioned carrier is introduced in push-pull fashion on the grids of a balanced modulator system. The same carrier is passed through a circuit having a 90-degree phase shift, through a narrow band suppression filter, and applied to the same two grids in parallel. A small 60-cycle voltage is also applied to the grids in parallel. The 60-cycle output voltage of the balanced modulators is applied through a transformer to the rewound current coils of a watt-hour meter. When the carrier frequency is that of maximum suppression for the narrow filter, equal voltages e_1 and e_2 will be applied to the grids of the two tubes forming the balanced modulator. If the carrier frequency shifts from this position, the voltage applied to each grid will be the vector sum of e_1 or e_2 and a voltage of variable magnitude and phase

e_ϕ, which appears in parallel on the two grids. The magnitude of this parallel voltage increases as the frequency of the carrier at intermediate frequency departs from its proper value causing the voltages on the two grids to change, one becoming higher than the other as shown by e_1+e_ϕ and e_2+e_ϕ of Fig. 7. As the amplitude of the applied radio-frequency voltage increases, the mutual conductance of the modulator tube decreases and consequently a greater amount of 60-cycle current flows in the plate circuit, the phase of which depends upon which tube has the higher mutual conductance. The voltage coil

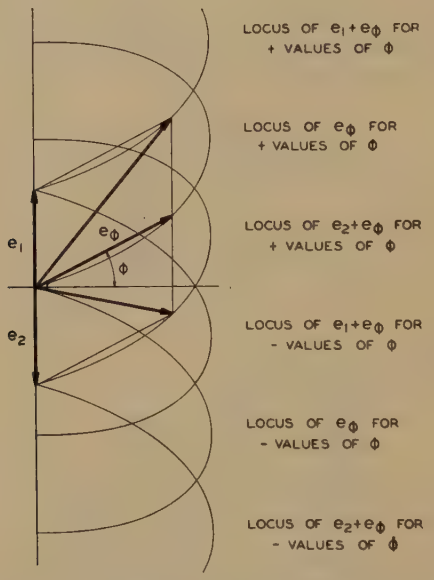
LOCUS OF e_1+e_ϕ FOR + VALUES OF Φ
LOCUS OF e_ϕ FOR + VALUES OF Φ
LOCUS OF e_2+e_ϕ FOR + VALUES OF Φ
LOCUS OF e_1+e_ϕ FOR - VALUES OF Φ
LOCUS OF e_ϕ FOR - VALUES OF Φ
LOCUS OF e_2+e_ϕ FOR - VALUES OF Φ
e_1
e_2
e_ϕ
Φ

Fig. 7—Vector diagram of input voltages to balanced modulators of the automatic tuning device.

of the watt-hour meter is permanently connected to the supply lead. When the frequency of the carrier at intermediate frequency is too high, the phases will be such that the watt-hour meter will run in one direction and when the frequency of the carrier is too low, the watt-hour meter will run in the other direction. A very small condenser is substituted for the registering mechanism of the watt-hour meter. This condenser is connected to the beating oscillator circuit and the whole circuit arranged in such a manner that the watt-hour meter runs until the beating oscillator gives the proper frequency, when the action stops.

Since this automatic tuning unit holds the carrier at intermediate frequency in a fixed relation with respect to a crystal filter, which may

drift slightly in resonant frequency from time to time, and not in synchronism with a local carrier oscillator, it is necessary that a separate mechanism be provided for synchronizing the local carrier if a local carrier is to be used. A schematic diagram of the circuit for doing this is shown in Fig. 8. The reconditioned carrier at intermediate frequency is introduced through amplifiers to two balanced modulators. The output of the local carrier oscillator is introduced to the same modulators, to one of them directly and to the other through

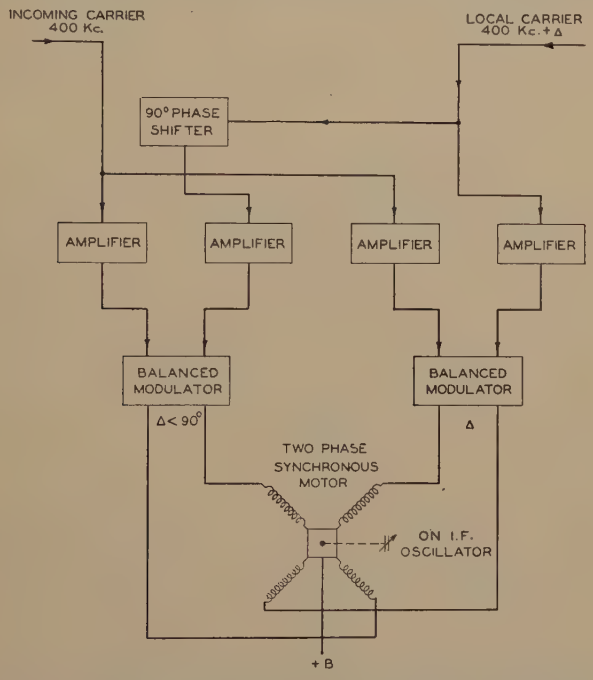

Fig. 8—Schematic of automatic synchronizing equipment.

a device which shifts the phase 90 degrees. The phases of the outputs of these balanced demodulators will be in quadrature and the frequency will be the beat frequency, Δ, between the incoming and local carriers. These voltages operate a variable reluctance type synchronous motor[3] which is mechanically connected to a condenser which forms a part of the local carrier oscillator circuit. The motor operates until the frequency of the local carrier oscillator is exactly the same as the carrier at intermediate frequency, when the frequency applied to the two-phase motor becomes zero.

[3] U. S. Patent No. 1, 959, 449.

For distortion-testing purposes the receiver can be used as a harmonic analyzer, the frequency of the beating oscillator being shifted so that only the desired distortion product passes through the narrow crystal filter. Measurements made in this way when the transmitter and receiver were close together checked very well with measurements made using the monitoring unit previously described.

A balanced second demodulator system was used, as the distortion is much less than with other types. No attempt is made to separate the incoming carrier from the side band in the second demodulator, the amplitude of the reconditioned carrier or the local carrier supplied to the second demodulator being several times the amplitude of the carrier transmitted with the side bands.

Experimental Results and Discussion

To determine experimentally in a quantitative manner the relative merits of two radio systems, such as the single and double side-band systems, is a matter of considerable difficulty. As a practical matter, the percentage of increased commercial time and the increased satisfaction which a customer may obtain are of great interest. Three types of tests have been used in the past for rapidly obtaining information on the performance of radio circuits. They are: (a) determining the signal-to-noise ratio, (b) articulation tests, and (c) observations of circuit merit.

A measurement of the signal-to-noise ratio is made by modulating the transmitter a given amount and measuring the tone at the receiving point. The tone is then removed and the noise measured with the same equipment. When fading conditions are severe a considerable degree of skill is needed to obtain consistent measurements.

Articulation tests may be made in the manner which has been described by Fletcher and Steinberg.[4] They may consist in the reading and recording of meaningless syllables, carefully chosen words inserted in a variety of sentences, or a simple list of words chosen at random from the dictionary and inserted in a common phrase.

In the routine operation of the transatlantic channels, the operators record a value of "circuit merit" which is a composite figure representing the operator's judgment of the commercial value of the circuit. All three of these types of tests were used in comparing the single and double side-band systems.

All observations were made on 9790 kilocycles with an audio-frequency band of from 250 to 2800 cycles. The carrier during single

[4] H. Fletcher and J. C. Steinberg, "Articulation testing methods," *Bell Sys. Tech. Jour.*, vol. 8, pp. 806–854; October, (1929).

side-band transmissions was ten decibels in amplitude below one of two equal side frequencies which loaded the transmitter to its maximum amplitude capacity. Only a single tone was used to modulate the transmitter when measuring signal-to-noise ratios. The degree of modulation of the double side-band comparison signal was 45 per cent when tone modulation was used. Speech modulation was made the same as for two tones for both double and single side-band transmissions. Directional antennas were used for both transmitting and receiving. Successive observations were made on single and double side-band

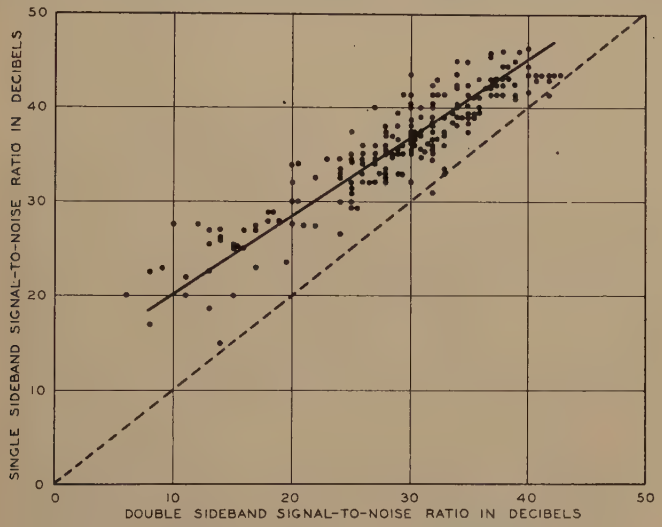

Fig. 9—Plot of signal-to-noise ratios on double side band vs. signal-to-noise ratios on single side band.

transmissions for nine-minute intervals. A reconditioned carrier was used at the receiver most of the time on account of the time required to synchronize the local oscillator when changing from double to single side-band reception. The signal-to-noise ratio as well as the articulation was found to be the same for either reconditioned or local carrier except when the fields were very low, at which times the local carrier was found to be more satisfactory. Since it was convenient to use a slightly different degree of modulation on double side-band than on single side-band transmissions and the filter on the single side-band receiver passed only 1.2 decibels less noise than the double side-band receiver rather than the theoretically possible three decibels, a theoretical difference of 8.1 decibels instead of nine decibels in signal-to-noise ratio was to be expected.

Each point shown on Fig. 9 represents the signal-to-noise ratio which was observed on the single side-band system at a particular period plotted against the average of the preceding and succeeding values of signal-to-noise ratio measured on the double side-band system. It will be seen that when the signal-to-noise ratio on the double side-band system was ten decibels the average signal-to-noise ratio on the single side-band system was ten decibels higher, and when the signal-to-noise ratio on the double side-band system was forty decibels the average signal-to-noise ratio on the single side-band system was five decibels higher. The lesser improvement with the single side-band

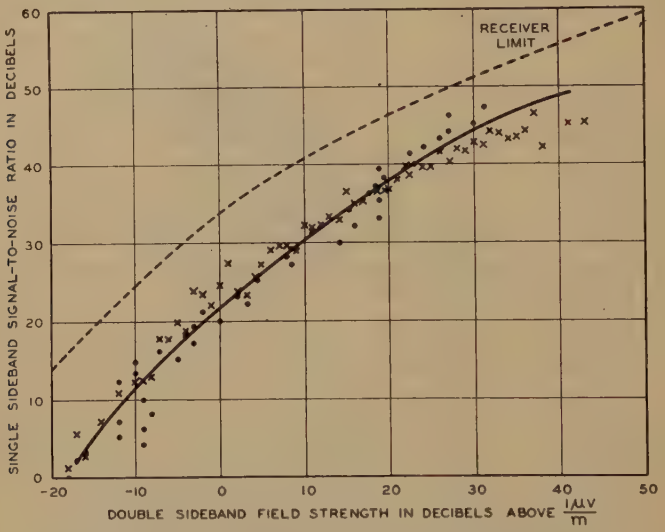

Fig. 10—Plot of signal-to-noise ratios on single side band vs. field strength.

system for the higher signal-to-noise ratios was probably due to limitations in the maximum signal-to-noise ratio obtainable from the transmitting experiment.

Figs. 10 and 11 are plots of the average signal-to-noise ratio versus field for the single and double side-band systems. Only double side-band fields were measured and the average single side-band signal-to-noise ratios are plotted against the average of the preceding and succeeding double side-band measurements. The crosses shown on the curve are the averages of all signal-to-noise ratios in one-decibel intervals of field and the dots shown are averages of all fields obtained when the signal-to-noise ratio lay within one-decibel intervals. The dotted lines represent the maximum signal-to-noise ratio which the

receivers will give for various values of field. It is seen that on the average the set noise was not the limiting factor determining the signal-to-noise ratios obtained.

Upon occasions, advantages considerably higher than the average were obtained for the single side-band system. Reeves[5] has shown that at times the two side bands of a double side-band radio system are likely to be shifted in phase relative to each other and the carrier in such a manner that the demodulated audio-frequency components add at random rather than directly in phase. Under such circumstances the received signal-to-noise ratio of the transmissions would

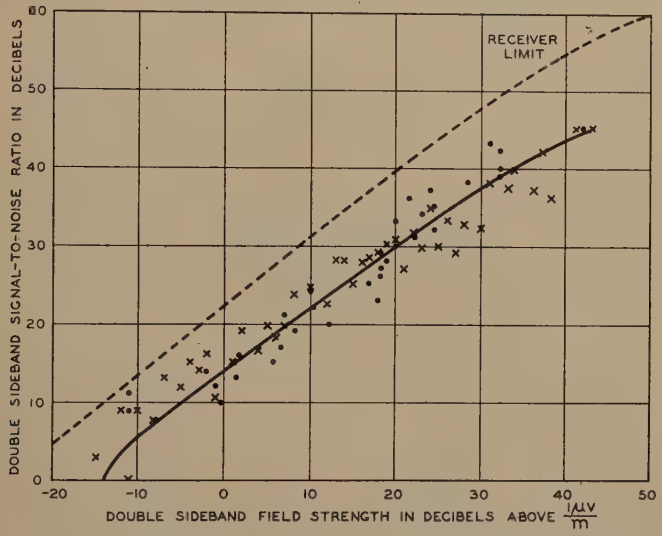

Fig. 11—Plot of signal-to-noise ratios on double side band vs. field strength.

be reduced by three decibels, and in comparison with the single side-band system the latter would show a correspondingly greater improvement. Further, under bad fading conditions, some advantage might be expected from using a receiver in which provision is made to insure an adequate carrier in the second detector at all times. The single side-band receiver used in these tests had such provision while the double side-band receiver did not.

The articulation of the two systems was compared by using words, which averaged approximately three syllables, taken at random from the dictionary. They were inserted in the phrase "Write down. . . ." Native English callers were used at the transmitting end of the circuit

[5] *Jour. I. E. E.* (London), vol. 73, p. 245; September, (1933).

almost exclusively and experienced articulation observers were used at the receiving end. Figs. 12 and 13 show the articulation errors ob-

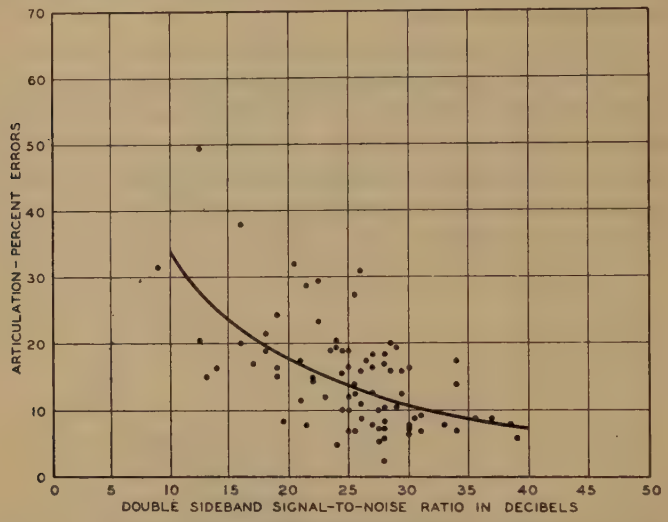

Fig. 12—Plot of per cent articulation errors on single side-band vs. double side-band signal-to-noise ratios.

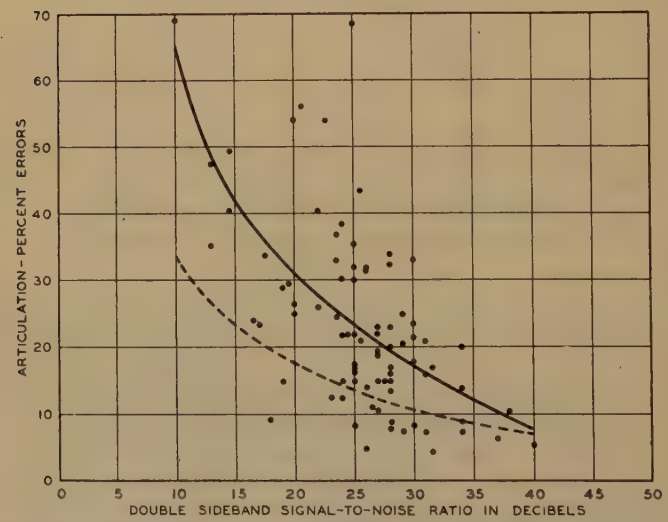

Fig. 13—Plot of per cent articulation errors on double side-band vs. double side-band signal-to-noise ratios.

served on the single and double side-band transmissions plotted against the signal-to-noise ratios measured on the double side-band receiver. When plotting the single side-band data, the average of two

successive signal-to-noise ratio readings on double side band was taken as the signal-to-noise ratio for plotting the intervening single side-

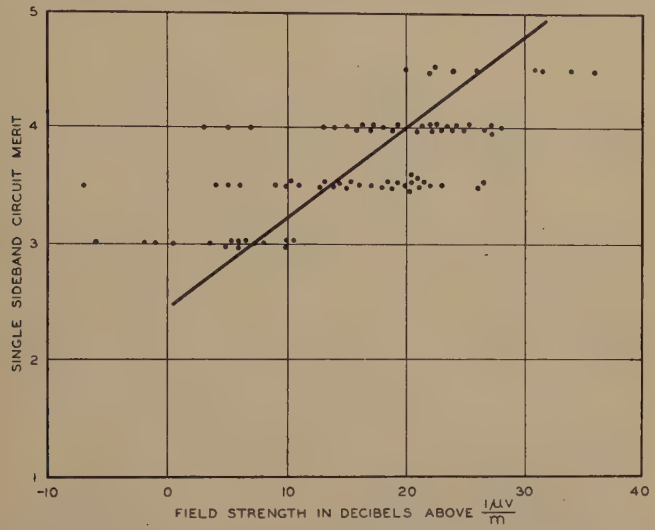

Fig. 14—Plot of circuit merit vs. field strength on single side band.

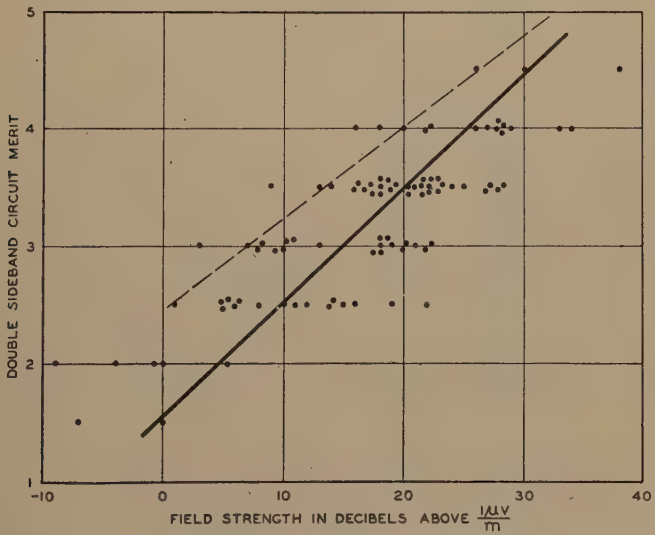

Fig. 15—Plot of circuit merit vs. field strength on double side band.

band observation. The improvement due to the use of the single side-band system expressed in decibels is the difference in the abscissas of the two curves for a given ordinate. The second curve of Fig. 12 has

been dotted in on Fig. 13 to facilitate the comparison of the two systems. The improvement is seen to average about eight decibels for intermediate values of signal-to-nose ratio.

Figs. 14 and 15 show the circuit merits obtained on the single and double side-band systems respectively plotted against the field strength measured on the double side-band receiver. A circuit having a merit of 5 is an extremely good circuit, while a circuit having a merit of 3 is only just commercial and one having a circuit merit of 2 is useful only as an order wire. It will be noted that the difference between the curves for a circuit merit of 3 is about eight decibels, for a circuit merit of 4 about 5.5 decibels, and for a circuit merit of 5 about 4.5 decibels. This is in fair agreement with the signal-to-noise and articulation data.

The comparison of two circuits in this manner is undoubtedly of value if the observations extend over a period of time and if the individual observations are separated by a sufficient interval. When the observations are spaced at short intervals, however, the observer is bound to be influenced by the previous observation and it seems likely that the resulting comparison may be considerably in error. For instance, the observer may notice a small difference in circuit merit and consequently consistently rate one circuit a half point higher than the other, when the actual difference might be nearer to three-fourths of a point. For this reason it is believed that the comparison of the two systems by means of circuit merit gives a less accurate result than by either signal-to-noise or articulation tests.

Outside of the general observation that, as might be expected, the improvement in signal-to-noise ratio at times when the circuit was poor was greater than at times when the circuit was good, no particular connection was found between the improvement obtained by the use of single side-band and transmission conditions. Only one magnetic storm of any consequence occurred during the test and the transmission was so poor on that day that no results were obtained, and, therefore, no conclusions can be drawn as to the effect of magnetic storms.

Proceedings of the Institute of Radio Engineers
Volume 23, Number 7 *July, 1935*

MONITORING THE STANDARD FREQUENCY EMISSIONS*

By

Evan G. Lapham

(National Bureau of Standards, Washington, D. C.)

Summary—*The method and equipment used in monitoring the standard frequency emissions are described in this paper. The emissions are continuously recorded in terms of the primary standard of frequency maintained by the Bureau of Standards. By means of selector circuits and frequency multipliers the received signal is heterodyned with the appropriate harmonic of the primary standard. The beat frequency is then recorded on a recording potentiometer by means of a circuit arrangement which produces a potential difference that is proportional to the frequency difference. The records show that the emissions have been in agreement with the primary frequency standard within two parts in one hundred million at practically all times, and the absolute value of the frequency transmitted is rarely in error by as much as one part in ten million.*

I. Introduction

THE radio transmitting station of the National Bureau of Standards is located near Beltsville, Maryland,[1] which is about thirteen miles northeast of the Bureau's principal laboratory. Standard radio frequencies are transmitted regularly from the Beltsville station. Prior to February 1, 1935,[2] an unmodulated wave having a frequency of 5000.000 kilocycles per second was transmitted each Tuesday from noon to 2 P.M. and from 10 P.M. to midnight, E.S.T. The transmitted frequency is obtained by means of suitable frequency multipliers from a piezo oscillator,[3] located at the transmitting station, which has a fundamental frequency of 200 kilocycles. A precise frequency adjustment is provided on this standard so that the transmitted frequency can be readily brought into exact agreement with the primary frequency standard[4] in the principal radio laboratory at Washington, D. C. Although the standard at the transmitting station nor-

* Decimal classification: R210. Original manuscript received by the Institute, January 31, 1935. Published in the *Bur. Stan. Jour. Res.*, vol. 14, pp. 227–239; March (1935). Publication approved by the Director of the National Bureau of Standards of the U. S. Department of Commerce.

[1] *Bur. Stan. Jour. Res.*, vol. 12, p. 1, (1934); RP630.

[2] Beginning February 1, 1935, and continuing each Tuesday and Friday thereafter, (except legal holidays), three frequencies will be transmitted as follows:

Time (E.S.T.)	*kc*
Noon to 1 P.M.	15,000
1:15 to 2:15 P.M.	10,000
2:30 to 3:30 P.M.	5,000

[3] *Bur. Stan. Jour. Res.*, vol. 11, p. 59, (1933); RP576.

[4] E. L. Hall, V. E. Heaton, and E. G. Lapham, "The national primary standard of radio frequency," *Bur. Stan. Jour. Res.*, vol. 14, p. 85, (1935); RP 759.

mally maintains agreement with the primary frequency standard within the desired limits for a period of two hours, which is the duration of a standard frequency emission, frequency comparisons against the primary standard are made continuously during the emissions, so that a readjustment of the frequency could be made if it became necessary and also as a check on the proper operation of the transmitter. Special apparatus was developed which automatically records the frequency difference between the transmitted frequency and the primary standard.

II. Method Used in Making Frequency Measurements

The method used in making the frequency measurements is indicated schematically in Fig. 1. Receiver No. 1 is connected to the antenna and to one of the outputs of the auxiliary oscillator. The frequency of the auxiliary oscillator is approximately 1000.120 kilocycles. The receiver being tuned to 10,000 kilocycles amplifies the second harmonic of the signal received from the transmitter and the tenth harmonic of the frequency of the auxiliary oscillator. The two signals which are amplified by receiver No. 1 differ by 1200 cycles. The result is that an audio frequency of 1200 cycles is produced in the output of this receiver. The other receiver, No. 2, is connected to the output of one of the units of the primary standard, No. 6 in Fig. 1, and the output of the auxiliary oscillator. This receiver is likewise tuned to 10,000 kilocycles and thus amplifies the 100th harmonic of the primary standard and the 10th harmonic of the auxiliary oscillator. Assuming the frequency of this primary standard to be 100.00004 kilocycles the two frequencies amplified by this receiver differ by 1196 cycles and an audio frequency of 1196 is produced in the output of receiver No. 2. The outputs of the two radio receivers are then combined and connected to an audio-frequency amplifier. These two audio frequencies alternately reinforce and interfere so that the resulting output of the audio-frequency amplifier carries a frequency which is equal to the difference between the two audio frequencies, or four cycles in the example cited. If one calculates the frequency difference between the second harmonic of the transmitted signal and the 100th harmonic of the primary standard, it is seen that it is four cycles. The beat frequency on the output of the audio-frequency amplifier, thus, is the difference between the frequency of the primary standard, No. 6, and the second harmonic of the transmitted signal, and is independent of the frequency of the auxiliary oscillator, the latter serving only to provide a carrier frequency. In order to determine the frequency of the transmitter at any given instant it is necessary to measure this beat

frequency. For this purpose a special form of beat recorder was developed. The frequency of the transmitter can then be calculated if it is known whether the transmitter is higher or lower than the corresponding harmonic of the primary standard. The direction of the difference is determined by making a check against another unit of the primary standard which is known to be higher or lower than the one previously used.

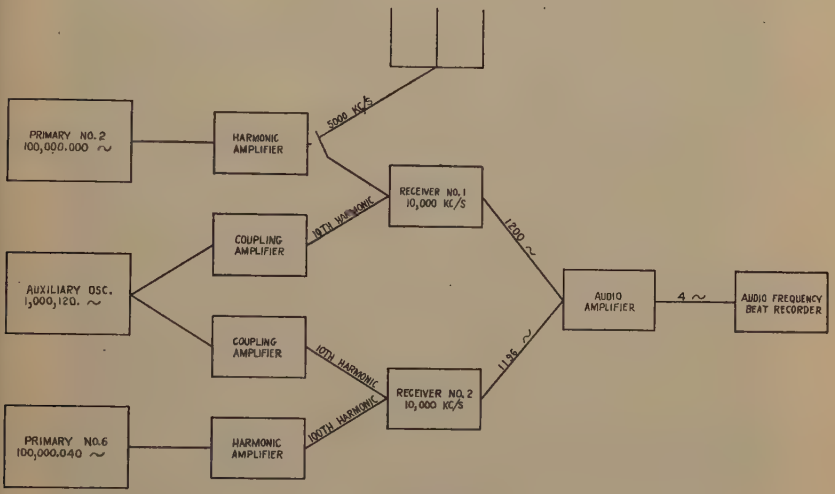

Fig. 1—The standard frequency monitor.

III. Description of Equipment

The complete monitoring equipment is shown in Figs. 2 and 3. The various sections are assembled on panels which are mounted on two relay racks. The equipment on each of the panels, except for the rectifiers and filters for the plate-voltage supplies, are shielded by metal covers. The shields are fastened to the horizontal subpanels by thumbscrews, and phosphor-bronze springs make low resistance contacts with the vertical panel along the top of the covers. The connections between circuits which carry radio-frequency voltages are made by means of concentric tube lines. These shielded lines are constructed of a five-eighths-inch brass tube with one-eighth-inch brass rod held centrally within it by means of bakelite insulators. Fig. 3 is a view of the back of the unit with the shields removed.

The receivers, indicated by *A* in Figs. 2 and 3, are commercial receivers of the regenerative type. Either receiver can be connected to an outside antenna by means of the double-throw switch mounted in the center at the top of the racks. They may be tuned from 2500 to

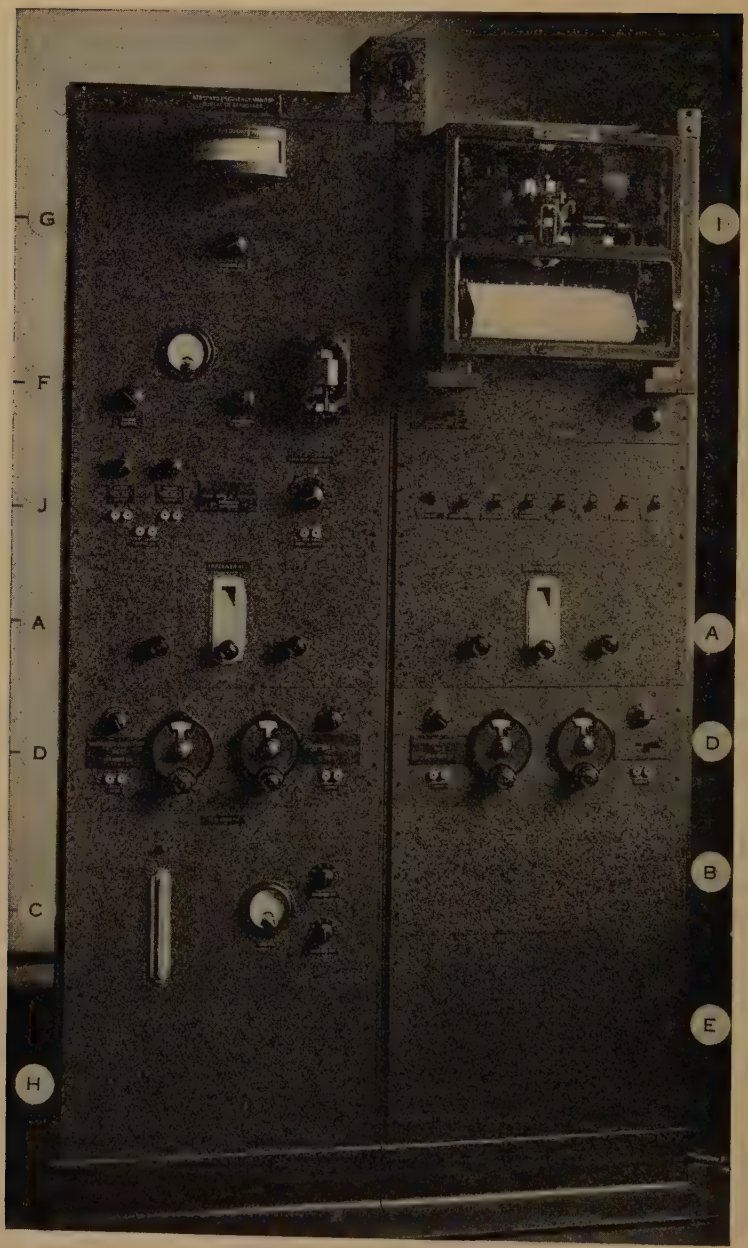

Fig. 2—Front view of the standard frequency monitor.

25,000 kilocycles by means of interchangeable coils, making possible the measurement of frequencies which are multiples of 1000 between

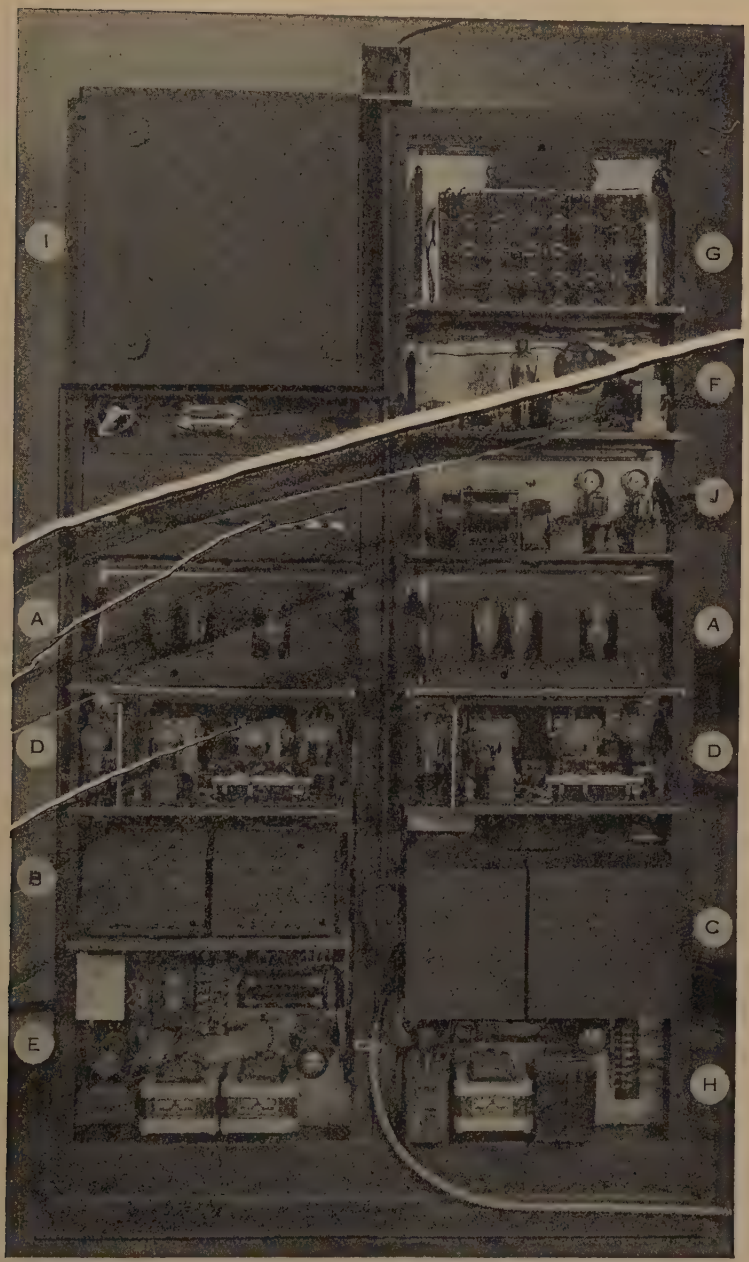

Fig. 3—Rear view of the standard frequency monitor with the shields removed.

3000 and 25,000 kilocycles. There is a single stage of radio-frequency amplification, a detector, and two stages of audio-frequency amplifica-

tion. The receivers were altered slightly in order to incorporate an automatic volume control which would maintain a relatively constant audio-frequency output voltage. The automatic volume control was obtained by shunting a portion of the output voltage through a copper-oxide rectifier and filter and applying this direct-current potential to the grid bias on the radio-frequency amplifier in the customary manner. The power supplies for the receivers are located at *B* in Figs. 2 and 3.

The auxiliary oscillator is a temperature controlled piezo oscillator. It is indicated by *C* in Figs. 2 and 3. The frequency of this oscillator is approximately 1000.120 kilocycles at 50.8 degrees centigrade. The piezo-electric element is a circular, *X*-cut quartz plate. The quartz-plate holder consists of two stainless-steel electrodes mounted in a horizontal position, which are spaced by a toroid of pyrex glass. The thickness of the spacer is such that an air gap of approximately 0.004 inch is left between the quartz plate and the upper electrode. The outside diameter of the pyrex spacer is one and three-quarters inches, the inside diameter one inch, and the thickness 0.15 inch, approximately. The pyrex glass spacer also serves to retain the quartz plate between the electrodes. The inner diameter is only very slightly larger than the diameter of the quartz plate and therefore permits very little lateral motion in any direction. The damping produced when the quartz plate makes contact with the spacer was minimized by grinding the inner surface of the spacer slightly conical from each face in such a way that the two conical surfaces intersect midway between the faces. The quartz plate thus makes contact with the spacer at only one point. The oscillator and amplifier circuit arrangements are conventional in every way and therefore require no explanation. Two separate coupling amplifiers are provided for connection to the two receivers. The coupling capacitors are variable 15-micromicrofarad condensers. The frequency of this piezo oscillator is constant to about one part in 300,000. The power supply for the piezo oscillator is shown at *E* in Figs. 2 and 3. A UX874 voltage regulator tube is used to supply the plate voltage for the oscillator tube.

The plate and filament voltages for the harmonic amplifiers are also supplied by the rectifier and filament transformer on the panel at *E*. The two harmonic amplifiers are shown at *D*. These units consist of an impedance-coupled input amplifier, two tuned amplifier stages, and an impedance-coupled output amplifier. In one of these units the first tuned amplifier is tuned to 200 kilocycles and the second to 1000 kilocycles. This harmonic amplifier has an output of 1000 kilocycles with an input of 100 or 200 kilocycles. The other harmonic amplifier has the

tuned amplifiers adjusted to 500 and 1000 kilocycles, respectively, and gives an output of 1000 kilocycles with an input of 100 or 500 kilocycles. The type 224 tube is used in these amplifiers.

Considerable difficulty was encountered in preventing the input voltage to one of the harmonic amplifiers from feeding into the other. The interaction between these two units was eliminated by having separate voltage dividers and 60-millihenry radio-frequency chokes in both the positive and negative leads of the plate voltage supply. The output of the harmonic amplifiers can either be connected to the receiver or to the jacks on the front panel, if used for other purposes, by means of the two-way switch on the right of each panel. When the switch is in the position to connect the output to the jacks, the receiver on the panel above can be connected to the antenna by properly setting the antenna switch previously mentioned. If the output of the harmonic amplifier is connected to the receiver the antenna connection is grounded. A 15-micromicrofarad variable condenser is provided to control the voltage input to the receiver.

The equipment used in measuring the beat frequency between the transmitted signal and the primary frequency is shown at *F*, *G*, *H*, *I*, and *J*, Figs. 2 and 3. The circuit arrangement is shown in the diagram, Fig. 4. The voltage divider and voltage regulator tube are mounted with the power pack for this unit on the panel *H*. The remainder of the circuits are on the panels *F* and *G*. The outputs of the two receivers are connected to the audio-frequency amplifier. The output of this amplifier is rectified by means of two half-wave copper-oxide rectifiers, *Q*, of the type used in rectifier type alternating-current meters, connected in a familiar voltage doubling arrangement. By rectifying the audio-frequency output a unidirectional potential is produced which is the envelope of the two audio-frequency notes. This direct-current potential is connected, as shown, to the grids of two type UY235 tubes. The plate impedance for these tubes is a 10,000-ohm voltage divider and the variable contact is used to balance the currents in the two tubes. The screen grid and plate are connected together as shown. A sensitive, polarized relay is connected across the plate resistor in series with a zero-center milliammeter which serves as a beat indicator. When the audio-frequency voltage reaches a maximum the resulting direct-current potential charges the one-microfarad condenser, *L*, positively through the two-megohm grid resistor, making this grid less negative, which accordingly increases the plate current in this tube. At the same time the one-microfarad condenser, *M*, is charged negatively and the current in this tube is decreased. The result is that a difference of potential is produced across the plate resistor,

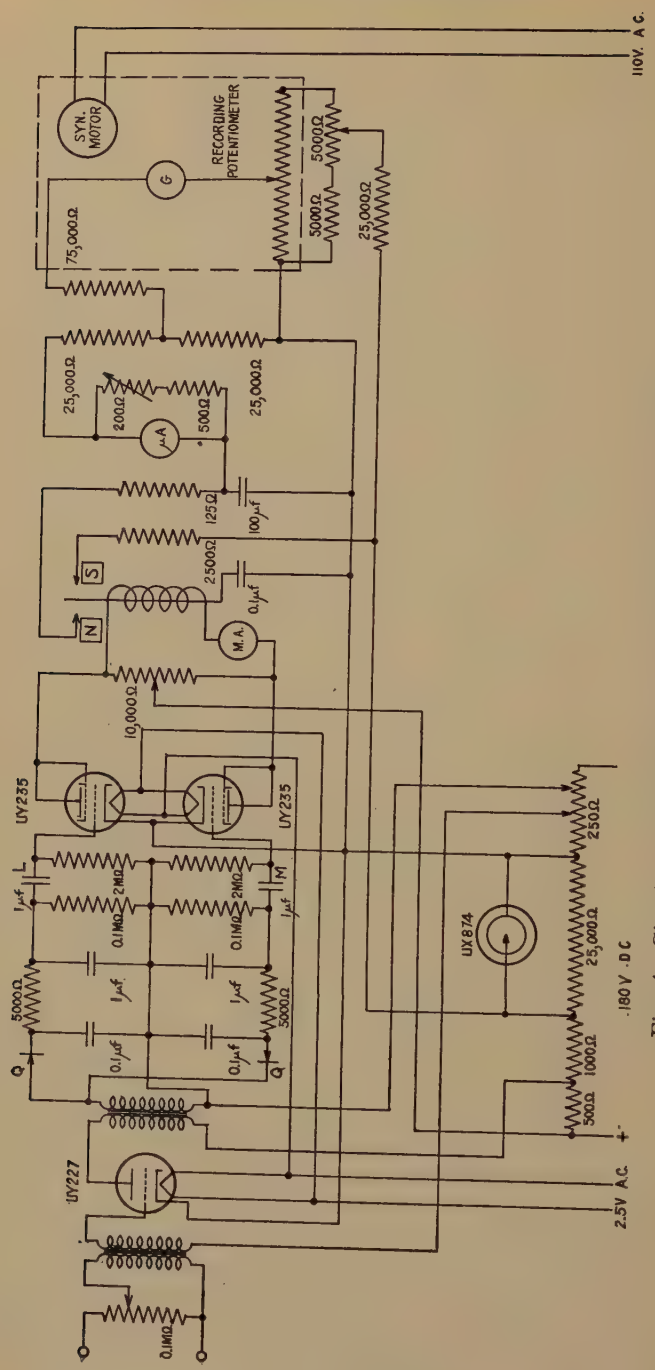

Fig. 4—Circuit arrangement of the beat indicator and recorder.

a current flows through the coil of the polarized relay and the reed moves in one direction. When the audio-frequency voltage decreases to a minimum the one-microfarad condensers discharge through the two-megohm grid resistors, which reverses the change in bias on the tubes, the potential difference across the plate impedance is in the opposite sense, and the relay reed moves in the opposite direction. The combination of coupling condenser and grid resistor which is used must be one which has a charging time somewhat greater than one fourth the period of the modulation frequency. The comparatively slow rate of charge and discharge of the one-microfarad condenser through the two-megohm resistor serves to prevent noise of short duration from interfering with the operation of the relay. The particular values used in this case make the relay operate over a range from 0.2 cycle to approximately 25 cycles. When the relay makes contact in one position, a 0.1-microfarad condenser is charged to 90 volts and when it makes contact in the other position the condenser is discharged completely into a condenser having a capacity of approximately 112 microfarads (indicated as 100 microfarads in Fig. 4). The 112-microfarad condenser discharges slowly through a 50,000-ohm resistor connected in series with a microammeter. After the relay has operated at a given frequency for a short time the voltage in the 112-microfarad condenser reaches an average value which is proportional, approximately, to the frequency operating the relay. The current through the microammeter is consequently approximately proportional to the frequency and the instrument can be calibrated to read frequency directly. The record of the frequency variations is obtained by connecting a recording potentiometer across a portion of the 50,000-ohm resistor which is in series with the microammeter. The Leeds and Northrup recording potentiometer, *I*, in Figs. 2 and 3, has been found to operate very satisfactorily for this purpose. The principal requirement is that the galvanometer have a high sensitivity and a low natural frequency. By adjusting the voltage across the slide wire the recorder is likewise made direct reading. The 90-volt supply which charges the 0.1-microfarad condenser also supplies the voltage for the potentiometer, which makes the recorder moderately independent of voltage fluctuations. The frequency indicating meter reads from zero to nine cycles with the smallest division 0.1 cycle or one part in one hundred million at 10,000 kilocycles. The recorder covers the range from zero to five cycles, with the smallest division 0.05 cycle, or 0.5 part in one hundred million at 10,000 kilocycles.

In order to be able to calibrate readily the frequency indicating meter and recorder it was necessary to have a source of known beat

frequency with which to operate the beat frequency measuring equipment. This was provided by constructing a device which would interrupt a 1000-cycle voltage at a known rate. The 1000-cycle voltage was used in this case as it was available in the laboratory, but practically any audio frequency, such as a small 60-cycle voltage from the power line, would be satisfactory. The interrupting device, *J*, in Figs. 2 and 3, consisted of a five-watt telechron motor which was geared to turn a shaft at the rate of twelve revolutions per minute. Four separate insulating disks were mounted on this shaft. One of the disks had two metal segments equally spaced on the cylindrical surface. The space between segments was equal to the length of the segments. Two phosphor-bronze springs pressed against this disk in such a way that they were connected together at the times that the metal segment was passing under them. The 1000-cycle voltage was connected so that it was in series with these sliding contacts. One revolution of this disk completed two cycles. With the disk rotating at the rate of twelve revolutions per minute the resulting beat frequency is twenty-four cycles per minute or 0.4 cycle per second. The other three disks had 5, 10, and 15 segments, respectively, and provided a beat frequency of 1, 2, or 3 cycles. A switch was provided so that any of these frequencies could be used for calibrating purposes.

IV. Results

The emissions on 5000 kilocycles were originally measured on the fundamental frequency. The received signal, however, was subject to considerable fading during the daytime emissions. The signal received during the night emissions was much more dependable for measurement purposes, although there were times when fading interfered with the measurements during this emission. Fading of the received signal makes the frequency record very unreliable. If the signal fades out completely the recorder operates as though the frequency difference were zero. If the fading has a period of the same order as the beat frequency being recorded, the intensity variations tend to operate the relay at the frequency of the fading and this obscures the actual beat frequency. If the fading is due to a movement of an ionized layer in the ionosphere a frequency change due to the Doppler effect is to be expected and has actually been observed at the receiving point. Such changes are very rapid and of short duration, so that the recorder responds only partially to such changes. The result is that fading tends to broaden the record obtained and limits the accuracy with which the transmitted frequency can be compared with the primary frequency standard. A representative record obtained on 5000 kilocycles during a daytime transmission is shown in curve *A*, Fig. 5. The

blank spaces which occur at ten-minute intervals are the periods during which the transmitter is keyed for identification purposes. During this period the recorder does not measure the frequency but drops to some other point which depends on the average keying speed. The beat frequency recorded was actually two to three cycles but in reproducing this record the coördinates were shifted so that they indicate directly the deviation in cycles from 5000 kilocycles. The variations in the transmitted frequency would appear from this record to be ± 0.5 cycle. Such variations in the transmitted frequency undoubtedly do not occur, however, as a record (curve *B*) of the frequency varia-

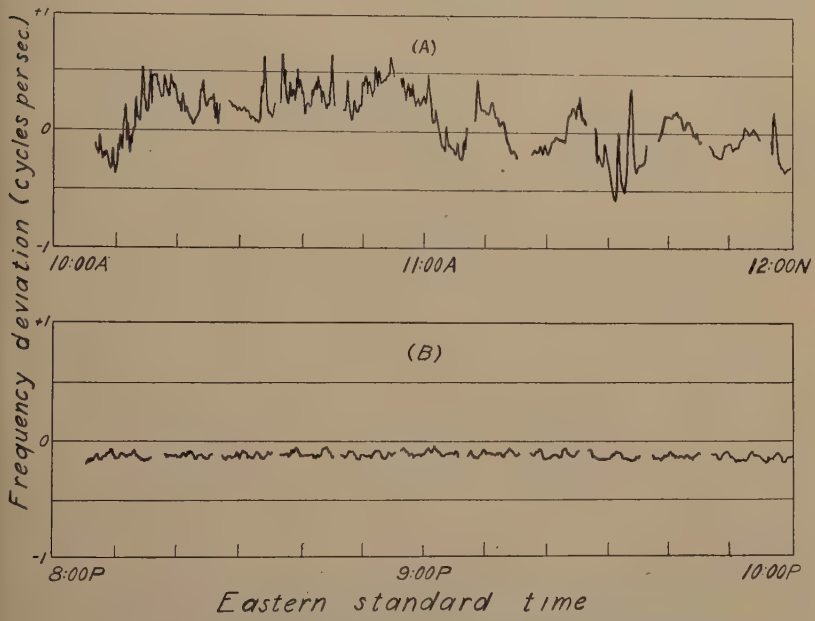

Fig. 5—Sample record of standard frequency emission on 5000 kilocycles.

tions ten hours later when no noticeable fading was present, and the frequency was obtained from the same frequency standard, indicates that the maximum variations are ± 0.1 cycle. The frequency variations indicated by the latter record may be due to variations either in the standard controlling the transmitter or in the reference oscillator, to the small amount of fading which may still be present in the signal but which is not noticeable as a variation in amplitude because of the action of the automatic volume control, or to hunting in the recording potentiometer. The latter variation is of the order of 0.02 cycle. The unreliable nature of the record obtained on 5000 kilocycles when fading was present made it necessary to make the frequency measurements in terms of the primary standard on another frequency.

It was found that the second harmonic of the transmitted frequency, 10,000 kilocycles, was sufficiently strong at the laboratory in Washington, D.C., to be measured and recorded dependably. The signal received on the second harmonic, moreover, was free from fading and records indicate frequency variations of the order of those in curve *B*, Fig. 5, both during day and night emissions.

The use of the standard frequency emissions where the received signal is subject to fading must be limited to the periods when the received signal is fairly steady if instantaneous measurements of a high order of accuracy are to be obtained.

In order to show the magnitude of the deviations of the emissions from agreement with the primary standard, the highest and the lowest frequencies indicated on the record for each of the emissions during the first ten months of 1934 were tabulated, and are presented in curves *A*, Figs. 6 and 7. The dates of the emissions are plotted as abscissas. The deviations from agreement with the frequency of the primary standard as indicated by the data available at the time of the emission are plotted as ordinates. The points directly to the left of a vertical line are for the daytime emission on that particular date, and the points directly to the right of the line are for the evening emission. The upper points indicate the highest value that the transmitted frequency attained during the two-hour period and the lower points the lowest value transmitted. The curves show that, during the ten-month period, the disagreement was at no time as great as one part in ten million. On all but a very few occasions the emissions were in agreement with the primary standard within about two parts in one hundred million. The average variation of the emission frequency from the primary standard was one-half part in a hundred million.

The absolute accuracy of the emissions depends on the determination of the absolute frequency of the primary standard. The determination of the frequency of the primary standard is made by comparing the time indicated by a synchronous motor clock controlled by one of the standards with standard time. The time signals received by radio from the Naval Observatory are used for this purpose. Since the time signals are somewhat in error, corrections are sent out by the Naval Observatory. These corrections were formerly received a month or more late, although recently the delay in the receipt of the corrections has been reduced to about one week. The frequencies as calculated in terms of the uncorrected time signals show variations of the order of four parts in ten million. For the standard frequency emissions it is necessary to extrapolate a curve through these points. After the corrections are received the variation in the frequency as indicated by

the time checks are narrowed down to approximately one part in ten million. For this reason the value of the primary standard assigned at the time of the emission differs from the final corrected value. Curves *B*, Figs. 6 and 7, give the frequency, on the date of the emission, of one of the units of the primary standard which was checked against standard time during this period. The solid line indicates the corrected values and the crosses the frequencies which were assigned at the time of the emissions. This error in the frequency of the primary standard decreases the absolute accuracy of the standard frequency emissions

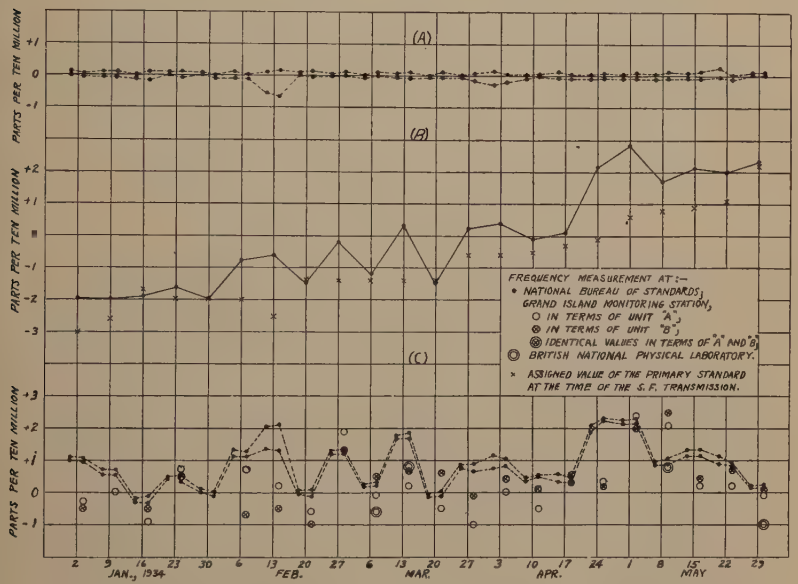

Fig. 6—Graphical representation, January to May, 1934, of the deviation of the standard frequency emissions from (*A*) the assigned value of the primary standard, (*C*) the corrected value of the primary standard, and (*B*) the frequency of a unit of the primary standard in parts per ten million above or below 100 kilocycles.

by a corresponding amount, as shown in curves *C*, Figs. 6 and 7, which give the transmitted frequency as determined in terms of the corrected values of the primary standard. It is seen that the absolute value of the transmitted frequency was rarely in error by as much as one part in ten million.

An interesting check on the measurements made at the National Bureau of Standards is shown in curves *C*, Figs. 6 and 7. Frequency comparisons are given which have been reported by the British National Physical Laboratory in terms of their national primary standard,

and also measurements by the Federal Communications Commission in terms of the standards at the monitoring station at Grand Island, Nebraska. These measurements show agreement within two parts in ten million at all times, and many are in agreement within one part in ten million. These measurements indicate not only the very close agreement between these independently operated standards, but also the very high accuracy of the frequency comparisons which can be made by means of standard frequency emissions.

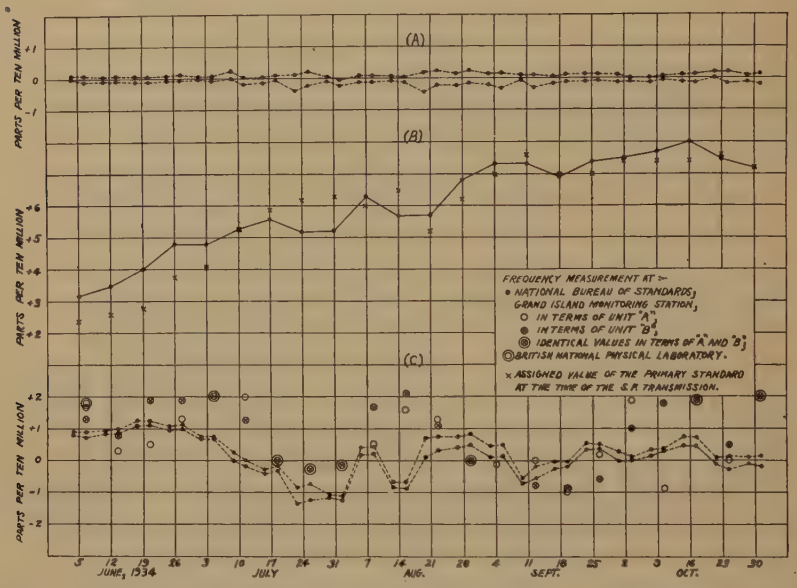

Fig. 7—Graphical representation, June to October, 1934, of the deviation of the standard frequency emissions from (*A*) the assigned value of the primary standard, (*C*) the corrected value of the primary standard, and (*B*) the frequency of a unit of the primary standard in parts per ten million above or below 100 kilocycles.

V. Additional Uses of Apparatus

The equipment which is described has also a useful application in comparing different frequency standards. If the standards have fundamental frequencies of either 100 or 200 kilocycles they can be connected to the two harmonic amplifiers and a record of the frequency difference obtained. Very minute variations can be detected in this way. The frequency of one unit in terms of the other can also be very accurately determined in this manner. Such frequency comparisons can be made at any harmonic frequency desired which is within the range of the receivers and is an integral multiple of 1000 kilocycles.

Proceedings of the Institute of Radio Engineers
Volume 23, Number 7 *July, 1935*

RECENT STUDIES OF THE IONOSPHERE*

By

Samuel S. Kirby and Elbert B. Judson
(National Bureau of Standards, Washington, D. C.)

Summary—*Results of ionosphere measurements utilizing transmissions at vertical incidence and made weekly over a period of eighteen months are discussed. Typical graphs of diurnal variations of the E-layer critical frequency and its relation to the ionizing force of the sun are shown for three seasons. Similar graphs for the F_2 layer are included as well as a seasonal curve of midday, and maximum critical frequencies of this layer. The absence of midday F_2 critical frequencies during the summer is pronounced.*

A sporadic E layer appearing at the same virtual height as the normal E, and after the normal E has reached its critical penetration frequency, is discussed. A comparison of its appearance with local thunderstorms, is tabulated.

The presence of a tentatively named G layer is indicated.

I. Introduction

OBSERVATIONS of the virtual heights of the ionosphere, made one day each week and extending over a period from June, 1933, to November 7, 1934, have presented an opportunity to continue the study of diurnal and seasonal effects and to compare them generally with other natural phenoma. Furthermore, other new and interesting phenomena have been observed, wholly due to the continuity of a day's "run" over a large range of frequencies. The purpose of this paper is to present and interpret this series of data.

The method employed in the experiment is essentially that of Breit and Tuve with modifications of technique similar to those described by Kirby, Berkner, and Stuart.[1]

Some data for diurnal variations of E critical frequencies have been contributed by T. R. Gilliland[2] of the National Bureau of Standards, from records of ionosphere heights made by his automatic recorder operating over a range of frequencies from 2500 to 4400 kilocycles. Since these continuous records were available in this band of frequencies, no manual measurements between these limits were necessary.

* Decimal classification: R113.61. Original manuscript received by the Institute, February 1, 1935. Presented before Ninth Annual Convention, Philadelphia, Pa., May 30, 1934. Published in the *Bur. Stan. Jour. Res.*, vol. 14, pp. 469–487; April (1935). Publication approved by the Director of the National Bureau of Standards of the U. S. Department of Commerce.

[1] Kirby, Berkner, and Stuart, *Bur. Stan. Jour. Res.*, vol. 12, p. 15; January, 1934; Proc. I.R.E., vol. 22, p. 481; April (1934).

[2] Gilliland, *Bur. Stan. Jour. Res.*, vol. 11, p. 561; October, (1933); Proc. I.R.E., vol. 22, p. 236; February, (1934).

It has been well established that in the latitude of Washington there are two major layers in the ionosphere at all times and a third present in the daytime, especially during the summer.[1,3] The first two are known as the E layer, 100 to 120 kilometers above the earth, and the F_2 layer, at approximately 230–350 kilometers virtual height. The third or F_1 layer appears at heights of 180–240 kilometers. Earlier experiments indicate that radio-frequency energy is returned to earth from these layers by a process of refraction, and these conclusions are further substantiated by the data given herein. The sharp rise in virtual height occurring at the critical penetration frequency and magneto-ionic double refraction, which is observed in the F_1 and F_2 layers, indicate refraction. When magneto-ionic double refraction is observed,

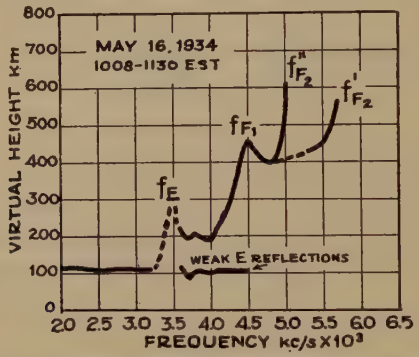

Fig. 1—Curve showing typical frequency sweep and the three major layers E, F_1, and F_2 with their critical frequencies.

the critical frequency occurring at the lower frequency is the ordinary ray while the one at the higher frequency is the extraordinary ray. These phenomena are clearly shown in the graphs in Fig. 1. Although well-defined critical penetration frequencies are usually found in the E region, no evidence of magneto-ionic double refraction has been observed.

The critical or penetration frequencies are indications of the maximum ionization density of the layers and are defined as the lowest radio frequency of a wave which penetrates a layer at normal incidence.

The relation between the maximum electron density and critical frequency for the ordinary ray in any layer in the absence of dissipation is given by the well-known equation

$$N = \frac{f_c''^2 \pi m}{e^2} \cdot 10^6 \qquad (1)$$

$$= 1.24 f_c''^2 \cdot 10^{-12} \qquad (1a)$$

[3] Schafer and Goodall, *Nature* (London), vol. 131, p. 804; June 3, (1933).

where,

N = number of ions per cm^3,

f_c'' = critical frequency of ordinary ray in kilocycles,

m = mass of ion in grams,

e = charge on the ion in electrostatic units.

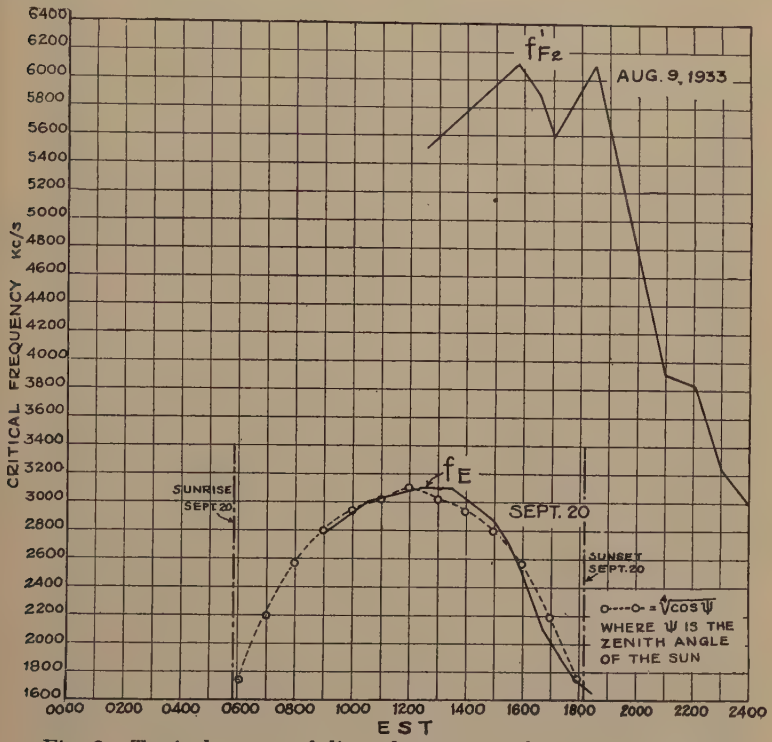

Fig. 2—Typical curves of diurnal variation of critical frequencies of E and F_2 layers for fall.

The relation between the critical frequencies for the ordinary and extraordinary rays is given by the well-known equation

$$f_c''^2 = f_c'(f_c' - f_H) \qquad (2)$$

where,

f_c' = critical frequency for the extraordinary ray,

$$f_H = \frac{He}{2\pi mc} \times 10^{-3} \text{ kilocycles}$$

$f_H \cong 1460$ kilocycles at Washington for electron ionization.

An indication of the diurnal variation of critical frequency for the various layers, corresponding to different seasons of the year, is given in the graphs of Figs. 2, 3, and 4.

II. E Layer

E-layer critical frequency measurements were made at frequencies of 2500 kilocycles or lower at early and late hours of day, and at night. Data for higher frequencies measured nearer noon were taken from

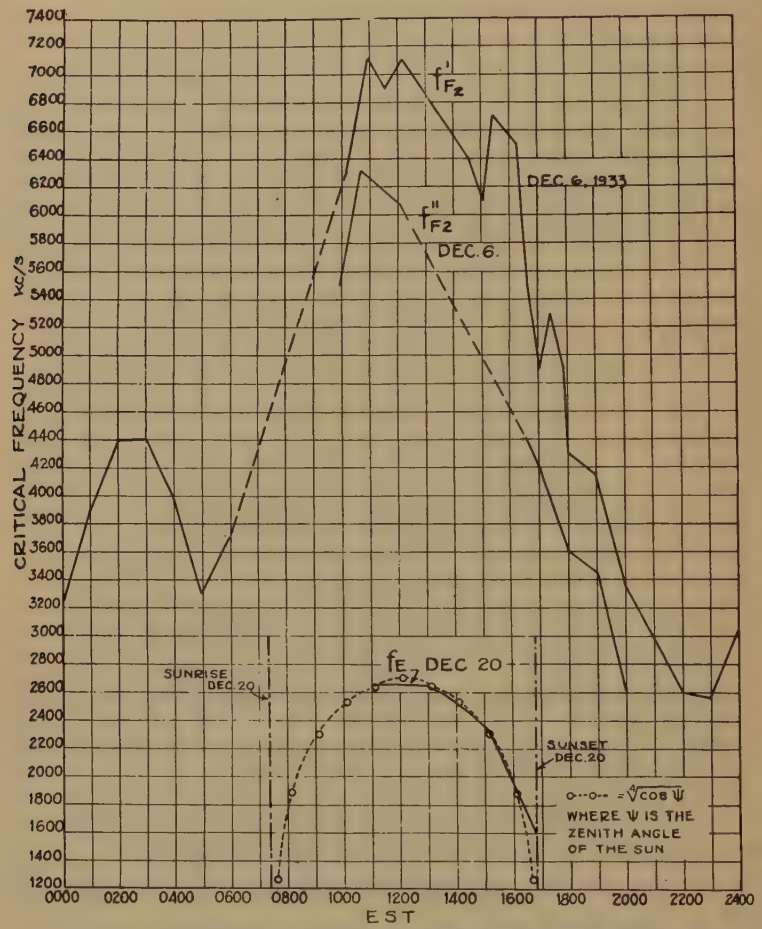

Fig. 3—Typical curves of diurnal variation of critical frequencies of E and F_2 layers for winter.

Gilliland's records. The critical frequency of the normal E layer is most clearly in evidence during the fall, winter, and spring. During the summer it is frequently obscured by the sporadic E which will be discussed later. The lower graphs of Figs. 2, 3, and 4 are for the E layer.

The normal E critical frequency rises rapidly out of the broadcast

band above 1500 kilocycles shortly after sunrise, comes to a broad maximum at noon, and falls rapidly into the broadcast band just before sunset. The graph of critical frequency vs. time of day is approximately symmetrical about the noon axis. These facts indicate a

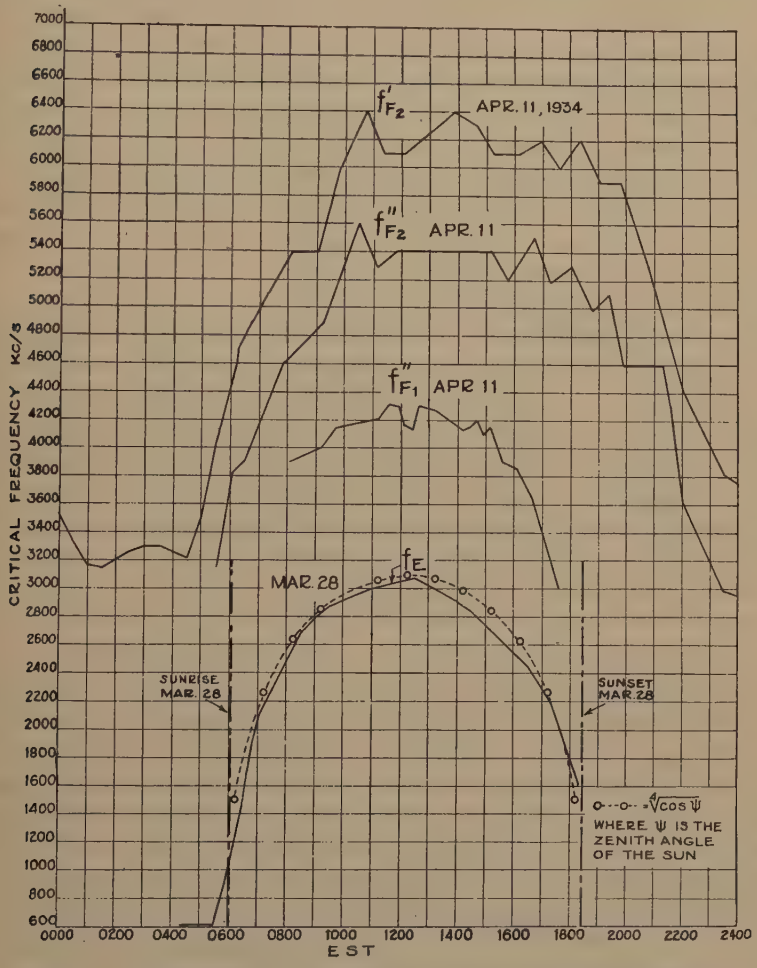

Fig. 4—Typical curves of diurnal variation of critical frequencies of E and F_2 layers for spring.

rapid recombination of ions and that the ionization density is a simple function of the ionizing force of the radiation from the sun during most of the time between sunrise and sunset. If recombination is rapid it may be shown from results of Pedersen[4] that the normal diurnal varia-

[4] Pedersen, "Propagation of Radio Waves," Chapters V and VI.

U OF I
LIBRARY

tion of f_c'' should follow the relation $f_c''=f_c''$ max $(\cos \psi)^{1/4}$ where ψ is the angle which the sun's rays make with the zenith. Data taken during the period preceding and following the eclipse of August 31, 1932, were found to agree well with this relation.[5]

The lower graphs of Figs. 2, 3, and 4 show the diurnal variation f_E (critical frequency for the E layer), determined experimentally and also the diurnal variation of $(\cos \psi)^{1/4}$ plotted in arbitrary units. From these figures it may be seen that the diurnal variations of f_E and $(\cos \psi)^{1/4}$ are approximately the same during most of the time that the sun is above the horizon. Also from (1) these figures indicate that N is proportional to $(\cos \psi)^{1/2}$ during most of the day.

The rate of change of ionization density may be expressed by

$$\frac{dN}{dt} = I - \alpha N^2 \tag{3}$$

where I is the number of ions produced per second by the ionizing agency, α is the coefficient of recombination, and N is the number of ions per cm^3. I is assumed to be proportional to $\cos \psi$. Since the diurnal variations of N and $(\cos \psi)^{1/2}$ have been found to be approximately equal dN/dt must be small and I is approximately equal to αN^2. To satisfy this condition it is necessary that αN^2 be large or, in other words, that recombination in the E layer during the daytime be rapid. Pedersen has shown from the work of Thompson and others[4] that α is of the same order of magnitude for electrons and heavy ions. Since αN^2 represents recombination, a rapid recombination would indicate a large value of N. From (1) a large value of N giving a moderately low value of critical frequency, such as the E critical frequencies, indicates a large mass for N. These results suggest that the E-layer ionization is composed mainly of heavy ions rather than electrons.

Further evidence in support of this conclusion is found by considering the phenomenon of magneto-ionic double refraction. This is commonly observed by the splitting of refractions in the F_1 and F_2 layers into ordinary and extraordinary rays with a frequency separation between the critical frequencies of approximately 800 kilocycles. This is just about the frequency separation obtained by calculations from (2) and (3) where the ionization of the layer is electronic and the earth's magnetic field is 0.52 gauss which is the approximate value at a height of 180 kilometers at Washington. Magnetic splitting has not been observed for E-layer refractions.[6] This point is considered as

[5] Kirby, Berkner, Gilliland, and Norton, *Bur. Stan. Jour. Res.*, vol. 11, p. 829; December, (1933); Proc. I.R.E., vol. 22, p. 247; February, (1934).

[6] At the I.R.E. convention, May 28–30, 1934, at which this paper was read, Schafer and Goodall presented a paper in which they stated that by the use of

further evidence for an E layer of heavy ions. It may be seen from (2) and (3) that for heavy ions, the critical frequency separations between the ordinary and extraordinary rays would be of the order of a few hundred cycles per second. This separation could not be resolved by the equipment used.

It is therefore concluded both from the rapid rate of recombination observed and from the absence of magnetic splitting that the normal daytime E layer is preponderantly made up of heavy ions rather than electrons.

So far it has seemed impracticable to follow the E-layer critical frequency down into the broadcast band in the evening because the transmissions would interfere with reception of broadcast programs. Measurements in the band, (600 to 1500 kilocycles) made between 0200 E.S.T. and sunrise show that the E layer is frequently penetrated at frequencies of 600 to 800 kilocycles. No definite E critical frequency has so far been observed at night. This phenomenon will be discussed under the section on "sporadic E layer."

During the months of May to August, E-layer critical frequencies below 2500 kilocycles during the early and late part of the day, if they existed, were usually obscured by sporadic E-layer reflections. Satisfactory measurements of diurnal variations were not obtained during these months at frequencies below 2500 kilocycles.

III. F_2 Layer

Characteristics of the F_2 layer were discussed in an earlier paper.[1] Some additions and modifications to the data and conclusions presented there are now desirable.

In general midsummer, midday measurements of F_2 layer heights and critical frequencies were unsatisfactory. Frequently no reflections or refractions could be received at frequencies above f_{F_1}'' (critical frequency of the ordinary ray for the F_1 layer) and sometimes none at lower frequencies. Fig. 5 shows a typical summer-day run. The general absence of F_2 refractions at frequencies above 5000 kilocycles may be caused by absorption.

Sporadic E reflections when present at these frequencies as they were frequently, were of medium amplitude, indicating that the absorption below the E layer was not extremely large. Also lower frequencies were not so highly absorbed in going to the E layer. Therefore it is believed that if the absence of refractions above 5000 kilocycles during the summer midday is due to absorption, the absorption is not

---

polarization receivers, magnetic splitting in the E layer had been observed. *See* Proc. I.R.E., vol. 23, pp. 670–882; June, (1935).

mainly below the E layer. The absence of refractions could be explained on a basis of low ion density although such would hardly be expected during the summer midday. The total number of ions formed

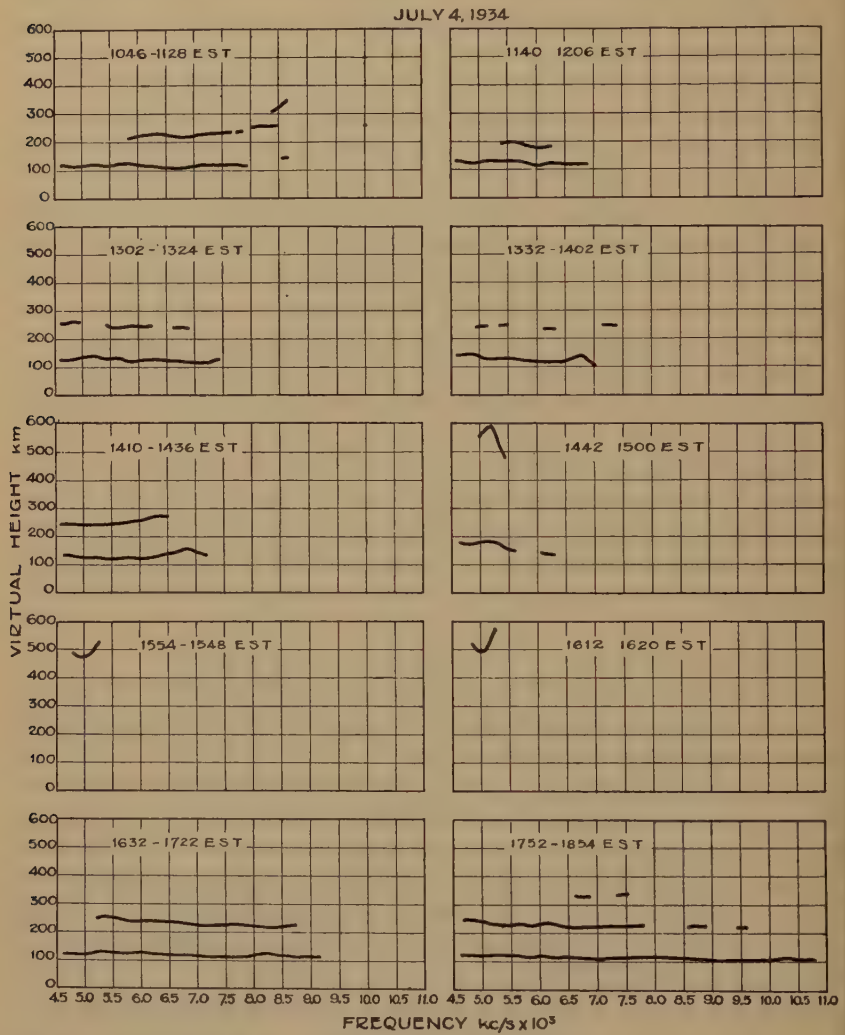

Fig. 5—Curve showing the absence of F-layer refractions and the formation of sporadic E-layer reflections, often experienced during the summer.

by the ionizing agencies, principally solar radiation, at this time might be a maximum and yet the ion density be low because of a thicker layer being formed. Fig. 6 shows the annual variation of the midday f_{F_2}'' which reaches maxima about November 1 and March 1. The

possibility that the F_2 layer loses some of its ionization to the F_1 layer during spring and summer may account for the lower critical frequency during this time. Consequently, high absorption is not needed to explain the absence of refractions from the F_2 layer above 5000 kilocycles during the midsummer day. Whether absorption or low ion density is the cause of the absence of these refractions is a question which remains unanswered.

Diurnal variations of f_{F_2}' (critical frequency of the extraordinary ray for the F_2 layer) are shown in the upper graphs of Figs. 2, 3, and 4. It should be noticed that these are not symmetrical about noon but are displaced toward the afternoon hours and have many irregularities in them. Also it should be noticed that the maximum value of f_{F_2} does not occur necessarily, at midday. f_{F_2} maxima occur at other times, mostly after noon. These maximum f_{F_2} values are also shown in Fig. 6. Furthermore, when no midday F_2 reflections are observed, they often appear after noon.

Fig. 6 shows the annual variation of noon values of f_{F_2}'. Summertime values are uncertain or missing. In the early fall the critical frequency rises until about November 1, then falls to a minimum after midwinter, rises to another maximum in March, and falls again in the spring. It was known from earlier results that f_{F_2} was higher in the winter than in the summer, although the two maxima in November and March were not previously discovered. It is not known that these appear every year but earlier data though not complete would indicate that they probably do.[7]

Experiments indicate that the F_2 critical frequency does not follow closely in phase with the ionizing force of the sun, either diurnally or annually. That the sun has a major influence is shown by the diurnal variation from day to night, f_{F_2}' rising rapidly after sunrise. The diurnal variations might be explained as a lag due to slow ionization and recombination, but the annual variations can hardly be explained on such a basis. From November to March the variations in the critical frequency of the F_2 layer are reasonably consistent with variations of the ionizing force of the sun.

IV. Sporadic E

Frequently, pulses are received with a retardation approximately that of E-layer refractions but for much higher frequencies than those for which E-layer refractions are normally observed. This effect is very common in the summer and is especially so during the summer evenings, although it may occur at any season, particularly in the evening.

[7] Schafer and Goodall[6] reported similar measurements at Deal, New Jersey.

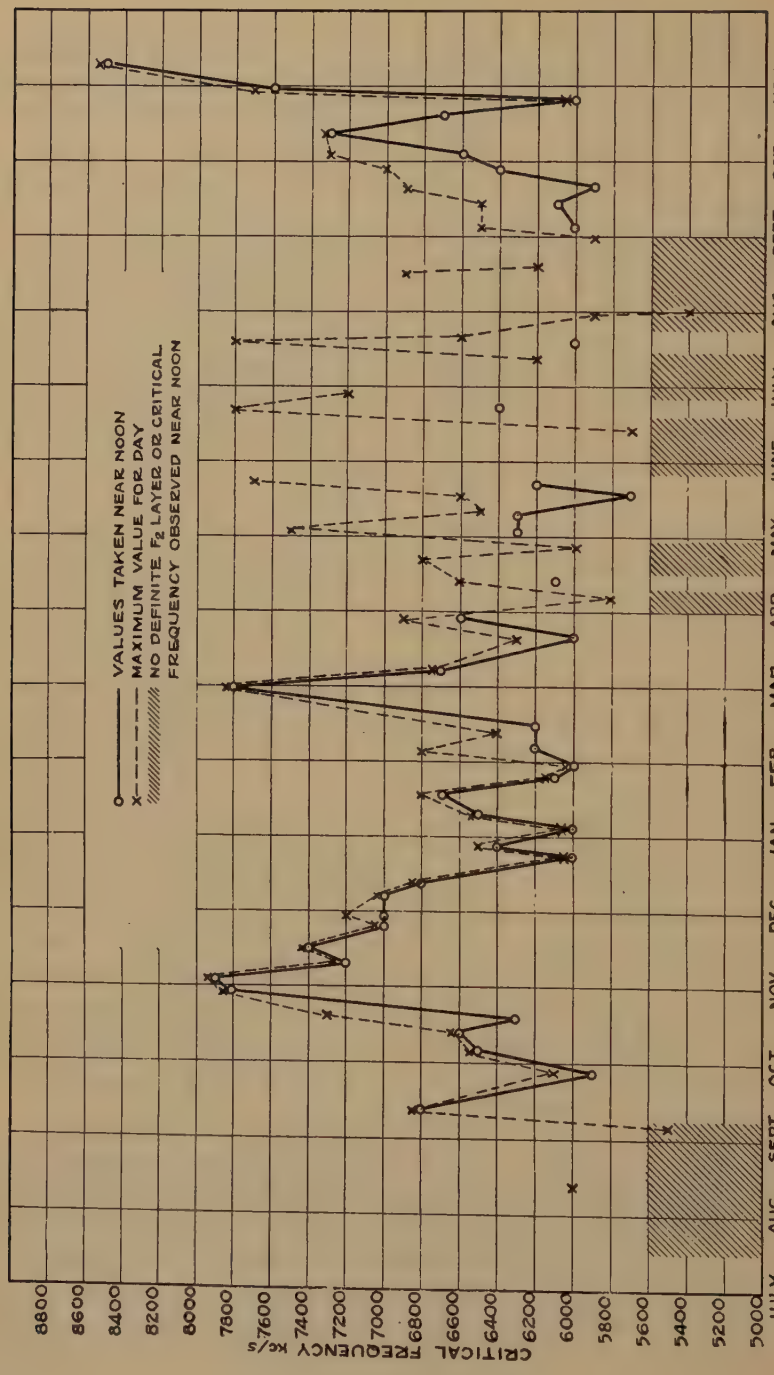

Fig. 6—Seasonal variation of the critical frequency of the extraordinary ray for the F_2 layer at midday, and of the maximum critical frequency obtained for the day.

This effect is believed to be due to reflection from the sharp boundary of the E layer. It has previously been attributed to an increase in ionization brought about at irregular periods by some geophysical phenomenon. The British, in particular, have advanced the view that an abnormal ionization was produced in the E layer by the charge in clouds during a thunderstorm. No correlation between the occurrence of thunderstorms and sporadic E reflection has been found at Washington; even local thunderstorms produce no noticeable effect. These re-

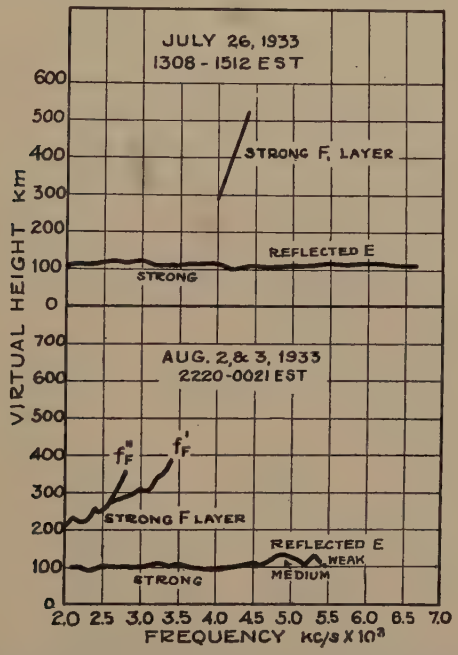

Fig. 7—Typical curves for summer, day and night, showing a strong F layer appearing through sporadic E-layer reflections.

flections have been received at frequencies up to 9400 kilocycles when the Weather Bureau reported no thunderstorms within a radius of 300 kilometers during the 24-hour period. So far no correlation between the occurrence of sporadic E and magnetic storms has been found.

Reasons for believing that the sporadic E is a reflecting rather than a refracting layer are as follows:

1. The E layer normally returns energy to some extent at frequencies far above the E critical frequency. Although these reflections are rather weak and unstable they seem to indicate a more or less sharp boundary.

2. Refractions from the F_1 and F_2 layers are received simultaneously with sporadic E reflections over frequency bands of several thousand kilocycles as is shown in Fig. 7. Refracting layers are not thus transparent except for frequencies above a critical frequency.

3. The disappearance of sporadic E reflections as the frequency is increased is not usually accompanied by a sharp increase in virtual height such as would indicate a critical frequency and such as is shown by the regular refracting layers. The disappearance of the sporadic E is marked by the gradual weakening of the pulses as the frequency is increased until their amplitude falls below the noise level.

4. Such large increases of E-layer ionization at night do not seem likely when the regular E-layer ionization follows so closely in phase with the ionizing force of the sun during the day. The ionization densities required to refract the waves at these frequencies would be six to eight times normal noon values of ionization density.

Table I shows the occurrence of sporadic E reflections during local thunderstorms. Table II shows the occurrence of sporadic E on days

TABLE I

SPORADIC E FOR DAYS ON WHICH LOCAL THUNDERSTORMS OCCURRED

Date 1934	Local thunderstorms		Sporadic E	
	Time of occurrence E.S.T.	Intensity	Time E.S.T.	Upper frequency of occurrence of sporadic E (above 4500 kc/s)
				kc/s
4/4	1200–1500	Moderate	1040–2032	No E reflections
6/6	1200–2200	Moderate	1012–2148	No E reflections
6/27	1430–1530	Severe	0822–1230	8400
			1315–1430	No E reflections
			1430–1524	No data
				Severe static
			1526	4500
			1608	6400
8/15	1500–1600	Severe	1612–1709	8800
			1716–1740	7000
			1758–2206	No E reflections
9/12	1200–1500	Severe	1003–1911	No E reflections
			1906–1927	5000

TABLE II

SPORADIC E FOR DAYS ON WHICH NONLOCAL THUNDERSTORMS OCCURRED WITHIN 100-KILOMETER RADIUS DURING SUMMER OF 1934

Date 1934	Upper frequency of occurrence of sporadic E (above 4500 kc/s)
	kc/s
7–4	10800
7–28	No E reflections
8–1	9200

when nonlocal thunderstorms occurred within a radius of 100 kilometers. The data for nonlocal thunderstorms were taken from the weather maps and other material furnished by the U. S. Weather Bureau. The thunderstorms were given only for the 12-hour periods

0800 to 2000 and 2000 to 0800 E. S. T. and no indication of the intensity was given, some of the storms being indicated by a single clap of thunder. On July 4 the weather was locally fair but one thunderstorm was reported just inside the 100-kilometer radius and another in the 100–200-kilometer zone. No precipitation was indicated so that it might be concluded that these were very minor storms. At about 1900 E.S.T. on the evening of July 4 sporadic E was found up to 10,800 kilocycles the highest so far recorded. This is shown in Fig. 5. Therefore close correlations in time between the occurrence of distant thunderstorms and sporadic E were not always possible. In the case of local thunderstorms, however, the time of occurrence was observed by us, and a fair estimate of the electrical intensity of the storm was also obtained. Therefore, if there is a correlation between the occurrence of thunderstorms and sporadic E, this correlation should be more positive for the case of local thunderstorms than for the thunderstorm data taken from the weather maps.

TABLE III

SPORADIC E FOR DAYS ON WHICH NO THUNDERSTORMS OCCURRED WITHIN 300 KILOMETER RADIUS DURING SUMMER OF 1934

Date 1934	Upper frequency of occurrence of sporadic E (above 4500 kc/s)
	kc/s
4–18	No E reflections
5–2	No E reflections
5–9	No E reflections
5–16	No E reflections
6–13	7000
6–20	7800
7–11	8000
7–18	6800
8–8	9200
8–22	No E reflections
8–29	7500

Table III shows the occurrence of sporadic E during the days on which no thunderstorms occurred within a radius of 300 kilometers of Washington. The above data fail to indicate a direct correlation between thunderstorms and sporadic E. Sporadic E is just about as prevalent on days when there are no thunderstorms within 300 kilometers as when there are severe local thunderstorms. Both phenomena are at a maximum during the summer months, and this fact in itself suggests a correlation but when the occurrences of thunderstorms and sporadic E are compared in more detail the correlation fails.

Another phenomenon believed to be a manifestation of the sporadic E layer occurred frequently during the early evening of the fall and sometimes winter on the frequency band 1600 to 2500 kilocycles. This is illustrated by Figs. 8 and 9 for October 6, 1933, and January 3, 1934. The E-layer critical frequency was observed to drop below 1600 kilocycles (Fig. 8, (a), (b), (c)) before sunset. E-layer reflections accom-

panied by strong F-layer refractions sometimes remained at frequencies above f_E as shown in Fig. 8. Later in the evening the E reflections became stronger, and still later they weakened as in (f) and later disappeared. There usually was little question but that the second

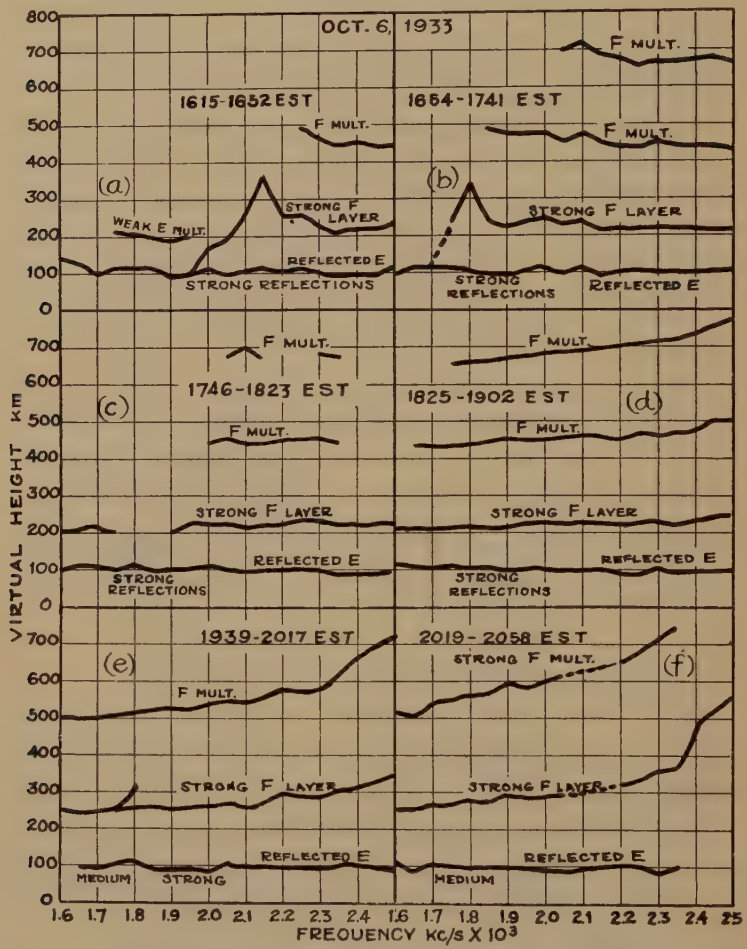

Fig. 8—Typical fall curve showing simultaneous appearance of F refractions and sporadic E-layer reflections after the normal E-layer critical had passed.

reflection was from the F layer rather than an E multiple. The second reflection was frequently stronger than the first E thus indicating that it was not a multiple of the first. The most prominent higher multiples were properly spaced to be multiples of the second reflection rather than the first. Also the F criticals sometimes appeared even while the

E reflections were still present, (e), (f), but no critical was found for the lower reflections.

More frequently as f_E decreased during the early evening the E reflections became very weak or disappeared as shown in Fig. 8 (a),

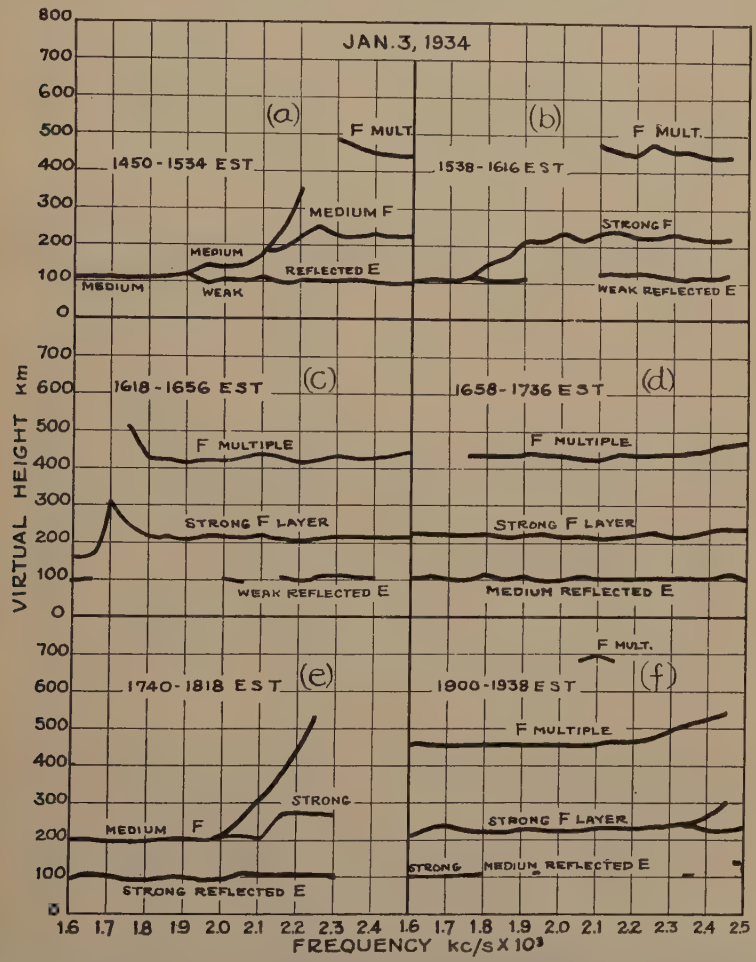

Fig. 9—Typical winter curve showing simultaneous appearance of F refractions and sporadic E-layer reflections after the normal E-layer critical had passed.

(b), (c). Later in the evening these E reflections became strong, (c), (d), while strong F layer refractions with multiples continued to come in, (d), (e). Usually except during the summer the sporadic E disappeared from this frequenty band later in the evening by a gradually weakening process and without showing a pronounced rise in virtual height such as indicates a critical frequency as shown in (f).

Somewhat similar results have been observed in the broadcast band during the early morning hours following 0200 E.S.T. E and F layers are frequently received simultaneously; no E critical frequencies were found and the disappearance of the E-layer reflections was marked by a gradual weakening rather than a critical and a sharp cut-off. It is believed that during much of the time at night E reflections at broadcast frequencies are manifestations of the sporadic E, and the E critical f_E if it exists is frequently at a frequency lower than 600 kilocycles. Fig. 10 shows a typical night run of this kind.

V. G and Higher Layers[8]

The F_2 layer is not very evident during the summer midday. One or two hours before sunset refractions from this layer attain moderate

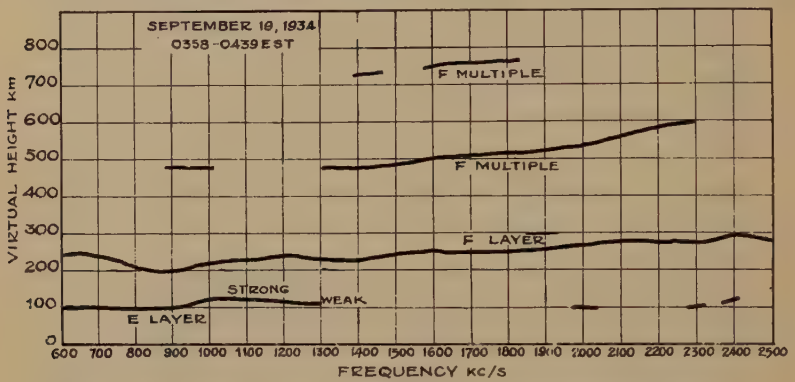

Fig. 10—Typical curve of sweep through the broadcast range of frequencies during the night.

intensity and the critical frequencies can be followed during the summer. At about the time of sunset or a little later, reflections of medium intensity suddenly appeared from a virtual height as great or greater than the F_2-layer virtual height and at frequencies higher than F_2 at any other time. During the earlier observations it was believed that the F_2-layer ionization increased rapidly to high values at these times. However, recent observations indicate that this phenomenon is produced by another higher layer which is either found about this time or more likely uncovered by lower absorbing layers at the approach of

[8] Reflections from heights greater than the F_2 region were reported in reference (1). In that paper, it was stated that such reflections might be phenomenon described by Taylor and Young, Proc. I.R.E., vol. 16, p. 561; May, (1928); vol. 17, p. 1491; September, (1929). The designation of certain of the reflections involving a G layer was first announced in the reading of the present paper at the May, 1934, Convention of the Institute of Radio Engineers, and the abstract published in vol. 22, p. 548; May, (1934). In a letter to *Nature* (London), vol. 134, p. 63; July 14, (1934), H. R. Mimno reported evidences of the existence of the G and higher layers.

sunset. We have tentatively called this the G layer. Fig. 11 shows six sweeps taken in the succession indicated by the lettering, on the evening of August 1, 1934. (a) and (b) show the F_2 critical frequency decreasing with advancing time; (b) shows the formation of the G layer;

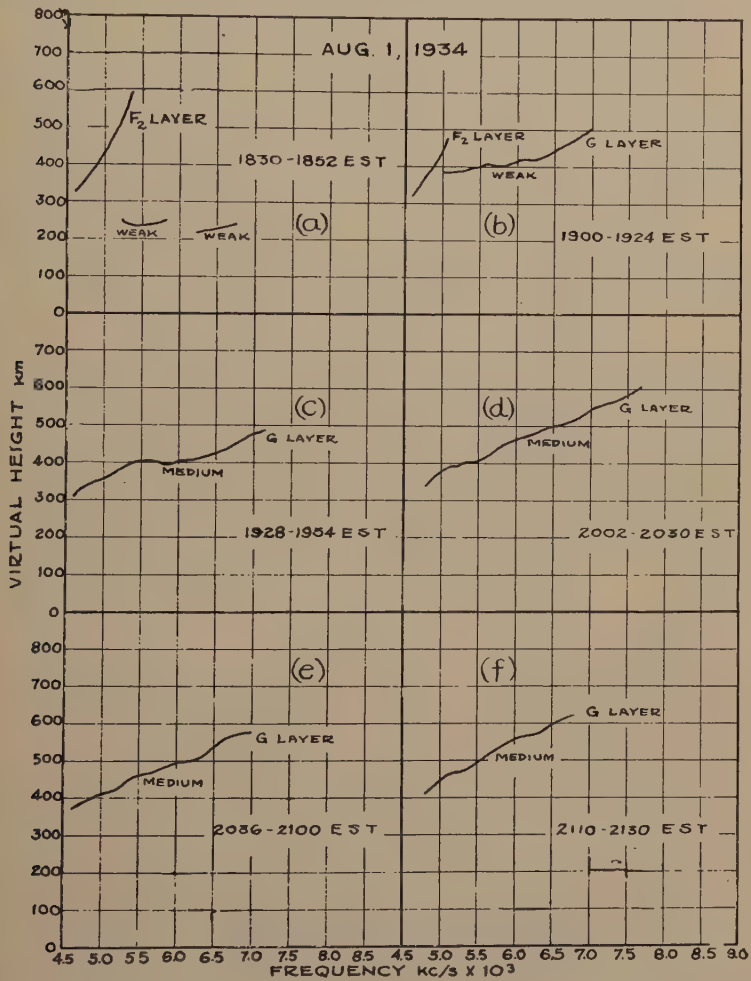

Fig. 11.—Curve showing formation of the G layer during a summer evening.

(c), (d), (e), and (f) show only the G layer remaining. The G-layer reflections were of medium amplitude. The virtual height increased with frequency in a peculiar manner. No critical frequencies and no magnetic double refraction were observed. The reflections at higher frequencies gradually became weaker and were finally lost in the noise. The effect shown in Fig. 11 occurs on summer evenings.

An additional effect which has been found at other seasons during both day and night [1] is shown in Fig. 12 for November 10, 1933. Complex reflections are returned from great virtual heights at frequencies above the F_2 critical frequencies. The virtual height vs. frequency

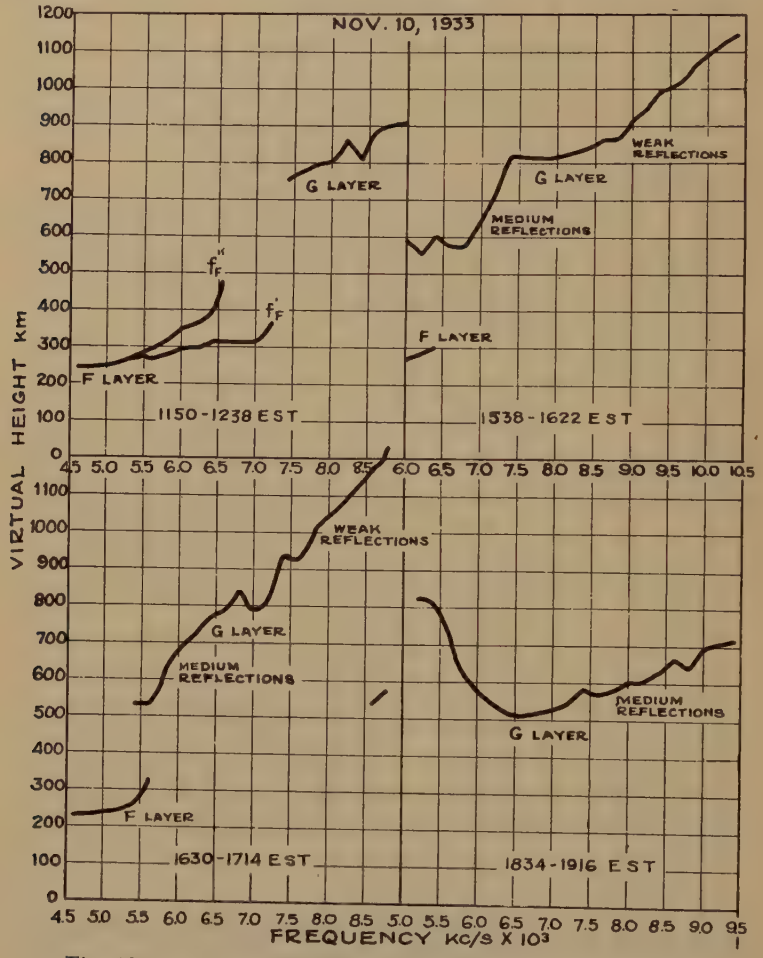

Fig. 12—Curve showing G-layer reflections for a winter day.

graphs have the characteristic slope found for the G layer during the summer evening and these reflections were probably from the same layer. The reflections shown in Fig. 12 were usually weaker than those of Fig. 11 and were complex so that even if they were present during the summer they would be more likely to be lost in the higher noise background.

VI. Conclusions

The variation of the normal E-layer critical frequency during the daytime was found to be approximately in accordance with the equation

$$f_E \approx (\cos \psi)^{1/4}.$$

Magneto-ionic splitting was not observed in this layer. These results indicated a rapid recombination and a layer of heavy ions.

The diurnal variation of F_2-layer critical frequency did not follow the above equation but in general lagged behind the variations of the ionizing force of the sun. Magnetic double refraction usually occurred. These results indicated a slower rate of recombination and a layer effectively of electrons.

The local noon maximum F_2 critical frequencies occurred in November and March. F_2 critical frequencies frequently could not be obtained near noon during the summer.

The data indicate the sporadic E layer returns the wave to earth by reflection at a sharp boundary rather than by refraction. This layer is frequently semitransparent and shows no critical frequencies. Most of the nighttime E layer observed is of this nature. It is common at much higher frequencies during the summer than during the winter.

G-layer reflections were observed at frequencies above the F_2 critical frequencies, especially during the summer evenings but also during the fall evenings.

Proceedings of the Institute of Radio Engineers
Volume 23, Number 7 *July, 1935*

ANALYSIS OF THE OPERATION OF VACUUM TUBES AS CLASS C AMPLIFIERS*

By

I. E. Mouromtseff and H. N. Kozanowski

(Westinghouse Electric and Manufacturing Company, East Pittsburgh, Pa.)

Summary *—The operation of class C amplifiers under carrier and modulated conditions is analyzed with the aid of constant-current charts. With these charts one can precalculate all operating factors such as output, efficiency, and grid driving power. The analysis discloses certain fundamental differences in the behavior of modulated amplifiers connected with self-bias and fixed, or generator bias operation. Audio harmonic distortion traceable directly to the amplifier is discussed in detail, together with methods for "compensating" the grid excitation to eliminate this distortion and to increase the operating efficiency. Oscillograms of the audio relations in modulated class C amplifiers experimentally verify the theoretical conclusions. The problems of grid excitation power, "true" grid dissipation, and "effective" plate dissipation for modulated amplifiers are treated for three tubes differing only in their amplification factors.*

BROADCAST transmitters in which vacuum tubes are used in the output stage as class C amplifiers, in combination with class B plate modulators,[1] because of their high over-all efficiency, are particularly suitable for high power installations.

Historically, class C amplifiers have evolved from the classical self-oscillator as frequency stability became a paramount requirement for broadcast transmitters. In both cases plate modulation was effected by means of very inefficient class A audio amplifiers. The necessity of using too great a number of modulator tubes augmented by the practical impossibility of the application of more than sixty or seventy per cent modulation subsequently forced radio engineers to give preference to the class B radio amplifier scheme. Here, modulation is applied to one of the earlier stages of power amplification and the output stage has only to reproduce faithfully the modulated wave. This scheme soon became standard in designing larger transmitters although the efficiency of the output stage for an average depth of modulation is in this case relatively low.

Quite recently, the advance in the art of designing high power audio transformers[2] made possible the application of high efficiency class B audio modulators and also permitted the realization of 100 per cent modulation in class C transmitters. As a consequence the latter have

* Decimal classification: R132. Original manuscript received by the Institute, March 21, 1935. Presented before Tenth Annual Convention, Detroit, Mich., July 2, (1935).

[1] J. A. Hutcheson, Proc. I.R.E., vol. 21, p. 944; July, (1933).

[2] J. A. Chambers, et al., Proc. I.R.E., vol. 22, p. 1158; October, (1934).

reappeared in the limelight. Therefore, a thorough study of this mode of operation of vacuum tubes has acquired a new importance as shown by numerous technical papers of recent times. The necessity of such a study is further emphasized by these two facts: (1) With the ever-increasing size of transmitters the economic side of operation begins to play a prominent rôle; hence, a thorough investigation of the actual limitations of transmitting tubes is highly desirable; (2) high modulation, up to 100 per cent, and occasional overmodulation bring about complications in tube performance which must be fully recognized both by the designer of transmitters and the tube engineer.

Problems Outlined

In this analysis, the first problem to be solved is: By what means can one accurately precalculate output power, efficiency, grid excitation power—in a word, all necesssary data for any assumed operating condition of a tube used as a class C amplifier?

The second problem is the application of the adopted method to a 100 per cent modulated amplifier with the purpose of investigating tube behavior during the entire audio modulation cycle.

Finally, the third problem involves the consideration of means and methods by which some inherent weak points of modulated class C operation can be improved.

During the investigation one must keep in mind that, by definition, the basic characteristic feature of a class C amplifier is the application of such a high negative bias that electronic current to the plate is allowed to flow during only a fraction of the half cycle corresponding to the positive grid swing. This enables the tube to deliver into the oscillating circuit large high-frequency power at high efficiency. The narrower the angle of the plate current the greater is the efficiency, all other conditions being the same. In this respect class C amplifiers and self-oscillators are alike. The main difference between a class C amplifier and a self-oscillator is in the grid excitation: *it is constant with the class C amplifier and strictly proportional to the radio-frequency plate voltage with the self-oscillator.*

Choice of Methods for Precalculation of Class C Performance

By virtue of the very character of class C operation the performance of a tube can be predicted accurately only in the case when one possesses a complete knowledge of tube characteristics, up to the highest feasible values of plate and grid currents. Unfortunately, no simple analytical expression is apt to supply this information. Thus, the basic 3/2-power law for static characteristics is valid only over a

very limited portion of the current-voltage curves; it does not hold either for very low plate currents, or for currents greater than half of the value of the available filament emission where saturation effects come to light. Yet, the greatest handicap in applying analytical methods to class C amplifiers is connected with the region of "quasi saturation" at high positive grid potentials: there, grid current becomes prominent, and the plate-current wave highly flattened, or even saddled-in. But just this region is the most interesting with class C amplifiers if high outputs and efficiencies are to be secured from the tube. In addition, one may point out that the region of reversed grid current, which is even harder to handle analytically, must also be explored if an exhaustive study of class C performance is to be considered.

In short, in the absence of a complete chart of tube characterists, one certainly is forced to look for suitable, even if approximate, analytical methods for precalculation of class C operation. But if such charts are available, results can be obtained more easily and accurately by a graphical treatment of this problem. A graphical method can be applied to any region of tube characteristics without restriction; it is independent of the shape of static characteristics. In addition, by a mere glance at a chart, one can better define tube limitations and preview the influence of various factors on tube operation.

Graphical Method for Studying Class C Performance

Dynamic characteristics for any mode of operation can be plotted on complete charts of the conventional type in which plate current is given as a function either of plate potential with grid voltage as parameter, or vice versa. However, in studying class C performance it proves to be much more convenient to employ different types of charts, occasionally mentioned in technical literature, but apparently seldom, if ever, used in engineering practice. These are *constant-current charts* with plate and grid potentials plotted on the two coördinate axes, respectively. These charts contain two families of curves, each curve drawn either for a constant plate, or a constant grid current (Fig. 1). The advantages of such a representation are evident:

(1) Plate and grid characteristics are conveniently combined in the same chart, in spite of the substantial difference in the magnitude of the two quantities.

(2) The operating point, for example, A, is *definitely located* on the chart as function of the operating direct plate voltage, E_p, and grid bias, e_c; this is not the case with any conventional chart.

(3) Every dynamic characteristic for class C operation is represented by *a straight line*, such as AB; this is true since the variation of both plate and grid potentials during oscillation can be considered synchronous and sinusoidal.

It may be noted in passing that for the same reason dynamic characteristics for class B and class A radio-frequency amplifiers are also represented in the adopted charts by straight lines. Therefore, the method which is outlined here is also applicable to these cases.

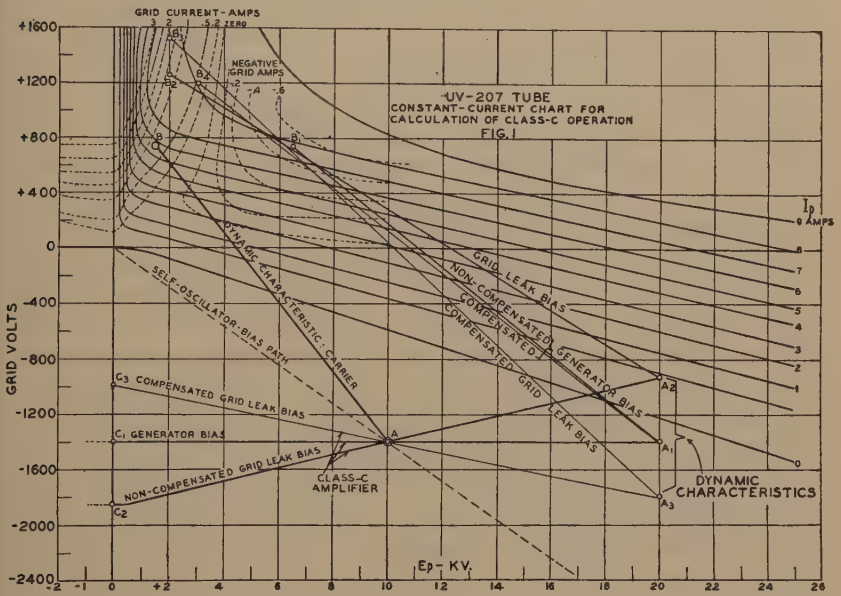

Fig. 1

Application of the Constant-Current Charts to the Calculation of Carrier Performance

The chart shown in Fig. 1 belongs to an individual tube of the UV-207 type having μ equal to 20. The chart has been prepared by the oscillographic method.[3] It may be noted that the inverted slope of the constant plate-current curve at any point of this chart gives the measure of the amplification factor, μ. This follows directly from the definition, $\mu = dE_p/dE_g$.

In order to describe better the method of application of the constant-current charts we shall proceed with the calculation of performance of the UV-207 tube for an arbitrarily chosen operating condition.

[3] H. N. Kozanowski and I. E. Mouromtseff, Proc. I.R.E., vol. 21, p. 1082; August, (1933).

Suppose the operating point is given by the direct plate voltage, $E_p = 10{,}000$ volts, and grid bias, $e_c = -1400$ volts. Let us assume that during oscillation the plate voltage on its downward swing reaches a minimum, $E_{\min} = 1500$ volts, so that the voltage amplitude is $E_0 = E_p - E_{\min}$ or 8500 volts. Let us further assume that grid excitation is such that maximum positive grid potential during oscillation reaches the value, $e_{\max} = +740$ volts. The grid voltage amplitude is then $e_0 = -e_c + e_{\max} = 2140$ volts. We draw a straight line AB through the operating point A and the end point of the operating characteristic B with coördinates $E_{\min} = 1500$ and $e_{\max} = +740$ volts. From this straight line dynamic characteristic we can easily plot a plate-current time curve by computing the electric angles corresponding to each point of intersection of the dynamic line with the individual plate-current curves. The values of electrical angles, which are proportional to time, will be obtained from the ratios of instantaneous plate voltages at each point found in the chart to the chosen amplitude, E_0, these ratios being sines of the respective angles. By virtue of the symmetry of the current-time curve with respect to its mid-ordinate, only one half of the actual curve is needed for calculation (Fig. 2). The current-time curve averaged over the entire cycle gives the value of the average or direct plate current, $I = 1.11$ amperes. This result is conveniently obtained from Fig. 2 by dividing the area of the time curve into nine narrow strips, each ten electrical degrees wide, measuring of the middle ordinates of each strip, summing up the middle ordinates and dividing the sum by $2 \times 9 = 18$; the factor 2 is necessary for averaging over the entire radio-frequency cycle.

Power output, P_0, can be determined graphically on the basis of the expression

$$P_0 = \frac{1}{2n} \sum_{n=1}^{n=9} i_n E_0 \sin \phi_n = \frac{E_0}{2n} \sum_{1}^{9} i_n \sin \phi_n \qquad (1)$$

where i_n is the instantaneous value of plate current in the middle of each strip, and E_0 is the plate voltage amplitude. Hence, multiplication of the measured middle ordinates of the strips by their respective sines summing the products, a further multiplication of the sum by the value of radio-frequency voltage amplitude, 8500 volts, and averaging of the result over the entire cycle by dividing by 18, will yield us the value of power output $P_0 = 8.5$ kilowatts. The plate input power and efficiency can be computed from $P_i = E_p I_p$ and $\eta = P_0/P_i$. They are: $P_i = 11.1$ kilowatts and $\eta = 77$ per cent, respectively. The entire calculation is tabulated in the table of Fig. 2.

Knowing E_0 and P_0 one can compute the value of the effective load resistance, R_L, which is to be connected across the tube on the output side from the expression

$$R_L = E_0^2/2P_0 = 4250 \text{ ohms.} \qquad (2)$$

Proceeding in a similar manner with the grid-current time curve (Fig. 2) we shall find

Average grid current, $I_g = 57$ milliamperes

Grid input power, $p_{gi} = 120$ watts

Bias loss, $p_c = 80$ watts

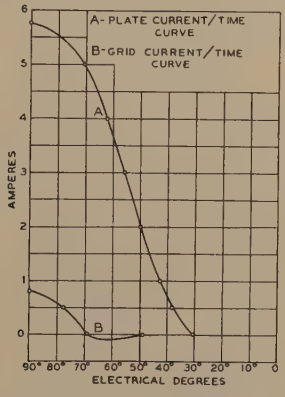

Values of Mid-Ordinates

5.87 amperes	×0.996	which is sin 85°	=5.65
5.27	.966	sin 75°	5.08
4.37	.906	sin 65°	3.96
2.87	.819	sin 55°	2.35
1.32	.707	sin 45°	0.93
0.28	.573	sin 35°	0.16
19.98			18.13

$I_p = 19.98/18 = 1.11$ amperes

$P_0 = 18.13/18 \times 8.5$ kilovolts $= 8.5$ kilowatts

$P_i = 11.1$ kilowatts

$\eta = 77$ per cent

Fig. 2

The power loss, p_{gh}, converted into heat in the grid itself might, at first thought, be calculated as the difference between the total grid input and the bias loss, $p_{gi} - p_c$. In reality, it can be shown that, generally

$$p_{gh} \gg p_{gi} - p_c.$$

However, we shall postpone the discussion of this statement to a later section.

It may be noted that the whole outlined procedure can be greatly helped by using a simple instrument, the *sine scale*, described elsewhere.[4]

Modulated Class C Operation

Choice of Carrier Conditions

In all practical cases, one may consider that the direct plate voltage, grid bias, and carrier output per tube are prescribed by the general design of a transmitter, in which the economic side plays no small part. Just for this reason, tubes are not always operated at their best ratings. Thus, for instance, the choice of the bias is often governed by the desire of reducing to a minimum the size and cost of the excitation stage and bias supply; thus, the use of sufficiently high biases required by ideal class C operation is precluded. Also, there is always a tendency to boost power output per tube in order to reduce as far as possible the number of tubes employed. In our further discussion we shall consider an actual case of a transmitter, with several UV-207 tubes in the output stage, operated as 100 per cent plate modulated class C amplifier with an output of 8.5 kilowatts per tube. This is somewhat in excess of the conservative tube rating, but through such a choice of a practical example some interesting facts regarding class C operation and its limitations will come to light more conspicuously.

With the assumption of $E_p = 10{,}000$ volts and $e_c = -1400$ volts the operating point in Fig. 1 is fixed at point A. We shall temporarily omit any consideration of the manner in which the bias is supplied. Now, we have to decide what grid excitation must be applied to the tube in order to obtain the desired output. For this, we shall first explore the variation of power output physically obtainable from the tube along several vertical lines in the chart, corresponding to $E_{min} = 1000$, 1500, 2000 volts, and so on. In each case we assume e_{max} equal in turn to +400, +800, +1000, and +1200 volts. For every combination of E_{min} and e_{max} we plot a straight line dynamic characteristic and proceed with calculation of all necessary quantities in the manner outlined in the previous section. Four points for each vertical line are in this case sufficient for shaping a smooth curve representing output power as a function of grid excitation for any assumed E_{min}. The calculated curves are plotted in Fig. 3. One can notice that:

(1) For low and medium grid excitation, all curves almost coincide.

(2) With higher grid excitation, there is an optimum for power output, at $E_{min} = 1500$ volts; below and above this value of E_{min}, power output decreases for any given grid excitation.

---

[4] This sine scale consists of a celluloid right-angled triangle on which are scribed slant lines corresponding to five-degree angle intervals from zero to ninety degrees. Any angle to be used in plotting the current-time curve can be read directly from the triangle. A detailed description of this scale is to be published in the *Electric Journal*.

(3) For higher grid excitation with the potential swinging to somewhat above +1200 volts, the output curves flatten and may even sink due to quasi saturation, which one may designate as grid saturation.

(4) Throughout the explored region, the output of 8.5 kilowatts can be obtained only with positive peak grid voltages definitely fixed within very narrow limits in the vicinity of 740 volts irrespective of the minimum plate voltage reached during oscillation.

Of course, for the realization of any particular value of $E_{min} = E_p - E_0$ the load resistance, R_L, must be appropriately chosen, as follows from equation (2). In each case the efficiency, η per cent, and average plate and grid currents will be different: the lower is E_{min}, the higher is

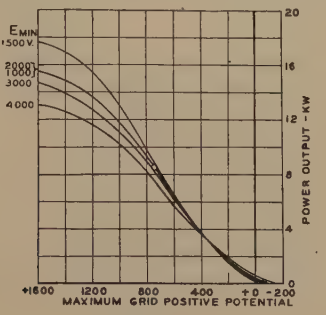

Fig. 3

the efficiency, and the lower the average plate current, but the higher is the average grid current. All this can be qualitatively foreseen from the direct plots of the dynamic characteristics in the chart. A compromise choice of the carrier condition will correspond to good efficiency and not too excessive grid excitation power. For our further discussion we shall choose $E_{min} = 1500$ volts, for which everything has been calculated in the above numerical example.

Tube Behavior During Modulation

With 100 per cent modulation applied to the plate of the tube, the average or input plate voltage swings at audio frequency down to zero and up to twice the original carrier voltage. With this, the output power varies down to zero and up to a certain maximum. In an ideal class C amplifier the maximum power is expected to be exactly four times the carrier output. Yet, as a rule, this never happens. The results of the present graphical investigation and of an oscillographic study corroborate the fact that even with a strictly sinusoidal modulation wave applied to the plate of a tube the output wave in a great many cases is distorted. This is not necessarily due to the lack of fila-

ment emission: it is inherent in the tube characteristics and may occur even with a large margin of electron emission left unused. It will be more clearly understood in the course of the analysis of the two following specific cases.

Case 1: Bias is Supplied by a Generator

At the crest of modulation in our numerical example the operating point in Fig. 1 will be at A_1 with $E_p = 20{,}000$ volts and $e_c = -1400$ volts. First, we shall calculate the output power for several dynamic characteristics plotted through the operating point and terminating on the horizontal line corresponding to the assumed grid excitation with $e_{max} = +740$ volts. Generally, for each of these dynamic lines the output power will have a different value. Then, in order to decide which line

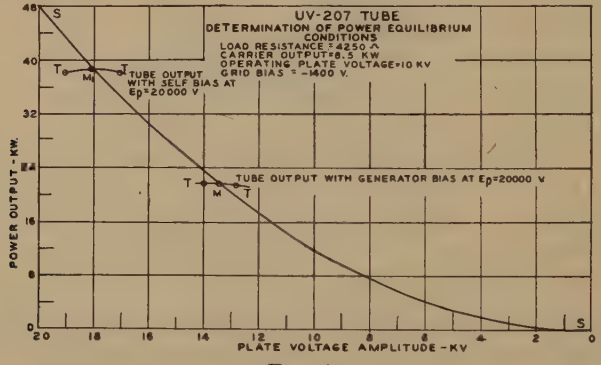
UV-207 TUBE
DETERMINATION OF POWER EQUILIBRIUM CONDITIONS
LOAD RESISTANCE = 4250 Λ
CARRIER OUTPUT = 8.5 KW
OPERATING PLATE VOLTAGE = 10 KV
GRID BIAS = -1400 V.
TUBE OUTPUT WITH SELF BIAS AT Ep=20000 V
TUBE OUTPUT WITH GENERATOR BIAS AT Ep=20000 V
S
T
M
POWER OUTPUT - KW.
PLATE VOLTAGE AMPLITUDE - KV

Fig. 4

will be followed in actual tube operation, we must keep in mind that the power output calculated for any dynamic characteristic is the output which the tube is able to supply when the correct load resistance, different for each line, is connected across the tube (see equation (1)). But in the present case one has to consider the resistance, R_L, *which has already been chosen in the adjustment of carrier conditions.* Therefore, we may proceed in the following manner.

Fig. 4 contains a curve, SS, showing amount of power which is consumed in the resistance, $R_L = 4250$ ohms, at different values of radio-frequency voltage amplitude, from zero to 20,000 volts, across the resistance. In the same drawing, another curve, TT, is plotted connecting several calculated points giving the power which *the tube is able to deliver* into the resistance correctly matched for each value of radio-frequency plate voltage. Hence, the intersection of the two curves at point M with $E_{min} = 6500$ volts indicates the dynamic characteristic along which the equilibrium between power delivered into the oscillat-

ing circuit and the power consumed in the load is established. Therefore, point M gives the only possible operating conditions for stable performance of the tube. The corresponding dynamic characteristic A_1B_1 is plotted in Fig. 1.

The calculation for this line yields the following figures:

Output power	$P_0 = 21.75$ kilowatts
Input power	$P_i = 37.1$ kilowatts
Efficiency	$\eta = 58.8$ per cent
Plate dissipation	$P_h = 15.35$ kilowatts
Direct grid current	$I_c = -100$ milliamperes

At a glance, one can notice the following shortcomings of such an operation:

(1) Power output at the crest of modulation instead of being 34 kilowatts as required for distortionless modulation, is only 21.75 kilowatts. This produces a strong second harmonic component in the output wave, approximately 10 per cent in magnitude.

(2) Efficiency at the crest of modulation drops enormously, from 77 to 58.8 per cent, thus minimizing the main advantage of class C operation.

(3) Plate dissipation increases disproportionately; in ideal class C operation it should not exceed four times the carrier loss, or 12 kilowatts. Although unfavorably affecting the average over an audio cycle the calculated dissipation, 15.35 kilowatts does not appear too excessive *per se* since it shows the plate dissipation only at the positive crest of an audio cycle; yet, one will note that the dynamic characteristic at this condition runs decidedly through the negative grid region. Under these circumstances, the "effective" plate dissipation is much higher than calculated and eventually may cause the cooling water to boil although the actually measured average loss does not exceed the rated 10 kilowatts. The discussion of the "effective" plate dissipation will be the subject of one of the later sections.

(4) The high negative average of direct grid current is due to the strongly emphasized portion of reversed grid current in the grid-current time curve. With this, the grid may easily become a generator of parasitic oscillations.

The enumerated defects of operation at or near the crest of audio modulation become greatly emphasized when over modulation is occasionally allowed to occur. For example, with 20 per cent overmodulation, which not so infrequently happens in real operation, the maximum effective plate dissipation in our case becomes 40 kilowatts; with this the average dissipation becomes quite prohibitive.

The above calculations and deductions are corroborated by an oscillographic study. Fig. 5 contains oscillographic records of the audio-frequency envelopes for grid current, plate current, and rectified radio-frequency current of the output wave, all taken simultaneously with sixty-cycle modulation of 100 per cent applied to the plate of a UV-207 tube operated under conditions similar to those of the above numerical example. Without paying attention, at this time, to the record at the extreme right, one can notice that the plate current on the positive swing of modulation distinctly exceeds its theoretical two-times-carrier value; at the same time, the output current is less than twice its carrier value. This is interpreted to mean that there is a "shortage" in output and that the efficiency is poorer at the crest of modulation than is appropriate for ideal class C operation. The phenomenon becomes intensified with reduced filament voltage and hence may become of more consequence when one considers worn-out tubes approaching the end of their career.

Another critical point in operation to be considered is the trough of audio modulation when the plate voltage becomes zero. Power input and output at this moment are both zero. Yet, it is obvious that with fixed grid excitation the grid current rises at this point to a very high value. Calculation gives the following figures:

Average grid current $I_c = 485$ milliamperes
Average input power $p_{gi} = 1000$ watts
Bias loss $p_c = 675$ watts.

Case 2: Operation with Self-Bias

In order to reproduce exactly carrier conditions adopted in the previous discussion one must choose the proper value of grid-leak resistance so that the following relation is fulfilled:

$$R_g = e_c/I_c. \tag{3}$$

With an average grid current of 57 millamperes in our case and $e_c = -1400$ volts, R_g must be 24,600 ohms.

With modulation applied, a self-biased tube behaves in a manner entirely different from a tube operated with generator bias. Indeed, with grid-leak bias there is no way to keep bias constant because the variation of average grid current during modulation is beyond our control. One may point out that in contrast to the case of a self-oscillator, the grid current and hence the grid bias of a class C amplifier during modulation *always decreases with increasing plate voltage, and vice versa.* This conclusion can be reached by a simple inspection of the chart of Fig. 1. Indeed, at higher voltages, dynamic characteristics are necessarily shifted toward and into the region of reversed grid currents

which brings down the average grid current and bias. Graphical calculation as well as oscillographic recording confirm this.

The actual value of grid current and bias at every particular instant of the modulation cycle depends on the actual position of the dynamic characteristic; its exact location is forcibly established by the simultaneous fulfilment of *two equilibrium conditions:* (1) The average grid current calculated along any dynamic characteristic plotted in the chart multiplied by the value of the adopted grid-leak resistance must be exactly equal to the bias assumed in plotting; and (2) as pointed out before, the tube output along the same dynamic characteristic must be balanced by the power consumed in the load resistance. One must keep in mind that both the grid-leak and the load resistances have been originally established by the carrier condition. The actual location of the dynamic characteristic at the crest of modulation for our numerical example is given in Fig. 1 as the line A_2B_2. In the same chart, the path AA_2AC_2A is also plotted, along which the operating point travels back and forth when 100 per cent modulation is applied to the carrier.

The inherent variation of self-bias in a certain sense constitutes self-adjustment of the tube. Thus, due to the lower bias at higher plate voltages the grid, being excited with the constant radio-frequency voltage, swings to higher positive potentials. Therefore, the power output at the crest of modulation is greater than in operation with generator bias. In fact, the output power can even exceed the "four-times-carrier" value with a resulting "negative" second harmonic component in the output wave. However, such self-adjustment is not without its drawbacks. These can be discussed more concisely after a glance at the following results of calculation:

Average plate current, I_p	2.82 amperes
Output power, P_0	38.8 kilowatts
Input power, P_i	56.4 kilowatts
Plate dissipation, P_h	17.6 kilowatts
Efficiency, η	69 per cent
Direct grid current, I_c	40 milliamperes
Grid bias, e_c	−930 volts
Grid excitation power, p_{gi}	85 watts
Grid bias dissipation, p_c	36 watts

This calculation actually confirms the statement that the output in this case is greater than the 34 kilowatts required for distortionless modulation. The ensuing second harmonic component amounts to 3.4 per cent. Then, efficiency, though higher than with generator bias, still is much lower than in the initial condition of the carrier. Yet, the most

important fact revealed by the calculation is the disproportionate increase in power input and in plate dissipation. This is a direct consequence of the loss of bias, which has dropped from −1400 to −930 volts. By going back to the chart of Fig. 1 one can perceive that the operating point at high modulation trespasses the zero plate-current line so that the tube ceases to be a class C amplifier: it shifts through the class B condition into nearly class A operation. Thus, in contradiction to the basic conception of class C operation, the current angle grows larger than 180 degrees; in our case it reaches 220 degrees. Hence, plate current flows at high instantaneous voltages and high negative grid potentials. As a result, due to the focusing action of the grid on the electron current to the plate, the "effective" plate dissipation increases more rapidly than the computed loss.

With heavy overmodulation the situation grows more serious in every respect: the bias drops further, input increases, the efficiency decreases so that finally the tube may run away. But even prior to such an extreme condition, the effective plate dissipation may reach quite a prohibitive value, causing the tube to boil; in our example, for instance, with 20 per cent overmodulation the effective plate dissipation at the highest point reaches a figure close to 50 kilowatts. In such a circumstance the electrons impinge on the plate at high instantaneous plate potentials so that X-rays may be generated abundantly within the tube. All such factors may contribute to the production of flashbacks, a very bothersome phenomenon in the operation of high power tubes.

At the negative swing of the plate modulation voltage bias self-adjustment becomes rather a beneficial factor in the respect that a heavier grid current builds up a higher bias, thus automatically preventing the radio-frequency potential from reaching as high positive grid values as in the case of the bias generator. Hence, lower grid current and grid excitation power ensue. The results of graphical calculation of the explored case are:

Average grid current, I_c	74 milliamperes
Grid bias, e_c	−1850 volts
Grid excitation power, p_{gi}	158 watts
Grid bias dissipation, p_c	136 watts

All conclusions regarding the operation of a self-biased class C amplifier, derived from the foregoing graphical calculation were also confirmed by oscillographic recording. A few typical records pertaining to this case are shown in Fig. 6. Temporarily, we shall again leave out of consideration the curves on the extreme right. In the records of the

first panel on the left, the output wave of a 100 per cent modulated tube with self-bias, the wave is designated as "output," proves to be

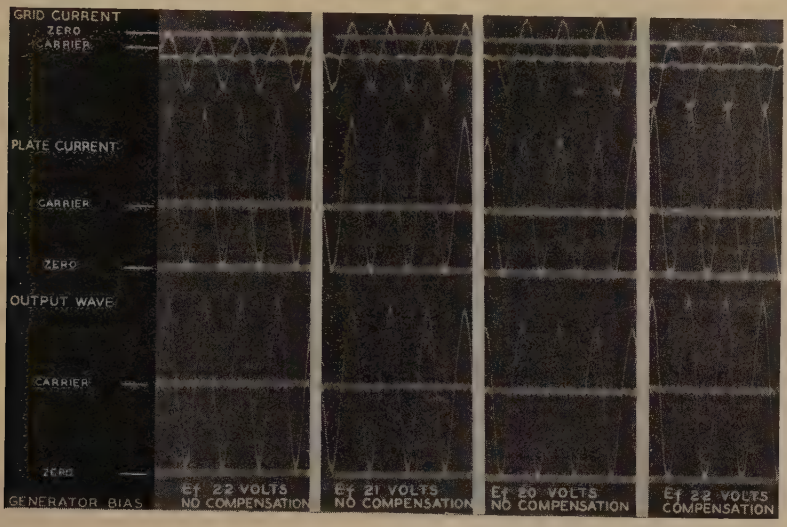

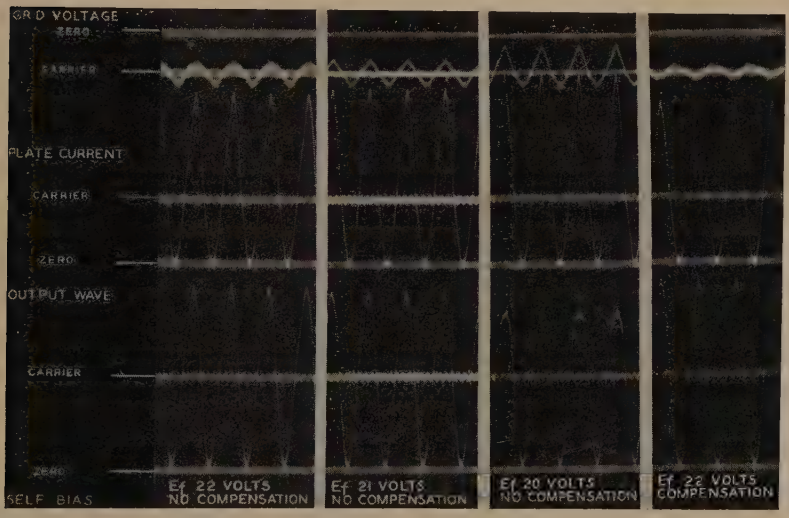

Figs. 5 and 6—UV-207 class C amplifier, 100 per cent modulated
Carrier:

E_p 10 kilovolts	I_p 1.1 ampere
E_g −1400 volts	I_g 0.100 ampere

essentially symmetrical with respect to the carrier, although more precise measurement can detect a slight overshooting on the positive half

cycle. It implies that in this case the power output actually varies from zero to approximately four times the carrier output, which is in a good agreement with our calculation.

The records of panels 2 and 3 are especially interesting. They reveal that with filament voltage reduced below normal the output wave loses its symmetry to a great degree, thus indicating a distinct "shortage" in power output at higher plate voltages just as in the case of generator bias. Again, one cannot ascribe this effect directly to a lack of filament emission, as might seem logical at first sight. Indeed, the plate-current amplitude should be directly affected by insufficient emission; yet, in this case it even goes up as the output drops. The coexistence of these two factors points to a reduced efficiency. The phenomenon is due rather to a more pronounced reversed grid current and to the redistribution of plate and grid characteristics compelling the establishment of a new and rather adverse state of "double equilibrium."

The same oscillograms distinctly show that the grid current and hence the tube bias in the case under consideration do not stay constant during an audio cycle; both vary in a sense opposite to the variation of the modulated plate voltage. Under special conditions, such as are met with during heavy overmodulation, the grid bias at the apex of audio plate voltage may become so low as to cause the tube to run away.

It is important to note that this variation of the grid bias during modulation with a self-biased class C amplifier occurs in just the opposite sense to that in a self-oscillator.

Comparison of Tubes Having Different Values of μ

Knowledge of class C operation is incomplete without an understanding of the manner in which this is affected by the amplification factor, μ, of a tube. A direct way to answer this question is to carry out a comparative analysis of the performance of tubes having structure similar in every respect except for the number of turns on their grids, determining their voltage factors. Such tubes are available: they are standard water-cooled sister tubes UV-863, UV-207, and UV-848, with respective values of μ 50, 20, and 8. The constant-current charts for the UV-863 and UV-848 are plotted in Figs. 7 and 8. Similar to the UV-207 chart of Fig. 1, they are mapped from oscillographic records. Once these charts are available one can pursue parallel calculations of class C operation for all three tubes with the assumption of comparable operating conditions. In our case, let them be determined primarily by the operating plate voltage $E_p = 10{,}000$ volts and the prescribed output power, 6 kilowatts, which is the rated carrier output. In addition, the

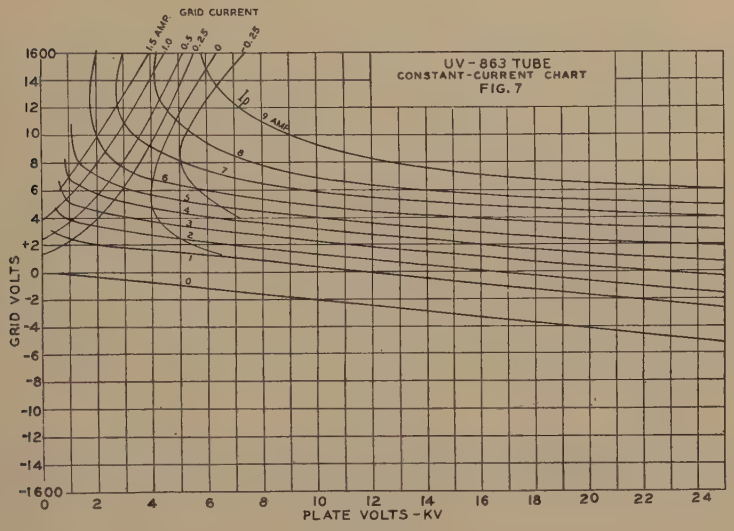

Fig. 7

biases are so selected that the plate-current angle, ϕ, is consistent with good class C operation and is approximately the same with each tube. After a preliminary computation it was found that with the respective

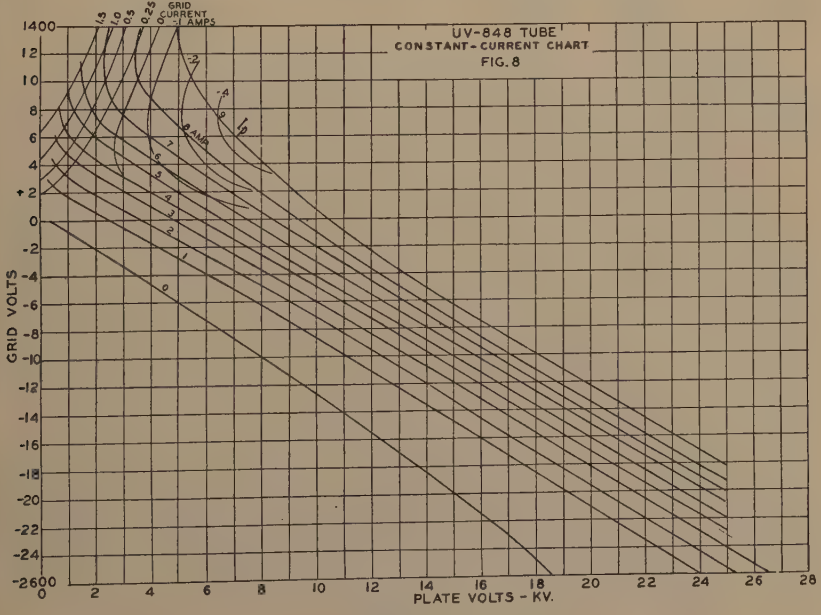

Fig. 8

biases of −2300, −2800, and −3700 volts the current angle with each tube is nearly 85 degrees. Incidentally, the −2800-volt bias on the UV-207 tube is twice as high as that used in the first example. With this the comparative effect on operation of low and high bias will come to light.

By the method outlined in the earlier sections the necessary grid excitation voltage is determined for each type of tube. The minimum plate voltage during oscillation was assumed to be $E_{min} = 1500$ volts with all tubes, which is equivalent to the assumption of the same load resistance, 6020 ohms, for all three tubes.

The calculated operating data, for a *constant grid bias* such as supplied by a generator, are assembled in Table I.

TABLE I

Tube Type	Plate Volts E_p	Grid Bias e_c	Plate Volts Min. E_{min}	+Grid Volts Max. $+e_{max}$	Plate Current amps. I_p	Output Power kw P_o	Input Power kw P_i	Eff. % η	Grid Current ma I_c	Excit. Power watts p_{gi}
Carrier Conditions										
UV-863	10 kv	−2300	1500	+765	0.760	6	7.6	79%	149	460
UV-207	10	−2800	1500	+720	0.760	6	7.6	79	60	190
UV-848	10	−3700	1500	+690	0.760	6	7.6	79	55	242
Positive Crest of Modulation Generator Bias										
UV-863	20 kv	−2300	6400	+765	1.21	15.4	24.2	63%	−93	0
UV-207	20	−2800	4000	+720	1.15	17.2	22.9	75	−25	0
UV-848	20	−3700	3750	+690	1.45	21.8	29.0	74	−19	0
Self-Bias										
UV-863	20 kv	−1880	2400	+1185	1.63	25.7	32.6	79%	121	370
UV-207	20	−2440	2100	+1080	1.63	26.5	32.6	82	60	213
UV-848	20	−3300	1870	+1060	1.64	27.3	32.8	83	49	214

Analyzing the carrier conditions one will note that in order to secure the same amount of output power from any of the explored tubes the grid must be swung to approximately the same positive grid potential in spite of a wide difference in values of μ and in the biases applied. However, the grid current goes down rapidly as the μ of the tube decreases. As the required grid excitation depends on the product of grid current and bias, medium-μ tubes such as the UV-207 are most apt to give the optimum solution for lowest excitation.

With 20,000 volts on the plate, twice the carrier voltage, none of the tubes satisfies the condition of distortionless modulation which requires the crest power output of 24 kilowatts. This only corroborates our previous conclusion. The largest distortion due to the "shortage" in power output is inherent in high-μ tubes and decreases as μ decreases. Expressed in percentage of second harmonic, distortions in-

troduced by the class C amplifier in the analyzed case are 10 per cent, 7.6 per cent, and 2.4 per cent, respectively.

The results of similar calculation for *self-biased operation* of the same tubes are also shown in Table I: Carrier conditions are the same as for generator bias.

In this case, the output power with all three tubes is *greater* than four times the carrier output with resulting second harmonic components, 1.7 per cent, 2.6 per cent, and 3.4 per cent, respectively, for the UV-863, UV-207, and UV-848 tubes. Thus, from the viewpoint of second harmonic distortion the last series of calculations distinctly exhibits the merits of the self-biased scheme and also of the application of high biases in class C operation. Self-biased operation also proves to be superior to that with generator bias with respect to the efficiency at the crest of the modulation voltage and the smaller grid loss on its negative swing. However, the action of self-bias on the negative swing of modulation voltage is such that harmonics of higher order can be introduced by the amplifier more readily than in fixed bias operation.

Before going into a general discussion of the foregoing results, we shall examine in greater detail the role of plate dissipation and grid losses from the viewpoint of limitations inherent in vacuum tubes.

Plate Dissipation

With all three types of tubes under investigation, 10-kilowatt plate dissipation has been experimentally established as a permissible limit for unmodulated class C operation. The associated rate of water flow is three gallons per minute. However, the 10-kilowatt maximum rating cannot be indiscriminately applied to all cases of modulated class C operation. This can be substantiated by the following discussion.

With 100 per cent modulation applied to the carrier the plate dissipation averaged over an audio cycle is theoretically equal to 1.5 P_{hc} if by P_{hc} we designate carrier plate loss. But this relation holds only in the case of "ideal" class C operation with constant efficiency throughout the audio cycle. In actual practice, one can express the average plate dissipation with good approximation as

$$P_{h\,\mathrm{av}} = 1/2\left(\frac{P_{hc} + P_{h\,\max}}{2} + \frac{P_{hc} + P_{h\,\min}}{2}\right) \tag{4}$$

where $P_{h\,\max}$ and $P_{h\,\min}$ are dissipation rates at the positive and negative crests of modulation, respectively. With 100 per cent modulation this expression turns out to be

$$P_{h\,\mathrm{av}} = 1/2P_{hc} + 1/4P_{h\,\max}. \tag{5}$$

Hence, $P_{h\ av}$ is equal to 1.5 P_{hc} only in the exceptional case when $P_{h\ max} = 4\ P_{hc}$. Yet, in the foregoing numerical examples we have seen that $P_{h\ max}$ may, and often does, depart considerably from the theoretical figure of 4 P_{hc}, thus affecting the average, $P_{h\ av}$.

The difference in plate dissipation between unmodulated and modulated operation may be further augmented by the focusing effect of the grid. This comes to light during a modulation cycle at higher plate voltages whenever appreciable instantaneous plate currents flow while the grid potential sweeps through its negative and low positive values. In this condition the heat generation is confined to narrow areas of the anode, formed as patterns of the grid mesh. Hence, local steam bubble

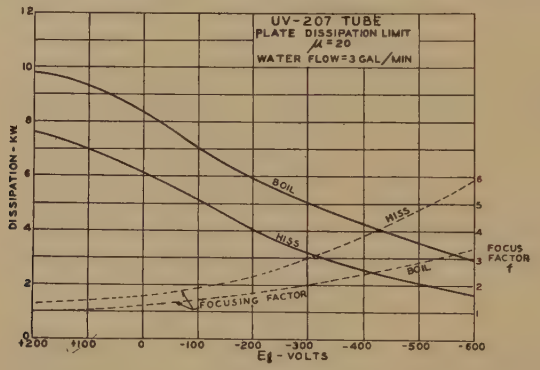

Fig. 9

formation may be started long before the average temperature of the cooling water warrants such a phenomenon. In order conveniently to take the focusing effect of the grid into consideration one may introduce conceptions of "focusing factor" and "effective plate dissipation." The focusing factor can be described as the ratio of the total available area of the active part of the anode to the actual area into which the impinging electrons are crowded in each specific case. The curve 1 of Fig. 9, taken experimentally on a UV-207 tube under static conditions, shows plate dissipation in kilowatts at different grid potentials; at each point this dissipation cannot be exceeded without producing steam bubbles at the anode accompanied by a hissing noise. Each ordinate of this curve divided into 10 kilowatts gives, then, the focusing factor, f, for the corresponding grid potential.

Thus, in calculation of plate dissipation along a dynamic characteristic one has to determine the factor f for each elementary strip of a current-time curve such as is dealt with in Fig. 2. Then the value of actual elementary dissipation, computed for each strip, is to be multiplied by the related value of f. The average of the sum of all such

weighted elementary dissipations over a radio-frequency cycle will be the average "effective" dissipation for the explored dynamic characteristic. The effective dissipation may in some cases affect modulated class C operation strongly, and must hence be taken into account. This is particularly true in the following specific cases: (1) If a relatively low bias is used; (2) if bias is strictly constant during a modulation cycle, such as is the case with a bias generator; and (3) if the tube has a low amplification factor, μ.

As an illustration of the importance of "effective" dissipation, it may be mentioned that in one particular case of operation of a UV-848 tube the cooling water was decidedly "boiling," while the temperature of the outgoing water was only 7 degrees centigrade.

Grid Excitation

The knowledge of grid excitation necessary to secure the desired output from the modulated stage is primarily important from the economic viewpoint. Indeed, the radio-frequency excitation voltage and power govern the construction of the exciter stage. The numerical value of grid excitation power in each case of operation can be computed conveniently and with a sufficient degree of accuracy as the product of the direct current and of the crest value of grid excitation voltage,[5] that is,

$$p_{exc} = i_c(e_c + e_{max}). \tag{6}$$

During modulation the average direct grid current and the excitation power both vary. They decrease as the positive peak of modulation is approached and may even become negative if generator bias is used. As the plate voltage falls to zero on the negative swing of modulation both quantities increase considerably.

In addition to economic considerations, one must realize how and in what degree the grid excitation can affect the tube itself. Grid-excitation power is consumed partly in the bias supplying source, grid-leak resistors, or bias generator, and partly in the grid itself, where it is converted into heat. The grid temperature therefore rises and eventually may reach a level where the grid starts emitting primary electrons of its own. With this, the grid loses its controlling action and may cause heavy overloading of the tube. In this manner the grid excitation may become a limiting factor in class C operation of a tube. Therefore, in each particular case, both carrier conditions and modulated operation must undergo scrutiny in this respect.

The amount of power which a grid can absorb without being heated

[5] H. P. Thomas, Proc. I.R.E., vol. 21, p. 1134; August, (1933).

to the emission point can be measured directly by a simple scheme.[6] A detailed consideration of the method is, however, out of the scope of this investigation. It has been found that appreciable emission of primary or thermionic electrons from the grid starts at the following conditions of dissipation:

With UV-863 tube at	450 watts
UV-207	350
UV-848	250

From completely undisturbed operation of these tubes these limits must be reduced; thus one may with safety assume permissible grid dissipation limits at 350, 250, and 175 watts, respectively.

The amount of power actually supplied to a grid by the excitation stage is found by simple calculation to be the difference between the total input power and the power lost in the bias device:

$$p_i = i_c(e_c + e_{max}) - e_c i_c = i_c e_{max}. \tag{7}$$

However, this is not the true total power converted into heat at the grid during oscillation. Actually the measured grid current at any instant represents the difference between the total incident grid current and the secondary emission current from the grid to the plate. In other words, at any instant the actual flow of electrons emitted from the filament and impinging on the grid is greater than the grid current recorded on a meter by the amount of the secondary emission current. Hence the total electronic flow to the grid can be viewed as though divided into two parallel streams with different external paths. One stream constitutes the current flowing into the grid circuit; the other component, being exactly equal in magnitude to the secondary emission current, is linked through this secondary emission current with the external plate circuit. Both primary electron streams physically end their career at the grid and contribute to its heating in proportion to their respective magnitudes. The comparatively small cooling effect due to the emission of secondary electrons can safely be neglected.

The amount of energy supplied to the grid by the exciter stage is, as we have seen, easily calculated from (7). The computation of the heat due to the primary grid current linked with and energized by the plate circuit is not so simple as this current blends completely with the main plate current in the external circuit. Fortunately the sum total of the electron current impinging on the grid is accessible by an indirect calculation. Some study carried out in our laboratory has

[6] Described in "Grid dissipation as a limiting factor in vacuum tube operation," presented before joint I.R.E.-U.R.S.I. meeting, Washington, D.C., April 26, 1935.

shown that one will not be far from the true value of actual grid dissipation if, in calculation along any given dynamic characteristic, one proceeds in the following manner:

(a) For instantaneous grid voltages above the diode line, or for $e_g \geqq E_p$ one can safely take the grid current values indicated in the chart.

(b) For all voltages such that $e_g \leqq E_p$ one can assume the *same instantaneous values of grid current as for the diode line*, $E_p = e_g$. By plotting such a "true" primary grid current as function of time, or of electrical angle, computing the grid dissipation for the narrow strips into which the time curve is divided, and then averaging the grand total over

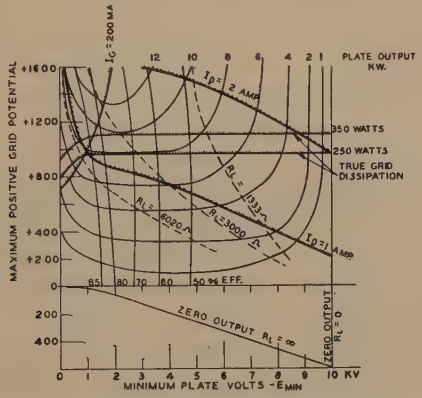

Fig. 10—Lines of equal output and efficiency for carrier conditions UV-207 tube $E_p = 10000$ v. $e_c = -2800$ v.

the entire radio-frequency cycle, one arrives at a more correct value of grid dissipation than is indicated by the externally recorded grid current alone. The final result will then contain a certain margin of safety.

General Discussion

In general, there is no rigorous common rule concerning the choice of tubes and grid excitation arrangements for modulated class C operation. Hence, in practice one encounters a great variety of independent solutions of these problems, sometimes differing basically from each other. Now, in the light of the foregoing analysis one can make a few statements which contribute to the general knowledge of modulated class C operation and which will help in the design of the output stage and in the proper selection of vacuum tubes.

(1) We have seen that with strictly constant grid bias, such as supplied by a bias generator, it is impossible to realize distortionless 100 per cent plate modulation with any type of tube unless the amplifica-

tion factor, μ, is extremely low; but then the other limitations come to the foreground. Therefore, the bias generator, or any other method supplying an essentially constant bias, must be generally considered unsuitable for modulated class C operation.

(2) Distortion of the output wave is also inherent in self-biased operation. Only here, in contrast to the previous case, distortion is due to an excess in power output at the crest of modulation. Yet, if one can tolerate some distortion introduced by the output stage, high-μ tubes are the most suitable for the purpose, giving the least distortion.

(3) A more flexible method of supplying bias is the simultaneous use of generator and grid leak in series. By combining the two methods exercising opposite effects on distortion one may adjust the output stage to a lower distortion than is possible with either method alone.

(4) Distortion changes greatly to the disadvantage of operation as the tubes in service become older. Hence, a periodical readjustmentof the bias and excitation is expedient.

(5) Distortion of the output wave inherent in class C operation is to some degree affected by the choice of the load resistance. From the very technique of the outlined graphical method one may arrive at the conclusion that the load resistance is to be chosen as high as possible in the case of constant bias and as low as possible in a self-biasing scheme. Nevertheless in either case the choice will be restricted by other factors such as grid excitation or tube efficiency.

(6) It is known that good class C operation requires the application of higher biases. On the other hand, from the economy viewpoint lower biases are advantageous. In addition too high a bias, necessitating high grid-excitation voltage, causes high dielectric loss in the press and other insulating parts of the tube; this may result in puncture of the tube. A compromise choice of the bias must be governed by the operating conditions at the apex of modulation rather than by the carrier.

(7) Plate dissipation at carrier conditions can hardly be a cause of concern to the designer. But when the tube may run into class B or even into class A operation during modulation, dissipation may become a limiting factor in choosing the best type of tube and appropriate operating conditions. In this respect low-μ tubes are particularly bad as their 100 per cent modulated operation is inherently accompanied by high "effective" plate dissipation.

(8) Grid excitation for producing a desired output is generally the highest with high-mu tubes and the lowest with tubes of medium μ, but power dissipation in the grid may become a limiting factor almost in the same measure with any of these tubes irrespective of the value of mu. This is because high-μ grids are usually built more massively,

have a larger cooling surface, and hence, can stand more dissipation without overheating.

With any tube, the grid excitation power increases rapidly as the minimum plate voltage touched during oscillation decreases; in other words, as the chosen load resistance increases. But this is not true with respect to grid dissipation. Indeed, we have seen that the true grid dissipation depends merely on the maximum grid excitation voltage, and this varies but little with different chosen values of $E_{\min}$, or of the load resistance.

(9) Correlating all results of the previous discussion one arrives at the verdict that the most suitable tubes for modulated class C operation are those of medium μ. Also, there appears to be no justification whatsoever in the application of low-μ tubes for this class of service. Nevertheless, if, for some reason, a low-μ tube is to be used as a class C amplifier, its rating must be decidedly lower than that of its sister tubes of higher μ. A bias generator in this case will be more suitable than a self-biasing scheme.

A general idea regarding the mutual relation of various factors in class C operation can be conveniently obtained from a map such as plotted in Fig. 10 for the UV-207 tube. In the map, lines of equal output are plotted for $E_p = 10{,}000$ volts and $e_c = -2800$ volts, which is the carrier condition in one of our numerical examples. The coördinates here are the same as used in the constant current charts, so that the two kinds of charts can be superimposed on each other. Any point of the new map represents the termination of a dynamic characteristic to which the inscribed values belong. The map also contains the curves of the conventional limits, $i_g = 0.200$ ampere and $I_p = 1.0$ and 2.0 amperes. The lines of true grid dissipation, $p_{gh} = 250$ watts and $p_{gh} = 350$ watts are also shown. In addition, the loci of the end-points of dynamic characteristics for three different load resistances are traced.

It may be of interest to mention the following relation between the instantaneous and average values of plate current in a modulated class C amplifier as they occur in the various cases of our calculation. The ratio of the maximum instantaneous to the average plate current at carrier conditions is from 6 to 7; it drops to 5 if a relatively lower bias is used. The ratio between the average plate current at the peak of modulation and that at carrier conditions is less than 2 with a constant bias and greater than 2 in a self-biasing scheme. The departure from the theoretical factor may be as large as ± 25 per cent. The maximum instantaneous plate current reached at the crest of a 100 per cent modulation audio cycle is from 9 to 9.5 times the average plate-current value at carrier conditions.

Compensated Class C Operation

From our entire discussion it is evident that the shortcomings inherent in conventional class C operation with high modulation have their primary cause in the fact that the radio-frequency grid excitation voltage is of constant amplitude. This is almost rigidly fixed in magnitude as soon as the carrier output, operating plate voltage, and grid bias are specified. However, the constant excitation voltage compatible with the carrier condition proves to be inadequate for other plate voltages during modulation as the positive and negative crests are approached.

Generally speaking, the excitation voltage is too high on the negative and too low on the positive swing of the audio plate voltage. Therefore, logically, any means that is capable of properly changing or "compensating" the grid-excitation voltage during each audio cycle will bring about a decided improvement in class C operation. One can imagine a variety of schemes which will effect the desired compensation. But essentially all of them can be described as *auxiliary modulation of the excitation stage.* For example, one can apply modulation directly to the plates of the exciter tubes by means of a special choke and audio transformer of small size, the primary of which is energized by the main modulators, or a suitable tap can be provided on the main modulating transformer for the same purpose. Another possibility in "compensation" is in the varying of the bias of the excitation stage or of earlier stages of the power amplifier, thus influencing the radio-frequency amplitude of the exciter voltage.

The effect of the compensation at the positive crest of modulation is this: In the case of a constant bias, due to the increased grid voltage amplitude the tube is able to produce greater outputs and hence the point of "power equilibrium" in Fig. 3 shifts in the direction of lower values of E_{min}, corresponding to higher outputs and higher efficiency. One can always adjust compensation so as to make the power output at the crest of modulation equal to exactly four times the carrier output. In operation with self-bias the immediate influence of compensation is an increase in the bias at higher plate voltages because of the grid swinging into the region of heavier grid currents. This, therefore, counteracts the natural loss-of-bias tendency in noncompensated modulation. In addition, the shift of the power equilibrium point also takes place. An important result common to both modes of operation is an increase in the efficiency and a reduction in the "effective" plate loss. Thus, in one instance, a UV-848 tube boiled vigorously when 100 per cent modulation was applied. One could clearly distinguish in the boiling the sixty-cycle pitch of the modulating frequency indicating that

boiling occurred just at the apex of the audio cycle. However, boiling disappeared as soon as compensation of the grid excitation was applied, and would reappear as soon as the compensation was taken off.

In self-biased operation it is possible to carry compensation so far that the bias will actually increase on the upswing of the modulation voltage and decrease on the negative half cycle of modulation. Such action reminds one of the classical self-oscillator. The main difference is that in a 100 per cent modulated self-oscillator the grid bias and grid excitation vary rigidly from zero to approximately twice carrier value at the modulating frequency, while in a compensated class C amplifier the magnitude of the audio bias variation can be adjusted at will. In other words in a self-oscillator the excitation is strictly proportional to the audio plate voltage and is therefore modulated to the same degree as is the plate, while in a compensated amplifier the percentage of auxiliary modulation of the excitation can be varied from zero to any desired level and will generally be much less than 100 per cent.

In Fig. 1 the paths of the biases are plotted both for compensated class C operation and for a self-oscillator. One may note that graphically the dynamic characteristics of a self-oscillator at any point of modulation may be represented by strictly parallel lines with slope equal to the ratio of grid and plate coupling turns, while in a class C amplifier, compensated or noncompensated, the slope of the instantaneous dynamic lines changes during the entire audio cycle.

At the negative crest of modulation, when the modulated plate voltage sweeps through zero, the grid compensation reduces the excitation voltage and thus tends to relieve the grid from excessive heat dissipation. In this respect the compensation scheme is superior to the grid-leak bias arrangement as it simultaneously decreases the bias, and with it, the unnecessary power loss in this region of operation. Generally, by the application of compensating methods, lower and more economical biases can be used, without impairing operation at high modulation voltages.

In Figs. 5 and 6 the extreme right panels demonstrate oscillographically the effect of compensation. In both cases the average audio variation in grid current is reversed 180 degrees in phase to that in the absence of compensation. Therefore, in self-biased operation the audio variation of bias during an audio cycle becomes more consistent with class C operation at any instant. At the same time in both cases the output wave, shown as the lowest record, *does not reveal any appreciable distortion.* In addition calculation indicates better efficiency as compared to noncompensated operation.

A simple though partial solution to the problem of compensating

the grid may be achieved by purposely making the exciter stage regulation high. From calculation as well as from the oscillographic records of Figs. 5 and 6 it is quite clear that with any noncompensated scheme the average grid current decreases with increasing plate voltage and vice versa. This means that the load on the exciter stage varies in the same manner. Hence if the regulation of the exciter stage is high the oscillation amplitude in the exciter tank circuit, which determines the excitation voltage, will increase and decrease elastically in the manner which is required for compensation. Such regulation can be preadjusted, for example, by inserting a resistor in the plate-voltage supply line to the exciter, or by other simple external means. The limitation of this method lies in the fact that on the positive half cycle of modulation the average grid current and bias may soon acquire a constant value, preventing a further unloading of the excitation stage.

Conclusions

The graphical method which has been described enables one to carry out a point-by-point analysis of the class C performance of a tube throughout an entire audio modulation cycle with accuracy and ease. It brings out the fact that operation with generator bias differs markedly from operation with self-bias when the process of modulation is considered. Detailed investigation shows that audio distortion is introduced into the output wave by the amplifier itself. In the case of generator bias this distortion is due to the shortage in output at modulation peaks while with self-bias it is due to an excess of power output on peaks. A study of the tube charts shows that in general the least distortion can be obtained by the use of a proper combination of the two bias methods. During modulation one must consider "effective" rather than actual plate dissipation; this becomes a distinct limitation on operation when the amplification factor of the tube is low. The audio distortion due to the class C amplifier itself can be eliminated by the use of grid "compensation" or auxiliary audio modulation of the excitation stage. This auxiliary modulation enables one to imitate the attractive features which exist in a self-oscillator so as to obtain an increase of bias and excitation at the crest of audio modulation and a corresponding decrease at its ebb. Operation under compensated conditions proves to be highly desirable in reducing the effective plate dissipation and in considerably increasing the over-all efficiency of the tube.

Compensation can also be instrumental in the improvement of modulated operation if "cathode" bias obtained from a series plate current resistor is used with class C amplifiers in accordance with recent tendencies in transmitter engineering practice.

Proceedings of the Institute of Radio Engineers
Volume 23, Number 7 *July, 1935*

NEW METHOD FOR ELIMINATING STATIC CAUSED BY TROLLEY AND ELECTRIC CARS*

By

E. W. Schumacher

(New York City)

THE ever-growing popularity of radio broadcasting has brought forward all problems concerning static and other disturbances. Besides various electrical apparatus and machines which could be made free of static through the connection of condensers, one of the main troubles is the collection of current by trolley cars and electric railways, because of the use of rolls or metal sliding bows as current collectors. The reason for these disturbances is mainly that between the roll or sliding bow and the overhead wires sparks will be generated which in turn produce high-frequency vibrations, whereby the overhead wires act like an antenna, sending out these vibrations. The usage of rolls on trolley cars is much more apt to be the source of disturbance, because the contact between the current collector and overhead wire converge to a point. The collection of current is better if sliding bows[1] are used, because the area of collector and wire is comparatively larger. It has been tried to eliminate static, etc., to a certain extent by adapting wider sliding surfaces, and also with the connecting of condensers. The fact remains however, that these experiments have not been proved to be entirely successful.

A thorough study and experimentation with all kinds of sliding-bow materials has shown that various metals and metal alloys have different reactions toward static. It was found, for instance, that bronze is the strongest source for disturbances, followed by copper, aluminum, brass, steel, lead glance, and bismuth sulphide. The lowest amount of disturbance could be observed with zinc, but it was found that carbon was especially free of static. The disturbances in units were as follows; bronze, 2000; steel, 1000; zinc, from 250 to 1500; and with carbon, never more than 240. By the usage of the carbon sliding bow, no static whatever could be noticed. It is a well-known fact that all metals, through formation of blowpipe beads, will roughen the wires, thus increasing static and generating sparks; whereas carbon will give the wires a smooth polish. Even if a metal bow were formerly in use, and

* Decimal classification: R430. Original manuscript received by the Institute, June 6, 1934.

[1] This paper is based in part on data on carbon sliding bows secured from the Noris Carbon Company, Inc., 160 Fifth Avenue, New York City, and C. Conradty, Nurnberg, Germany.

the wires already show a formation of ripples, this condition would soon be rectified, by using carbon sliding bows *only*, because of their smoothing and polishing effects. The question of wear and tear on the wires also plays an important part. There is in Nurnberg, Germany, a trolley car company that is using carbon sliding bows exclusively, and it has been found that the wear and tear on the wires was 0.1 millimeter per year with a five-minute operating service. If the overhead wires are well polished, the wear and tear on the carbon bow is very little, and several trolley car companies have testified that they can use a carbon piece for 80,000 to 100,000 miles. If, however, a metal bow is being used on a line, on which a carbon bow is used at the same time, the life of the carbon bow will be shortened, because the wires, through the use of metal, will be roughened and will cut into the carbon. Therefore it would be advisable to use carbon bows exclusively, thus assuring a 100 per cent efficient service through continous polishing. It is safe to assert that a carbon sliding bow is the only current collector that eliminates static entirely, and at the same time will not only not affect adversely, but will prolong the life of overhead wires. All research work, as far as the adaptability of carbon sliding bows is concerned, must come to the same conclusions.

In Germany there is a law in preparation which will force the operators of trolley car companies to use these carbon bows, in order to safeguard static-free radio reception.

Proceedings of the Institute of Radio Engineers
Volume 23, Number 7 *July, 1935*

ANOMALOUS TRANSMISSION IN FILTERS*

By
J. G. Brainerd
(Moore School of Electrical Engineering, University of Pennsylvania, Philadelphia, Pennsylvania)

Summary—*It is well known that the terminating impedance plays an important rôle in the action of a filter. Using a terminating impedance which approximates the negative of the usual iterative impedance is shown to result in transmission not specified by ordinary filter theory in addition to that in the customary pass bands. The effect is essentially one of resonance which can be produced in a suppression band.*

WHEN several equal passive linear electric transducers are joined in series to form a filter or chain, it is customary to assume that definite cut-off frequencies limit the transmission and suppression bands of the filter, and that these cut-off frequencies are determined by some rule such as that which states that a cut-off frequency is any frequency which makes the factor[1] ρ equal 0 or -1 ($\varrho \equiv \mathbf{z}_M/4\mathbf{z}_N$ where $\mathbf{z}_M$ is the total series impedance and $\mathbf{z}_N$ the shunt impedance of the equivalent T section either of one of the constituent transducers or of the major transducer formed by the filter). It is proposed in this paper to discuss an apparently anomalous problem—transmission in suppression bands, where "transmission" is used in the same sense as in "transmission band."

As a preliminary the elementary theory of filters may be briefly reviewed. The ratio of output current ($\mathbf{I}_n$) to input current ($\mathbf{I}_0$) of a chain of n equal symmetrical sections in series is

$$\frac{\mathbf{I}_n}{\mathbf{I}_0} = \frac{2\mathbf{z}_K}{(\mathbf{z}_r + \mathbf{z}_K)\epsilon^{\gamma n} - (\mathbf{z}_r - \mathbf{z}_K)\epsilon^{-\gamma n}} \tag{1}$$

where $\mathbf{z}_K$ is the iterative impedance and $\gamma(\equiv\alpha+j\beta)$ the propagation factor of one section, $\mathbf{z}_r$ is the impedance terminating the chain at the end of the n section, ϵ is the base of the natural logarithms and $j \equiv \sqrt{-1}$. In terms of the parameters of a section,

$$\mathbf{z}_K = \sqrt{\mathbf{z}_M\mathbf{z}_N(1 + \varrho)} \tag{2}$$

and,

$$\epsilon^{\gamma} = 1 + 2\varrho + 2\sqrt{\varrho(1 + \varrho)} \tag{3}$$

* Decimal classification: R386. Original manuscript received by the Institute, June 12, 1934.

[1] Boldface symbols denote complex quantities; symbols in italics and not boldface denote modulus values.

from which it may be shown that, neglecting resistance in the section elements, $\alpha = 0$ and $\mathbf{z}_K$ is a pure resistance when $0 \leqq \rho \leqq -1$, whereas outside this range $\alpha > 0$ and $\mathbf{z}_K$ is a pure imaginary. From (1), $\mathbf{I}_n/\mathbf{I}_0 = \epsilon^{-\gamma n}$ when $\mathbf{z}_r = \mathbf{z}_K$, hence so long as the latter equation holds $I_n/I_0 = 1$ when $\alpha = 0$ and $I_n/I_0 = \epsilon^{-\alpha n}$ when $\alpha > 0$. Thus those frequencies which make ρ fall between 0 and -1 lie in transmission bands (a current of a frequency in such a band is passed with little or no attenuation through the filter) and all other frequencies are in suppression bands (a current of a frequency in the latter group is attenuated in passing through the filter since $I_n/I_0 = \epsilon^{-\alpha n}$). It is usual to terminate a filter with a resistance ($\mathbf{z}_r$ real) which may equal $\mathbf{z}_K$ at some frequency in a pass band. Under these circumstances

$$\frac{I_n}{I_0} = \frac{1}{\sqrt{\left(\frac{z_r}{z_k}\sin \beta n\right)^2 + \cos^2 \beta n}} \tag{4}$$

in a transmission band. So long as z_r does not deviate too far from z_K, this ratio remains near unity.

Much work has been devoted to the design of proper terminations for a filter, and it has long[2] been recognized that the terminating impedance plays an important role in the over-all action of the filter. From (2) it is seen that $\mathbf{z}_K$ may have two values, only one of which has a positive real part. This is the one almost always used. Since however the usual filter theory outlined above neglects resistance in the section elements, it is reasonable to inquire into the significance of that value $\mathbf{z}_K'$ of the iterative impedance which has a negative real part when resistance is not neglected. By (1) it is seen that when $\mathbf{z}_r = \mathbf{z}_K' = -\mathbf{z}_K$

$$\frac{\mathbf{I}_n}{\mathbf{I}_0} = \epsilon^{\gamma n}. \tag{5}$$

It is only outside the pass bands that $\mathbf{z}_K'$ can be approximated; in the suppression bands it is primarily a reactance (assuming that the resistances of section elements are small) and in these bands $\alpha > 0$. Hence, by (5), $I_n/I_0 > 1$ in suppression bands and $I_n/I_0 = 1$ in the pass bands. The filter has thus been "inverted" and transmission of currents of frequencies in the usual suppression band is better than that of currents of frequencies in the usual pass bands.

The above theory is too rough for use. Neglect of resistance in ordinary elementary filter theory leads to results which approximate

[2] Zobel, "Transmission characteristics of electric wave-filters," *Bell Sys. Tech. Jour.*, vol. 3, no. 4, October, (1924); Campbell, "Physical theory of the electric wave-filter," *Bell Sys. Tech. Jour.*, vol. 1, no. 2, November, (1922).

experimental results; in the present case, resistance is of much greater relative importance. This results from the $(\mathbf{z}_r+\mathbf{z}_K)\epsilon^{\gamma n}$ part of the denominator in (1). Even though it be assumed that $\mathbf{z}_r$ has no resistance component (as can be effectively realized when it is a capacitative reactance), nevertheless if $\mathbf{z}_K$ has an appreciable real part r_K, the product $r_K\epsilon^{\alpha n}$ usually will be the predominating factor in the denominator. This is particularly true when α is large. The result is that the transmission effect appears, that is, the ratio I_n/I_0 is maximum near a frequency which makes $\mathbf{z}_r=-jx_K$, but there is a large loss.[3] The curve I_n/I_0 versus frequency in this case (fixed capacitance, suppression band) has the general shape of a resonance curve.

From (1) it follows that when $\mathbf{z}_r=-jx_K$

$$\frac{\mathbf{I}_n}{\mathbf{I}_0}=\frac{2(r_k+jx_k)}{r_K\epsilon^{\gamma n}-(r_K-j2x_K)\epsilon^{-\gamma n}} \tag{6}$$

whence it is seen that by making x_K very large the ratio I_n/I_0 may also be large, assuming r_K as small as possible.

From throwing (1) into the form

$$\frac{\mathbf{I}_n}{\mathbf{I}_0}=\frac{2\epsilon^{\gamma n}}{\left(\frac{\mathbf{z}_r}{\mathbf{z}_K}+1\right)(\epsilon^{2\gamma n}-1)+2} \tag{7}$$

it appears that $(\mathbf{z}_r/\mathbf{z}_K+1)\ (\epsilon^{2\gamma n}-1)$ may be taken as a measure of the approximation to "inversion." The ideal value for this quantity is zero for inversion of the type indicated by (5).

It may be noted that theoretically very large values of I_n/I_0 may be obtained in the usual pass band. If $\mathbf{z}_r=jx_r$ then

$$\frac{I_n}{I_0}=\frac{r_k}{\sqrt{r_k^2\cos^2\beta n+x_r^2\sin^2\beta n}} \tag{8}$$

and $I_n/I_0=\infty$ when $x_r=0$ and $\beta n=(k+1)\pi/2$ (k an integer). This assumes $\alpha=0$ in the pass band, which is not true.

There are several possible uses for the "inversion" effect discussed above. For one, it may add a pass band (not as sharply defined as the usual band) to a filter, and thus extend (or restrict) the range of use of the latter. For another, it permits control of a pass band by the terminating impedance, and in consequence allows a partially variable

[3] The loss in the usual pass band of an ordinary filter may be large. For example, a filter to pass only a band of 100 cycles at 20,000 cycles may have a loss of 25 decibels (order of magnitude). The loss in several filters in the case of inversion was less than this.

filter; i.e., one in which some of the cut-off frequencies can be varied, to be made with no varying parameters inside the filter itself. Particularly when z_K' is a capacitative reactance are the inversion properties obtained, in part because of the very small real part which z_K' may have. In this case a partially variable filter can have one pass band dependent on a value of the capacitance at the receiving end, which may be changed rather easily. Terminating a filter with a capacitor is practicable when the voltage across the capacitor is applied to the grid of an amplifying tube, and when the variation of impedance with frequency is not important or is small as in narrow pass bands at high frequencies.

ACKNOWLEDGMENT

The above results have been checked and the author is indebted to Mr. S. Nathan Lev, CWA research associate in the Moore School, for having carried out the experimental work.

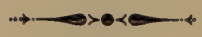

Proceedings of the Institute of Radio Engineers
Volume 23, Number 7 *July, 1935*

A SIXTY-CYCLE BRIDGE FOR THE STUDY OF RADIO-FREQUENCY POWER AMPLIFIERS*

By

ATHERTON NOYES, JR.
(Harvard University, Cambridge, Massachusetts)

Summary—*A selective bridge, consisting of three resistive arms and a fourth arm comprising a sinusoidal sixty-cycle voltage, has been devised and applied to the study of radio-frequency power amplifiers. In Part I the measuring circuits are described, and in Part II some typical data on a type 10 tube are presented. The observed linearity of contours of constant plate loss on a diagram plotted to the coördinates of output carrier-frequency voltage and plate-battery voltage is discussed, and a very simple circuit, based on this result and useful for rough measurements, is described.*

SYMBOLS

$\bar{I}_p$, $\bar{E}_B$, etc. —steady value of current or voltage
I_p, E_o, etc.—r-m-s values of fundamental component of a periodic wave
$\hat{E}_o$, $\hat{E}_m$, etc.—peak values of fundamental components
i_p, e_p, etc. —instantaneous values
$\boldsymbol{I}$, $\boldsymbol{Z}$ —complex values
R_o —antiresonant impedance, to the fundamental applied frequency, of a parallel tuned output circuit at resonance.
Z_o —replaces R_o when the tuned circuit is not resonant to the applied fundamental frequency.
P —power in watts

Subscripts:
i—input
o—output
g—grid
p—plate
m—modulating
C—used to indicate quantities, such as bias, in the grid circuit
B—used to indicate quantities, such as plate-battery potential, in the plate circuit

INTRODUCTION

CIRCUITS, such as those of oscillators or radio-frequency power amplifiers which involve the operation of a vacuum tube over a large and nonlinear region on its characteristic, are usually most easily studied by experimental methods. At radio frequencies, however, the precautions necessary to obviate the effect of stray capacities and

* Decimal classification: 621.374.2. Original manuscript received by the Institute, January 10, 1935; revised manuscript received by the Institute, March 18, 1935.

inductances of leads, and of undesired couplings, complicate the experimental technique.

In 1929 E. E. Spitzer[1] of the General Electric Company made a study of the power input requirements of heavily biased radio-frequency power amplifiers, using for his measurements a fundamental frequency of sixty cycles instead of radio frequencies. This shift to a low frequency eliminated many of the difficulties inherent in high-frequency measurements. It required, however, a parallel-tuned output circuit resonant to sixty cycles—of necessity a cumbersome affair.

Previous to this time E. L. Chaffee, at Cruft Laboratory, had conceived the idea of studying oscillators at sixty cycles, using for the plate and grid loads not tuned circuits but transformer secondaries whose primaries were to be connected to the power mains. The secondaries were to be so connected as to apply voltages in approximately opposite phase to the grid and plate of the tube under test. Thus the voltages from the transformers were to simulate the alternating voltages which, in an actual oscillator, are developed across the grid-circuit and plate-circuit impedances.

Chaffee and Kimball[2] have now applied this method to the study of oscillators with considerable success. As in the scheme originally proposed by Chaffee use was made of wattmeters to measure grid-circuit and plate-circuit power relations, and much interesting information has been presented compactly in the form of contours of constant power output, tube loss, efficiency and the like plotted against the coördinates of alternating grid and plate voltages. This simple scheme has now been elaborated somewhat to facilitate the study of class B and class C amplifiers used as modulators. The principles of the method are described below.

Fig. 1. illustrates the basic principle of the two-transformer method as applied to a radio-frequency power amplifier. In (a), which shows diagrammatically a typical stage of class C amplification, a radio-frequency voltage e_i is impressed on the input terminals of the stage. An effort is generally made to keep e_i sinusoidal. The tube is biased beyond its quiescent plate-current cut-off by $\bar{E}_c$, and e_i is of such magnitude as to swing the grid considerably positive during a portion of each cycle.

The resulting plate current i_p therefore consists of a train of rectified current loops corresponding to the swings of the grid in a positive direction, with zero plate current flowing during all of the negative and a part of the positive half cycles of grid excitation. This plate

[1] "Grid losses in power amplifiers," Proc. I.R.E., vol. 17, pp. 985–1006; June, (1929).

[2] E. L. Chaffee and C. N. Kimball, paper to be published shortly.

current may be shown by Fourier analysis to consist of a steady component $\bar{I}_p$, a sinusoidal component of the frequency of the input voltage, I_p, and a series of components harmonically related to this frequency.

The plate load Z_o is generally tuned to resonance with the excitation frequency. The voltage e_o that appears across this load is, therefore, due almost wholly to the fundamental frequency component I_p of plate current, (for the impedance of Z_o to harmonics of this frequency is small) and is, therefore, practically a pure sine wave.

It will be seen that the circuit of (b) will be equivalent to (a) provided the voltages e_i and e_o are nearly sinusoidal. These voltages are

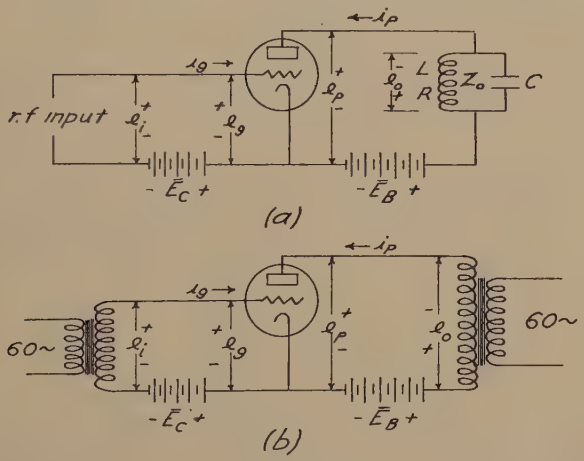

Fig. 1

derived from the secondaries of transformers whose primaries are connected to the city power supply. Tests carried on by means both of a harmonic analyzer and of an oscilloscope have proved that the impedance to harmonic components of grid or plate currents offered by suitable transformers is so low that, in general, no harmonic component of either voltage exceeds one per cent of the fundamental, regardless of the character of the current wave flowing through the transformer secondary.

Thus the plate transformer introduces a sinusoidal voltage in the plate circuit corresponding to that which would occur across a tuned impedance in the actual case, and the ratio of this sinusoidal voltage to the fundamental component of plate current is equal to the value of the impedance Z_o which it simulates.

Chaffee and Kimball[2] used essentially the circuit of Fig. 1(b) in their work, with wattmeters in grid and plate circuits for the measurement of tube losses, and interpreted their results as bearing on an

oscillator on the assumption that the voltage e_i is fed back from the plate circuit. Many of these results can be interpreted equally well in terms of an unmodulated amplifier. In fact, a modulated amplifier can, over a certain region of the tube characteristic, be studied by the use of this same circuit. With the carrier frequency supplied dynamically at sixty cycles, the modulating voltage swing applied to the tube can be simulated by a point-to-point variation of the steady battery voltages in either the plate or the grid circuit, depending on the type of modulation under consideration. Since, however, a wide assortment of wattmeters would be required to trace the changes in carrier frequency power during the modulation cycle, a bridge has been devised for use in the output circuit. This has the combined advantage of eliminating the plate-circuit wattmeter and of making possible the taking of all data directly in terms of any desired value of load impedance Z_o.

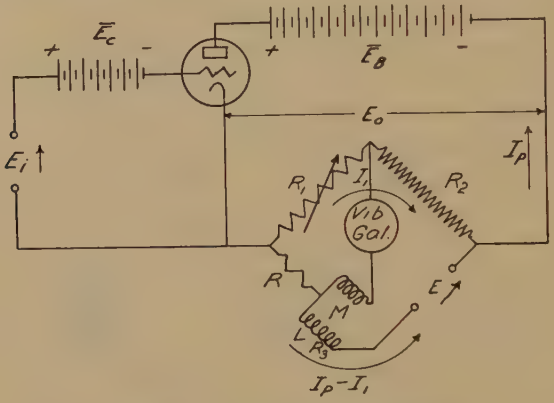

Fig. 2—Plate circuit bridge (schematic).

In Part I these circuits will be briefly described, and in Part II data illustrative of their use in the analysis of amplifier circuits will be given.

PART I

The Experimental Circuits

Fig. 2 is a schematic diagram of the plate-circuit bridge. The bridge has four arms. The resistive elements R_1 and R_2 form two of them; the resistance R and (for certain measurements) the inductance L of the rotor of a variometer, are contained in the third, and a sixty-cycle voltage from the secondary of a transformer takes the place of the

usual fourth impedance. The detecting device is a vibration galvanometer which is connected from the junction of the arms R_1 and R_2 to the stator of the mutual inductance M. A vibration galvanometer is used as an indicator because of its extremely sharp frequency selectivity. The bridge must be balanced for sixty-cycle currents, yet harmonic currents of very substantial magnitude are normally flowing through the bridge arms.

At balance the bridge simulates an impedance Z_o through which the plate current is flowing, and having across its terminals a voltage:

$$E_o = Z_o I_p \tag{1}$$

where I_p is the complex value of the fundamental component of plate current. I_p, of course, and therefore the condition of balance for any given adjustment of the bridge, is dependent upon the value of $\overline{E}_B$ as well as upon E_i and E_o.

If, as will usually be the case, Z_o is assumed to be a resonant circuit offering a resistance R_o to the fundamental component of plate current, the mutual inductance M may be eliminated. In this case solution of the bridge equation gives

$$R_o = \frac{E_o}{I_p} = R\left\{\frac{R_1 + R_2}{R_1 + R}\right\}. \tag{2}$$

The variometer is used only in cases where it is desired to simulate a load impedance with a reactive component. The bridge equations are only slightly complicated by inclusion of the variometer.

At balance, then, and with $M\omega = 0$ the bridge offers a pure resistance R_o to plate current of fundamental frequency, while having negligible impedance to currents of harmonic frequencies. With $M\omega \neq 0$ the bridge may be made to simulate any impedance desired. Equation (2) is plotted in Fig. 3 against the axes of R_o and R_1 with $R_2 = 100{,}000$ ohms and $R = 10$ ohms. Throughout the work here described R_o was fixed by adjusting R_1 according to this relation.

From current and voltage readings at bridge balance, moreover, the plate-circuit power relations are completely determinable without the use of a wattmeter. The total power input to the plate circuit from the plate battery or generator is the product of battery voltage $\overline{E}_B$ and direct plate current, $\bar{I}_p$. This supplied power divides into two parts, namely the output power in the load, P_o, and the plate loss, P_p. If we make the assumption that the plate load impedance has a negligible resistive component for harmonic frequencies and for direct current the power in the load is then derived wholly from components of the fundamental frequency, and is

$$P_o = E_o I_p = \frac{E_o^2}{R_o}, \tag{3}$$

then since, as above stated,

$$P_B = P_o + P_p \tag{4}$$

$$P_p = \bar{E}_B \bar{I}_p - \frac{E_o^2}{R_o} \tag{5}$$

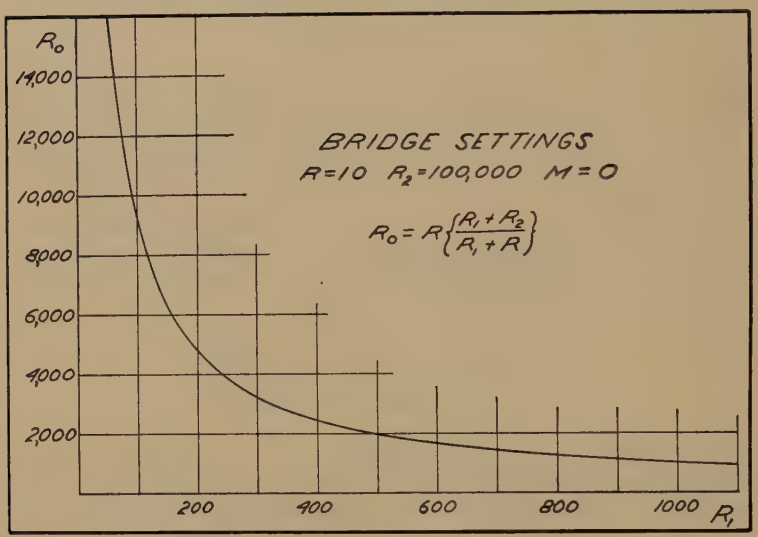

Fig. 3

and the plate circuit efficiency is

$$\text{Plate Eff.} = \frac{P_o}{P_B} \times 100\%. \tag{6}$$

To calculate all of the above quantities it is necessary only to balance the bridge for any required value of R_o by variation of such circuit voltages or bridge impedances as may be desirable and, with the bridge at balance, to observe E_o, $\bar{E}_B$, and $\bar{I}_p$—quantities all easily measurable with instruments readily obtainable. In testing a type 10 tube it has been found easy to balance the bridge for values of E_o ranging from two or three volts to several hundred volts and thus to calculate power output and plate loss for values between a few hundredths of a watt and forty or fifty watts.

It is sometimes desirable to extend the investigation into regions of the tube characteristic in which, with continuous operation, the tube losses would be dangerously high. To safeguard the tube in such regions cam-operated contacts may be employed to apply potentials to the tube for, say, half-second periods at two-second intervals. In Fig. 4, which shows the experimental circuit used, such contacts appear near the center of the figure with the designating numbers 1 and 2. These contacts closed in such order that the vibration galvanometer

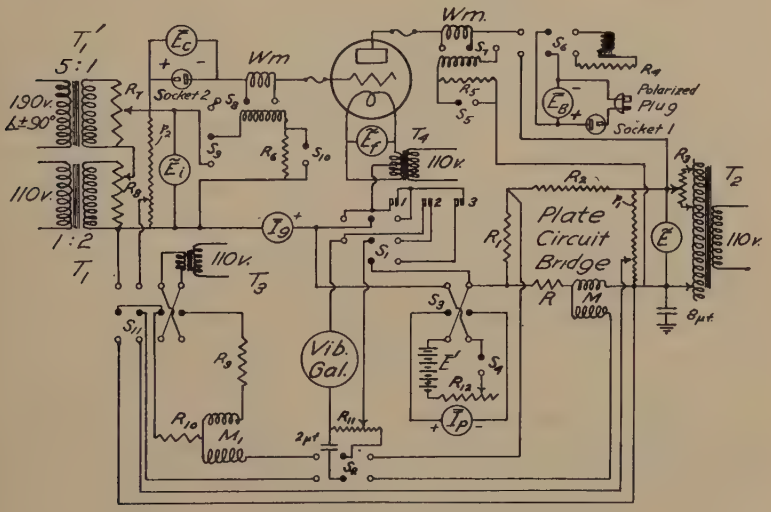

Fig. 4

was connected in circuit only when the power was on and after all transients had died down, so that balance of the bridge was readily obtained with the cam shaft in rotation. When balance was not perfect the galvanometer received a deflecting impulse once every rotation of the shaft. Contact 3 permitted measurement of $\bar{I}_p$ by a null method.

Fig. 4 is a much more complex circuit than is necessary for analysis of simple and usual cases. A circuit hardly more elaborate than that indicated by Fig. 2 is all that would be required for most purposes. The wattmeter shown in the plate circuit was used solely as a check on the operation of the bridge; after a number of measurements in which plate-circuit power relations as computed from the bridge adjustment were closely checked by measured values, it was discarded.

Similarly, much of the apparatus shown in Fig. 4 for adjustment and measurement of the phase of input and output voltages will be, as a rule, unnecessary. Under normal operating conditions the alternat-

ing voltage appearing on the plate of a class C amplifier is presumed to be opposite in phase to the voltage applied to the grid. In certain cases, however, this may not be true. Consequently the experimental set-up of Fig. 4 was designed to allow for sizable variations of the phase angle between grid and plate voltages from the normal 180 degrees. The phase of the plate swing, or output voltage, was fixed by the phase of the sixty-cycle mains by way of the transformer T_2; the phase of the input voltage could be varied as desired by means of the slide-wires R_7 and R_8 across the transformers T_1 and T_1', fed in quadrature from Scott-connected three-phase transformers. The resistances R_7 and R_8 were of sixty ohms each, thus keeping the impedance of the source at a low value. The relative phases of input and output voltages were measured, with the vibration galvanometer as an indicating instrument, by comparing each in turn with the phase of a current driven through R_{10} and M_1 by the small transformer T_3. S_2 was used to connect the galvanometer to this circuit.

Either input power P_i or grid-dissipated power P_g could be measured by the use of the wattmeter shown. Switch S_9 served to connect the voltage coil of the wattmeter directly to the input voltage for measurements of P_i and to the grid side of the biasing battery when measuring P_g.

Assuming negligible harmonic voltages in E_i (R_7 and R_8 were made small to justify this assumption, which, as will be shown later is thoroughly admissible) the power relations in the grid circuit are

$$P_i = E_i I_g \cos \theta_g \tag{7}$$

$$P_c = \overline{E}_c \overline{I}_g \tag{8}$$

$$P_i = P_c + P_g. \tag{9}$$

These relations can easily be checked by direct wattmeter measurements.

As will be illustrated by the data of Part II, these circuits are well adapted to an easy experimental study of the relations existing between any of the circuit parameters $\overline{E}_c$, $\overline{E}_B$, E_i, Z_o and the associated quantities E_o, P_o, P_p, P_i, P_g.

The bridge may be balanced either by adjustment of any circuit voltage or, if Z_o is the dependent variable, by manipulation of the bridge arms. For each balance of the bridge, data obtained from simple and rugged low-frequency measuring equipment suffice for the calculation of all quantities of interest.

PART II

Experimental Tests of a Type 10 Tube

Modulation in the Plate Circuit

The bridge circuit previously described makes possible an easy approximate analysis of the operation of a class C amplifier modulated by the introduction of a series voltage in the plate circuit.

In Fig. 5 is shown a family of curves radiating from the origin. Each of these curves shows the relation between E_o, the carrier-frequency voltage across the output impedance of the amplifier, and the battery voltage $\bar{E}_B$, in the plate circuit. Each curve is plotted for a different value of output impedance R_o obtained by adjustment of the bridge impedances according to Fig. 3. Each point corresponds to a balance of the bridge achieved by experimental adjustment of either $\bar{E}_B$, the plate-circuit battery voltage, or of E_o, the carrier-frequency plate-circuit voltage derived from transformer T_2. The data for each point included readings of E_o, $\bar{E}_B$, $\bar{I}_p$, $\bar{I}_g$, and P_i. From these data curves of P_i, P_o, P_p, I_p and plate efficiency were computed and plotted. Cross-sections of these curves of P_p and P_o at constant power levels were then transferred to Fig. 5, where they appear as contours of constant power superimposed on the original diagram.

Contours of constant P_i obtained by the same process could be plotted on the same figure. However, they would complicate an already complex diagram, and it has been considered advisable to plot them separately. The original data for Fig. 5 gave points for contours of constant input power which appeared to lie in straight lines, just as the plate-loss contours do. The points were not well enough spaced, however, to establish this fact with certainty. Fig. 6 shows a family of curves taken to determine the input power relations more precisely. Each curve was observed with E_0 fixed at the value indicated. Cross sections of these curves, at a constant value of P_i, give five points on a constant power-input contour for Fig. 5; the contours derived from Fig. 6 by this method, together with reference curves of E_0 versus $\bar{E}_B$ taken from Fig. 5, are plotted in Fig. 7.

Figs. 5, 6, and 7 give direct information on most of the quantities of interest in the operation of a plate-modulated class C amplifier. Plate-circuit efficiency, while implicit in the curves of Fig. 5, is not directly shown there. In Fig. 8 the plate efficiency for each of the values of R_0 of Fig. 5 is plotted against $\bar{E}_B$. Contours of constant efficiency would lie nearly parallel to the $E_o - \bar{E}_B$ curves of Fig. 5 and would needlessly confuse the diagram.

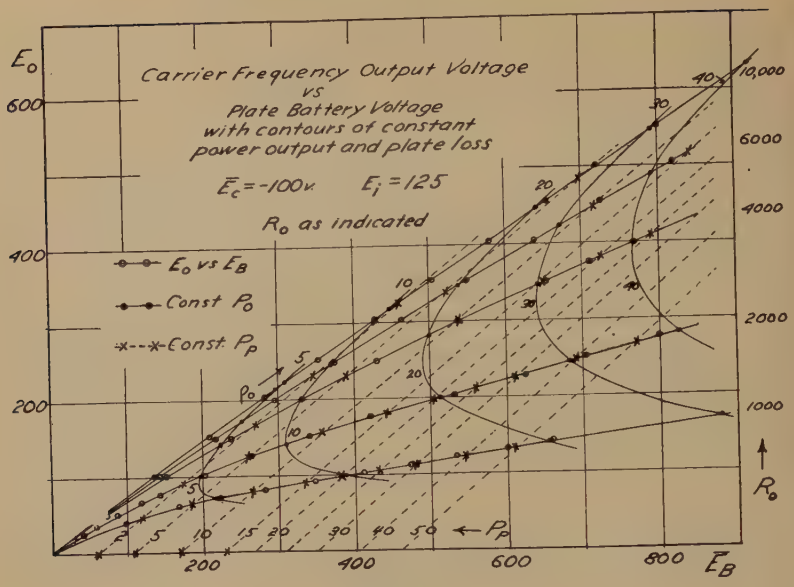

Fig. 5

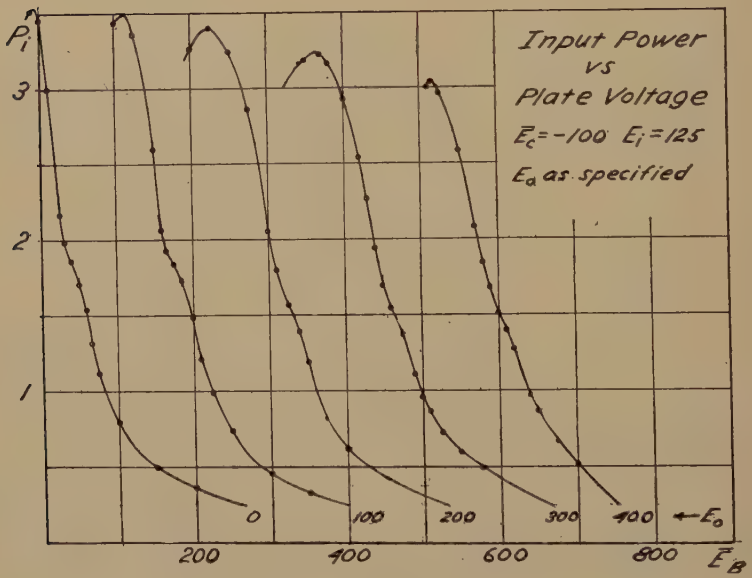

Fig. 6

The primary curves of Fig. 5, E_o versus $\bar{E}_B$ at constant R_o, are of especial interest from the viewpoint of distortion of the modulation

envelope when the amplifier is modulated in the plate circuit. In this case we consider the voltage $\bar{E}_B$ of the diagram to be replaced, in an actual modulator, by a steady battery voltage $\bar{E}_B$ on which is superimposed a modulating voltage $\hat{E}_m \cos at$. We further require that the

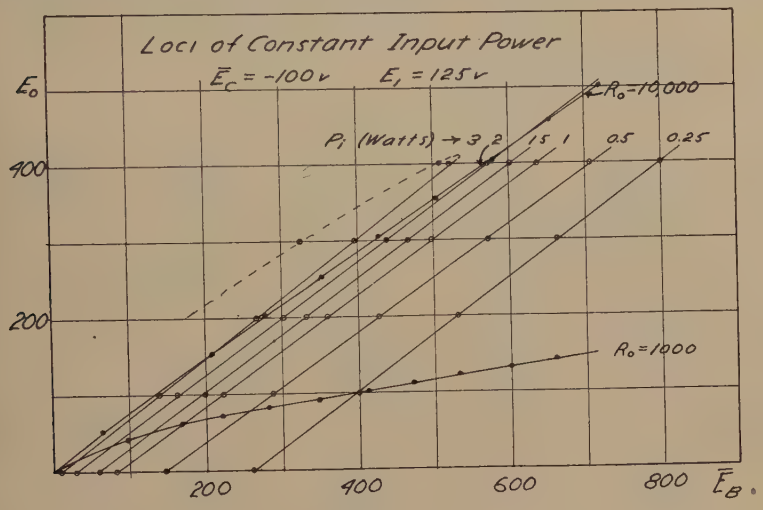

Fig. 7

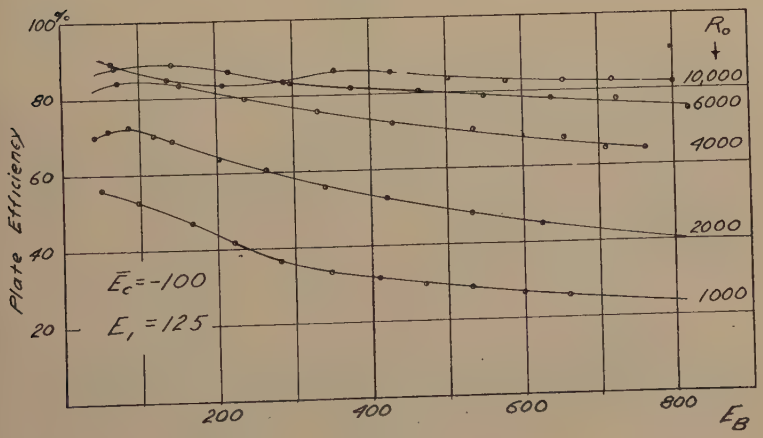

Fig. 8

side-band frequencies produced by modulation do not differ sufficiently in frequency from the carrier to invalidate the tacit assumption that R_o is constant for carrier and side bands. Thus the radio-frequency voltage across the load is varied at the audio frequency $a/2\pi$ in a manner determined by the shape of the $E_o - \bar{E}_B$ curve for the value of R_o

in the circuit. In regions where E_o is linearly related to $\overline{E}_B$ (Fig. 5) the envelope of the modulated output carrier wave will be a faithful duplicate of the modulating wave. That is, there will be no modulation distortion. When the characteristic is curved the carrier envelope will contain audio harmonics not present in the modulating voltage.

An an illustration, let us assume a second order term in the equation of the characteristic and let

$$E_o = a + be_B + ce_B^2. \tag{10}$$

Such an equation, with constants chosen to fit it to the observed points of one of the curves of Fig. 5, is shown in Fig. 9. On the same diagram is indicated an assumed modulating swing $\widehat{E}_m$.

Now it is very simple to show that, given a peak modulating swing $\widehat{E}_m$, varying sinusoidally at a frequency $a/2\pi$, the carrier-frequency voltage across the load will be represented by

$$e_o = A(1 + m_1 \cos\ at + m_2 \cos 2\ at) \sin \omega t \tag{11}$$

and that fractional modulation coefficients are given geometrically in Fig. 9 by

$$\begin{aligned} m_1 &= \frac{|v|}{2E_{0q} + u} \\ m_2 &= \frac{|u|}{2E_{0q} + u} \end{aligned} \tag{12}$$

where u, the departure of the curve at the point of peak audio swing from the tangent to the curve at the quiescent point, is taken as positive in sign if the curve lies above the tangent, negative if below. The per cent second harmonic to be expected after distortionless detection is, of course, by (12)

$$\text{per cent second harmonic} = \left|\frac{u}{v}\right| \times 100 \text{ per cent.} \tag{13}$$

Fig. 9 thus illustrates an easy method of estimating the distortion due to small curvatures in the $E_o - \overline{E}_B$ characteristics of Fig. 5. If the curvature is such that the curve may be represented by an equation of the form of (10) the ratio of second harmonic to fundamental in the envelope will be given by the ratio of $|u|$ to $|v|$. In the actual case illustrated in Fig. 9 the second harmonic will be 4.89 per cent of the fundamental.

The data taken for Fig. 5 included observation of direct plate current $\bar{I}_p$. These curves are shown in Fig. 10, and may be used to compute

the audio-frequency power necessary to modulate the tube under any given conditions. For example, in the case previously chosen for Fig. 9, $\bar{E}_B = 400$ and $\hat{E}_m = 300$. The peak audio current which flows

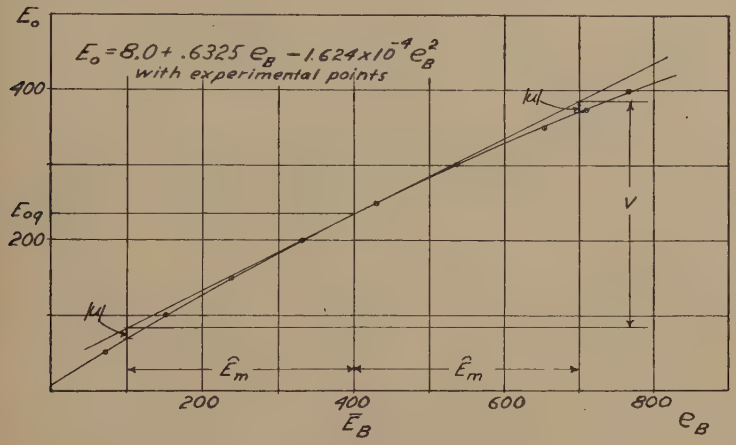

Fig. 9

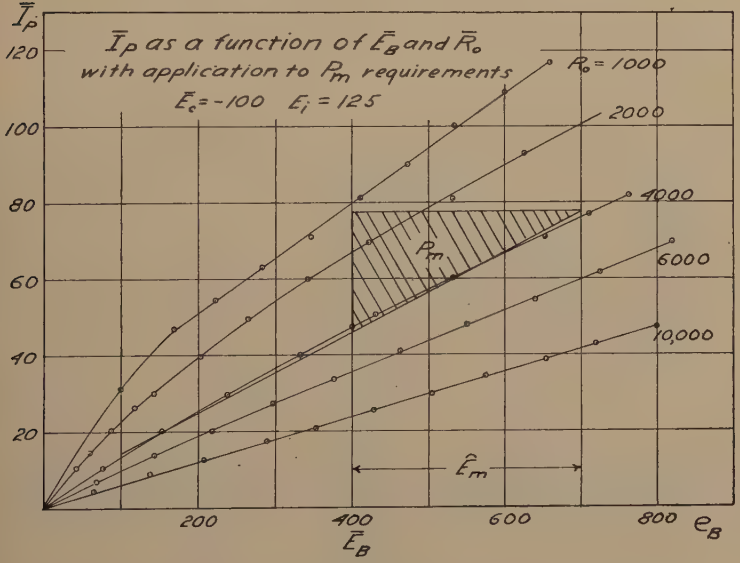

Fig. 10

from the modulating source is equal to the altitude of the shaded triangle of Fig. 10 (30 milliamperes). The audio power required then is

$$P_m = E_m I_m = \frac{\hat{E}_m \hat{I}_m}{2} = 4.5 \text{ watts} \qquad (14)$$

and the resistance to which the modulation supply should be matched is

$$R_m = \frac{E_m}{I_m} = 10{,}000 \text{ ohms.} \tag{15}$$

As has been seen the data, taken at suitable bias and input voltages, for the primary curves of E_o versus $\bar{E}_B$ at constant R_o, may be made to yield much information as to linearity of plate modulation, power output, power input, and tube loss under any operating conditions.

A short digression will now be made to describe an extremely simple experimental set-up for approximating the foregoing data. The approximate linearity of the contours of constant P_p and P_i (Figs. 5, 6, and 7) suggests the method. Reference is made to the appendix, where it is shown that, if the pulses of grid current and of plate current occur

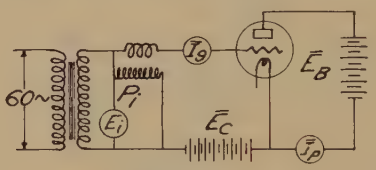

Fig. 11

during a relatively small fraction of the half period of the driving voltage, the contour lines of constant plate loss P_p and of constant input power, P_i on the $E_o - \bar{E}_B$ diagram are very nearly linear, with a slope slightly greater than $1/\sqrt{2}$. Furthermore, to a very rough approximation, the contours of constant P_p are also contours of constant direct plate current $\bar{I}_p$ and of plate current of fundamental frequency I_p. Also, the ratio of I_p to $\bar{I}_p$ is roughly equal to $\sqrt{2}$.

Consequently, it is extremely simple to construct a crude $E_o - \bar{E}_B$ diagram similar to that of Fig. 5 from data obtainable by very little effort.

The experimental set-up necessary is shown in Fig. 11. The data required consist of readings of direct plate current $\bar{I}_p$ and of input power P_i as a function of $\bar{E}_B$. $\bar{E}_c$ and the exciting voltage E_i are to be held constant for any one diagram.

In this experiment $R_o = 0$ and $P_o = 0$ so that the product of $\bar{E}_B$ by $\bar{I}_p$ at any setting gives P_p directly. Such a value of P_p is, it will be observed, the lower extremity of a linear contour of constant P_p, and these contours can be drawn at once from points on the $\bar{E}_B$ axis as determined by the data. The slope of the contours should be slightly greater than $1/\sqrt{2}$.

Similarly, if desired, contours of constant input power can be drawn in the same manner, their intersections with the $\bar{E}_B$ axis being determined by the experimental values of $\bar{E}_B$ which yielded suitable wattmeter readings. Of course, if necessary, a still further simplification can be introduced here by applying the approximation suggested by Thomas,[3] and computing P_i from readings of $\bar{I}_g$ and E_i.

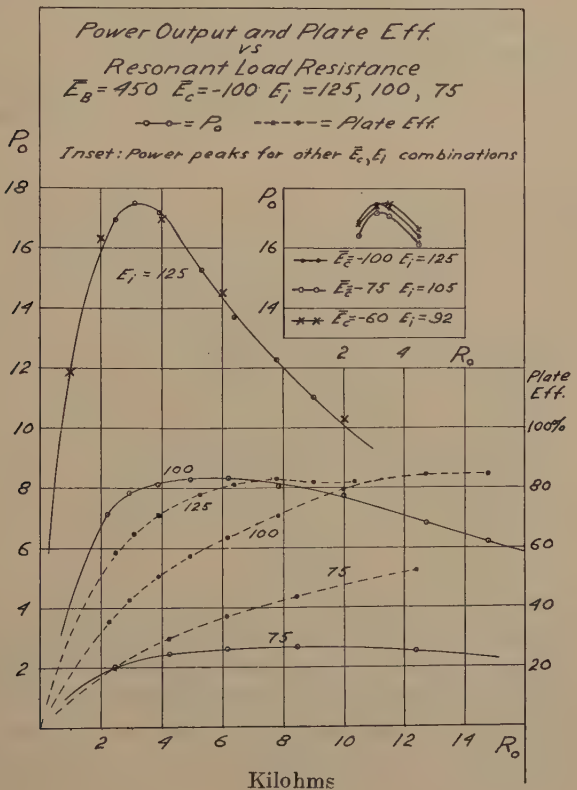

Fig. 12

Next a third set of parallel contour lines should be drawn. These are contours of constant I_p, and are to be obtained by multiplying the observed values of $\bar{I}_p$ by $\sqrt{2}$.

By the use of these last contours the rest of the diagram can be computed. Each curve of E_o versus $\bar{E}_B$ for constant R_o can be located from the intersection of these contours with the coördinate lines of E_o by the use of the relation $R_o = E_o/I_p$.

[3] Proc. I.R.E., "Determination of grid driving power in radio-frequency power amplifiers," vol. 21, pp. 1134–1142; August, (1933).

Finally, the contours of constant output power, P_o, can most readily be obtained by using the equation $P_o = E_o^2/R_o$, which determines points on a contour in terms of the intersection of the curves for constant R_o with the appropriate value of E_o.

A diagram constructed in this manner is not, of course, very accurate, and will become less accurate as the bias voltage is decreased and the duration of the current pulses becomes relatively longer. It will, however, aid in estimating the potentialities of a tube whose actual performance characteristic is unknown.

Returning now to the more complete circuit, we see that the application of the bridge is not limited to the data just described. Grid-

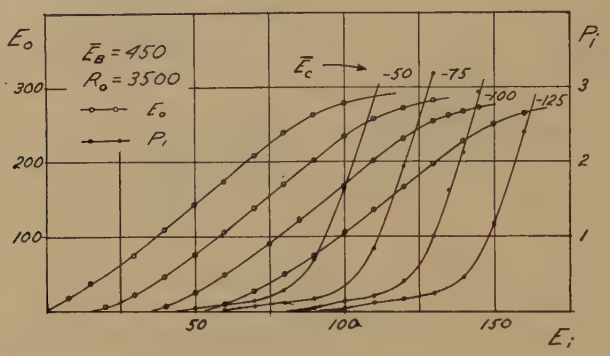

Fig. 13

circuit modulation may be investigated by allowing $\bar{E}_c$ to be the experimental independent variable, and obtaining curves of E_o versus $\bar{E}_c$ which are interpretable in the same manner as those of Fig. 5. Or, if we choose, we may fix the direct potentials and excitation voltage at suitable values and investigate output power as a function of load resistance. Such curves are obtainable by fixing, for any point, either E_0 or R_0 (by the relation of Fig. 3) and adjusting the other for bridge balance. Fig. 12 is a specimen of this type of data.

Again, it is extremely simple to obtain the relationship between input and output voltages as dependent on any other of the circuit elements. Fig. 13, taken with a bridge setting fixed to simulate a 3500-ohm resonant load, is illustrative. In Fig. 13 are shown curves of E_o versus E_i and P_i versus E_i, for four values of bias. The data for these curves permitted the computation of the corresponding curves of output power, plate loss, and plate efficiency, and these curves are given in Fig. 14. The curves of Figs. 13 and 14 are of interest in connection with the amplification of a modulated wave.

It may at times be desirable to investigate conditions when the input and output voltages are not in phase. At radio frequencies such a situation may arise as a result of the grid-plate capacity or of nonresonance in the load circuit. The effects of grid-plate capacity upon phase angle and other quantities may be studied by increasing the capacity to such a value as to yield the same coupling reactance at sixty cycles as would exist at radio frequencies due to the actual tube capacity. A nonresonant load circuit can be simulated by the utilization of the mutual inductance element indicated by M in Fig. 2 or Fig. 4. By proper setting of this variometer the bridge may be adjusted,

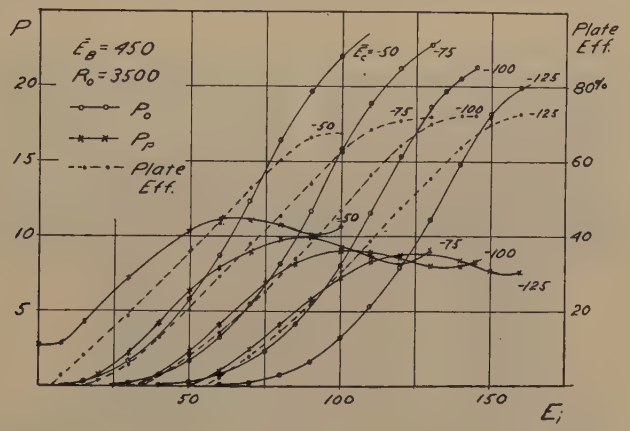

Fig. 14

to balance at a vector ratio of E_o and I_p and thereby to offer, at balance, any desired complex impedance to the fundamental-frequency plate current. Provision must be made, of course, for adjusting the phase relationship of E_i and E_o, as for example, by the method shown in Fig. 4. Such data have been taken for a type 10 tube, but are probably not of sufficiently general interest to warrant inclusion here.

An obvious advantage of making measurements at low frequencies lies in the ease with which the harmonic content of current and voltage waves may be observed, or the actual waves recorded by the oscillograph. An audio-frequency harmonic analyzer of the heterodyne type manufactured by the General Radio Company has been found to be well adapted to the measurement of the harmonics of waves of fundamental frequency as low as sixty cycles. The wave shapes have also been examined on a cathode ray oscilloscope. A few oscillograms, obtained by superimposed photographic exposures, are reproduced in Figs. 15, 16, and 17.

Fig. 15 shows the plate current i_p for five values of E_o, with $\bar{E}_c$ constant at -100, and $\hat{E}_i = \sqrt{2} \times 125$. The maximum instantaneous grid voltage was thus 76.6 volts positive. The five curves, from top to bottom, were observed at $\bar{E}_B = 400$ and E_o as specified in the accompanying table:

Trace	E_0	$e_{p\min}$	$\bar{I}_p$
1	125	223	73
2	175	153	62
3	225	78	49.4
4	250	47	39
5	282	0	23

Data for Fig. 15

Note the effect of secondary emission from plate to grid in the lower traces.

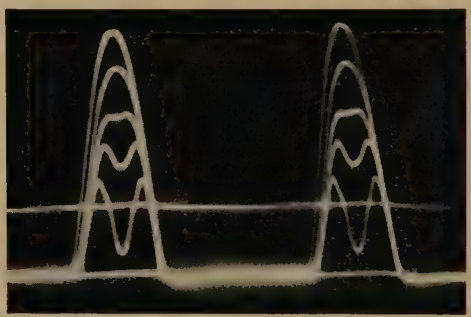

Fig. 15

Fig. 16 (a), (b), and (c) show, respectively, the grid current of the tube for the conditions of traces 1, 2, and 4 of Fig. 15. Loss of secondary electrons by the grid as well as secondary emission from the plate is evident in these traces. For low values of E_o the central portion of the grid-current loop may drop below the zero axis.

Fig. 17 (a) shows plate current and plate voltage with $\bar{E}_B = 400$, $\bar{E}_c = -100$, $E_i = 125$, and $E_0 = 190$. Fig. 17 (b) gives the grid current and grid voltage for the same conditions. The average plate current was 57 milliamperes and the average grid current 3.15 milliamperes. Calibrating lines at the battery voltages and at 75 and 10 milliamperes are also included in the figure. Note that the tube voltages are nearly the sum of a steady and a sinusoidal component, as was required to make the experimental method valid. Harmonic analysis, as mentioned above, showed second and third harmonics of the voltages to be of the

order of 0.5 or one per cent, with higher harmonics even more negligible. The current waves, in contrast, contain harmonics of the same general magnitude as the fundamental.

(a)

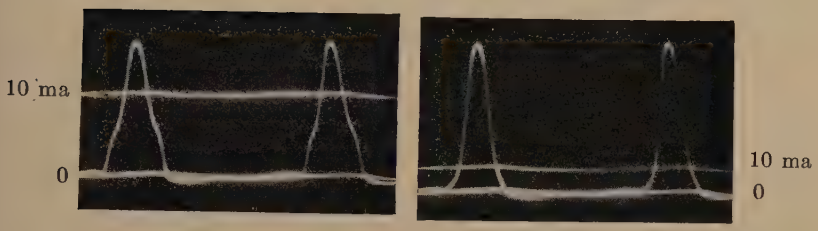

(b) (c

Fig. 16

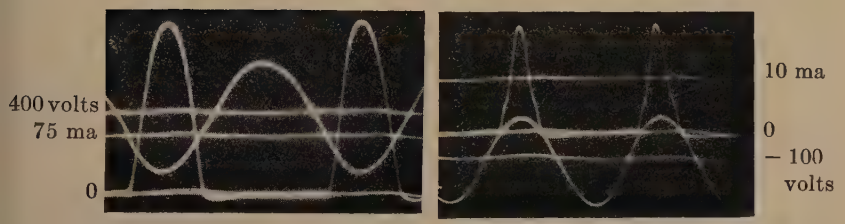

(a) (b)

Fig. 17

Conclusion

The data which have been presented are merely illustrative of the uses to which the measuring circuits can be put. The operation of a power tube, as amplifier, modulator, or oscillator, can be studied by these methods even when a very wide range of the characteristic surface is utilized. The circuits are not limited, of course, to triodes, but can be advantageously employed in the study of multielement tubes, or of almost any nonlinear circuit involving the flow of a distorted current wave through a selective impedance.

For most purposes the circuit of Fig. 4 is far more complicated than necessary. It can, usually, be simplified, as by the omission of the phase-measuring equipment and of the commutating mechanism used only at high power level, until it is hardly more complicated than the schematic circuit of Fig. 2. And, for very rough work, it has been shown possible to make a useful estimate of a tube's potentialities and approximate circuit requirements by the extremely elementary set-up of Fig. 11.

Appendix

The Linearity of the P_i and P_p Contours of Fig. 5

Let the plate current, as illustrated by the oscillograms of Fig. 16, be represented by

$$\begin{aligned} i_p &= f(\omega t) = f(\theta) \quad \text{for} \quad -\theta_o \leqq \theta \leqq \theta_o \\ i_p &= 0 \qquad\qquad \text{for} \quad \begin{cases} -\pi < \theta < -\theta_o \\ +\theta_o < \theta < \pi \end{cases} \end{aligned} \tag{16}$$

and,

$$e_p = \overline{E}_B - \widehat{E}_o \cos\theta. \tag{17}$$

Now,

$$\begin{aligned} P_p &= \frac{1}{2\pi}\int_{-\pi}^{\pi} i_p e_p d\theta \\ &= \frac{\overline{E}_B}{2\pi}\int_{-\theta_o}^{\theta_o} f(\theta)d\theta - \frac{\widehat{E}_0}{2\pi}\int_{-\theta_o}^{\theta_o} f(\theta)\cos\theta d\theta. \end{aligned} \tag{18}$$

The first integral of (18) represents the area under a loop of plate current; the second integral gives a slightly smaller area obtained by multiplying the ordinates of plate current by cos θ when cos θ is near unity. In the limit, as θ approaches 0, the second integral approaches equality with the first. If we let

$$\int_{-\theta_o}^{\theta_o} f(\theta)d\theta = A$$

we may then set the second integral of (18) equal to $(1-\alpha)A$, where α represents the decrease in area due to the cosine factor. Moreover,

$$\frac{A}{2\pi} = I_p \text{ and } \widehat{E}_0 = \sqrt{2}E_o \tag{20}$$

so that (18) may be rewritten as

$$P_p = \bar{I}_p\{\overline{E}_B - \sqrt{2}\,E_0(1 - \alpha)\}. \tag{21}$$

From (21) the generic equation of the contours becomes

$$E_0 = \frac{1}{\sqrt{2}(1 - \alpha)}\left(\overline{E}_B - \frac{P_p}{\bar{I}_p}\right). \tag{22}$$

It will be seen that (22) represents a straight line provided α and $P_p/\bar{I}_p$ are constant.

Let us examine the case in which θ_0 is so nearly zero that $\alpha \ll 1$. In such a case (17) becomes, for the duration of the pulse,

$$e_p = \overline{E}_B - \widehat{E}_o \tag{23}$$

and (21) gives

$$\overline{E}_B - \widehat{E}_o = e_p = \frac{P_p}{\bar{I}_p}. \tag{24}$$

Assume now that for any contour $\bar{I}_p$ is constant. Then e_p is also constant during the pulse, and, with bias and grid excitation remaining unchanged, the pulse $i_p = f(\theta)$ is always the same in shape and magnitude. If the pulse does not change, $\bar{I}_p$ and I_p are evidently constant and the assumption is justified.

A derivation of the generic equation of the contours by another method gives the ratio $\bar{I}_p/I_p$. Since with a resistive load

$$P_p = \overline{E}_B\bar{I}_p - E_oI_p \tag{25}$$

the equation of the contours is evidently

$$E_0 = \frac{\bar{I}_p}{I_p}\left(E_B - \frac{P_o}{I_p}\right). \tag{26}$$

A comparison of (26) with (22) shows that

$$I_p = \bar{I}_p\sqrt{2}(1 - \alpha).$$

Summarizing, then, if the pulse is of such short duration that $\alpha \ll 1$, the contours of constant P_p on the $E_o - \overline{E}_B$ diagram are linear with a slope of $1/\sqrt{2}$. They are also contours of constant $\bar{I}_p$ and of I_p, and, for any point $I_p = \sqrt{2}\,\bar{I}_p$.

In general, α is not negligible, and, actually, both α and $\bar{I}_p$ vary somewhat along a contour. The net result is that, while the variations

of α and $\bar{I}_p$ appear to be nearly compensatory so that the contours of P_p are very closely linear, they are not accurately contours of constant currents, and they are not precisely parallel.

From similar reasoning it becomes evident that contours of constant P_i (and, for that matter, of $\bar{I}_g$ and P_g) are approximately parallel straight lines. It will be observed that since θ_0 is smaller for the pulse of grid current than for the plate-current wave, α is smaller in the grid circuit, and the grid contours have a slope more nearly equal to $1/\sqrt{2}$ than do those of the plate circuit.

Acknowledgment

It is a pleasure to acknowledge the debt I owe to the earlier work of E. L. Chaffee and C. N. Kimball, and I wish to express my thanks to Professor Chaffee for his assistance both in pointing out the problem and in helpfully criticizing the results.

Professor G. W. Pierce also has been most kind both in making possible the undertaking of the work and in encouraging its progress.

Proceedings of the Institute of Radio Engineers
Volume 23, Number 7 *July, 1935*

MEASUREMENT OF RADIO-FREQUENCY IMPEDANCE WITH NETWORKS SIMULATING LINES*

By

W. L. Barrow

(Round Hill Research Division, Massachusetts Institute of Technology, Cambridge, Mass.)

Summary—*The complex value of an impedance may be measured at radio frequencies by measuring voltage ratios on a transmission line terminated in the unknown impedance. The line may often be replaced advantageously by an equivalent network. Several new methods of carrying out the measurement have been developed and a study of the factors affecting the accuracy and the technique of manipulation has been made. Optimum accuracy obtains when the characteristic impedance of the network and the impedance to be measured are equal. Only two quantities need be accurately known; viz., (1) the capacitance of a variable condenser, and (2) the frequency of the applied voltage; this is a decided advantage at radio frequencies. The conditions imposed on the voltmeter are easily satisfied in practice. A common lead connecting generator, voltmeter, network, and unknown impedance makes grounding and shielding simple. Experimental results at frequencies from 50 to 1500 kilocycles have agreed well with the computed performance of the device and they demonstrate the practicability of the method.*

THE USE of either a radio-frequency transmission line or its equivalent circuit as an impedance measuring device has been described by Labus[1] and others[2,3,4]. This general method has some valuable features that particularly adapt it to the frequency range above about fifty kilocycles and to impedance values from about ten ohms up to about fifty thousand ohms. The fact that the reference standards may be taken as (1) the frequency and (2) either the constants of the line or the value of a variable capacitance, is an important advantage, because both of these quantities may be determined at radio frequencies with greater accuracy than may resistance, inductance, etc. In this paper the results of an investigation of the conditions for optimum accuracy and of the technique of manipulation are presented. Several new methods of using equivalent networks are de-

* Decimal classification: R240. Original manuscript received by the Institute, November 22, 1934; revised manuscript received by the Institute, April 15, 1935. Presented before joint meeting of U.R.S.I. and I.R.E., Washington, D. C., April 26, 1935.

[1] J. W. Labus, "Measurement of resistance and impedance at high frequencies," Proc. I. R. E., vol 19, pp. 452–460; March, (1931).

[2] E. J. Sterba and C. B. Feldman, "Transmission lines for short-wave radio systems," Proc. I.R.E., vol. 20, pp. 1163–1202; July, (1932).

[3] R. King, "Amplitude characteristics of coupled circuits having distributed constants," Proc. I.R.E., vol. 21, pp. 1142–1181; August, (1933).

[4] O. Schmidt, "Das Paralleldrahtsystem als Messinstrument in der Kurzwellentechnik," *Hochfrequenz. und Elektroakustik*, vol. 41, pp. 2–16; January. (1933).

scribed. Their performance has been investigated and it gave very satisfactory results. Some of the details of construction are brought out. A large part of the discussion applies equally to the use of lines or of networks.

Impedance Measurement with Transmission Lines

Although the measurement of impedance with a radio-frequency transmission line and a voltmeter or an ammeter is fairly well known, it is helpful to review briefly the principles of measurement before going on to the use of equivalent networks with which this paper deals more specifically. The procedure consists in connecting the unknown impedance Z_r to the output terminals of a line and in measuring the voltages or the currents at three points on the line. From these readings the resistive and the reactive parts of Z_r may be determined in terms of the ratios of these voltages and the characteristic impedance of the line. The three points of measurement are usually selected $\lambda/8$ distance apart measured from the terminal end, as the computations are then easier.[5] If the absolute magnitude of Z_r is wanted, rather than its complex value, measurements need only be taken at two points.[1]

The equations for impedance measurement may be obtained from conventional transmission line theory under the assumption that,

$$r \ll L, \qquad g \ll C \tag{1}$$

where,

r = resistance per unit length
g = leakage conductance per unit length
L = inductance per unit length
C = capacitance per unit length.

These conditions are usually well satisfied by radio-frequency lines[2] and they will be made basic to the following development. A discussion of their validity in the equivalent networks will be made later. With the simplifications resulting from (1), the current I_x and the voltage V_x at a distance x from the unknown impedance Z_r at the receiving end are given by

$$\begin{aligned} I_x &= I_r\left(\cos mx + j\frac{Z_r}{Z_0}\sin mx\right) \\ V_x &= V_r\left(\cos mx + j\frac{Z_0}{Z_r}\sin mx\right) \end{aligned} \tag{2}$$

[5] The author's first knowledge of the three-meter modification came from a colloquium by Dr. P. B. Taylor, "High-frequency transmission lines," delivered to the Electrical Engineering Department, Massachusetts Institute of Technology, 1933.

where $m = \omega\sqrt{LC} = 2\pi/\lambda$, Z_0 = characteristic impedance = $\sqrt{L/C}$, and V_r = voltage across the receiving end. The measurement equations will first be derived in terms of voltage. At the three specified points on the line, Fig. 1, the voltages are found from (2) to be given by

$$\begin{aligned} x &= 0, & V_1 &= V_r \\ x &= \frac{\lambda}{8}, & V_2 &= \frac{V_r}{\sqrt{2}}\left(1 + j\frac{Z_0}{Z_r}\right) \\ x &= \frac{\lambda}{4}, & V_3 &= jV_r\,\frac{Z_0}{Z_r}. \end{aligned} \tag{3a}$$

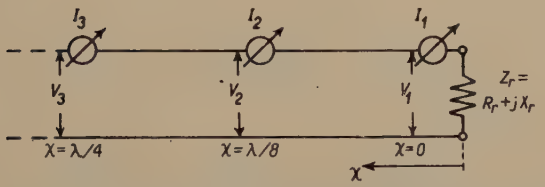

Fig. 1—Diagram illustrating impedance measurement on a high-frequency transmission line.

If the notation

$$\frac{Z_0}{Z_r} = c + jd, \tag{3b}$$

is adopted the squares of the absolute magnitudes of the voltage ratios V_2/V_1 and V_3/V_1 are as follows:

$$\begin{aligned} B_1 &= \left|\frac{V_2}{V_1}\right|^2 = \tfrac{1}{2}\left[(1-d)^2 + c^2\right] \\ B_2 &= \left|\frac{V_3}{V_1}\right|^2 = c^2 + d^2. \end{aligned} \tag{3c}$$

Solving these two simultaneous equations for c and for d gives

$$\begin{aligned} c &= B_1\left[(B_2 - B_1 + 1) - \tfrac{1}{4}(B_2 - 1)^2\right]^{1/2} \\ d &= \tfrac{1}{2}(B_2 + 1) - B_1 \end{aligned} \tag{3d}$$

and these equations, together with (3b), give the values of the resistive and of the reactive components of the unknown impedance as

$$\begin{aligned} R_r &= \frac{c}{c^2 + d^2}\cdot Z_0 = \left[a_2(a_1 - a_2 + 1) - \tfrac{1}{4}(a_1 - 1)^2\right]^{1/2}\cdot Z_0 \\ X_r &= \frac{-d}{c^2 + d^2}\cdot Z_0 = \left[a_2 - \tfrac{1}{2}(a_1 - 1)\right]\cdot Z_0 \end{aligned} \tag{3}$$

where,

$$a_1 = \left|\frac{V_1}{V_3}\right|^2, \qquad a_2 = \left|\frac{V_2}{V_3}\right|^2.$$

In a similar manner, the measurement equations in terms of the three currents, Fig. 1, may be shown to be

$$\begin{aligned} A_1 &= \left|\frac{I_2}{I_1}\right|^2, \qquad A_2 = \left|\frac{I_3}{I_1}\right|^2 \\ R_r &= [A_1(A_2 - A_1 + 1) - \tfrac{1}{4}(A_2 - 1)^2]^{1/2} Z_0 \\ X_r &= [\tfrac{1}{2}(A_2 + 1) - A_1] Z_0. \end{aligned} \tag{4}$$

The general advantages possessed by this method of measuring the resistive and the reactive components of an impedance at radio frequencies are mainly the following:

(1) It is not necessary to know the values of the currents or of the voltages in amperes or in volts, because only the current or voltage ratios are needed;

(2) The characteristic impedance Z_0 can be calculated in many cases from the geometry of the line; and

(3) No calibrated decade boxes are required.

Opposed to these advantages is the inconvenient size of the line, which practically limits the method to the ultra-high-frequency region.

Impedance Measurement with Simulated Lines

Method I

The disadvantage of a lengthy transmission line may be removed by substituting for each $\lambda/8$ section its equivalent lumped constant network. The operation of this lumped network will be identical to that of the line. The complete apparatus comprising the impedance measuring device can then be contained in a small space and made convenient for manipulation.

Of the several types of equivalent networks available, the T has been used in most of these experiments. Under the assumed conditions (1), the series and the shunt arms, Fig. 2a, have the following values:[6]

$$\begin{aligned} \tfrac{1}{2}Z_1 &= jZ_0 \tan \pi/8 & Z_2 &= -j\frac{Z_0}{\sin \pi/4} \\ &= j0.4142 Z_0 & &= -j1.4142 Z_0. \end{aligned} \tag{5}$$

[6] *See*, for example, A. E. Kennelly, "Electric Lines and Networks."

The network therefore has two series inductances and a shunt capacitance, Fig. 2b. The characteristic impedance Z_0 is a factor of both $\frac{1}{2}Z_1$ and Z_2 and hence it does not affect their ratio α:

$$\alpha = \tfrac{1}{2}Z_1/Z_2 = 0.2928. \tag{6}$$

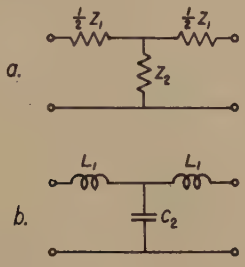

Fig. 2—Equivalent T network replacing a $\lambda/8$ section of the line.

The equivalent network will represent a line $\lambda/8$ long when this ratio α is established, independently of the absolutely magnitudes of $\frac{1}{2}Z_1$ and Z_2. This fact is of importance from a constructional viewpoint. Since $\left|\frac{1}{2}Z_1\right| = \omega L_1$ and $\left|Z_2\right| = 1/\omega C_2$, equation (6) gives at once

$$C_2 = 0.2928 \frac{1}{\omega^2 L_1}. \tag{7}$$

This expression gives the associated values of C_2 and L_1 as a function of the frequency. The value of Z_0 for the equivalent network is found from (5) to be

$$Z_0 = \frac{\omega L_1}{0.4142} = \frac{1}{1.4142\omega C_2}. \tag{8}$$

The ratio of the series and the shunt arm impedances must be made equal to α at the measurement frequency. This may be checked by measuring these impedances separately. Or preferably, one may make use of one of the following methods for adjusting the network to the $\lambda/8$ condition. In these methods, it is assumed that both the frequency of the applied voltage and the value of the capacitance C_2 are known quantities. Furthermore, it is assumed that C_2 is adjustable and that fixed identical coils having about (but not necessarily exactly) the desired value of inductance are available. All four of these conditions are generally easy to satisfy in practice. The network is brought to the proper condition for a $\lambda/8$ equivalent network by adjusting the capacitance C_2 to its proper value, using the Criterion I or the Criterion II below. *Criterion I:* Adjust C_2 until resonance takes place in the series branch L_1, C_2 at a frequency $\omega' = 1/\sqrt{L_1 C_2} = 1.849\ \omega$, where ω is

the frequency at which the measurements are to be made. This adjustment is best made by short-circuiting the input to one section, leaving the output open-circuited, and coupling loosely to the first coil with a coil carrying the radio-frequency current. A similar procedure should be carried out with both sections. *Criterion II:* The output of one $\lambda/8$ section is open-circuited and the voltage ratio B_1 is measured as C_2 is adjusted; C_2 has the proper value when the sending end voltage V_2 and the receiving end voltage V_1 are related by the factor $V_2 = V_1/\sqrt{2} = 0.707\ V_1$. Criterion II is quite easy to carry out and it has the advantage that the network is connected exactly as it will be during the later measurements.

If the network is brought to its proper adjustment as above, *the standards of reference are the frequency and the capacitance* C_2. These two quantities are probably the safest ones to select as standards for radio-frequency measurements.

The complete circuit comprising the two sections is shown in Fig. 3. In measuring the resistive and the reactive components of an unknown impedance with this circuit, the procedure is identical with that for the transmission line.

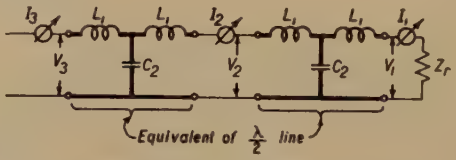

Fig. 3—Complete network for measuring the complex value of impedance Z_r at high frequencies.

Accuracy is the factor that governs the value of Z_0 to be used in a given network, as will be shown below, although the optimum value of Z_0 may not correspond to any actual line. In fact, (7) and (8) allow the transmission line ideas to be completely divorced, except in so far as they are useful in advancing the network measuring technique.

Method II

The following method of measuring the complex value of an impedance has the advantage of requiring only one equivalent network. The measurement is carried out with a single network that is first adjusted to represent a $\lambda/4$ line; the voltage V_1' across the receiving end impedance Z_r and that across the sending end V_2' are measured. The value of the capacitance C_2, Fig. 2, is then changed to a new value C_2' for which the network represents a $\lambda/8$ line, the inductance elements L_1 remaining the same, and the voltage across the receiving end V_1

and that across the sending end V_2 are again measured. Using the notation

$$B_1 = \left|\frac{V_2}{V_1}\right|^2 \cdots \lambda/8 \text{ network}$$
$$B_2 = \left|\frac{V_2'}{V_1'}\right|^2 \cdots \lambda/4 \text{ network} \tag{9}$$

and proceeding as in Method I, the values of the unknown resistance and of the unknown reactance are found to be

$$c = \left[B_1\left(\frac{B_2}{h^2} + 1 - B_1\right) - \frac{1}{4}\left(1 - \frac{B_2}{h^2}\right)^2\right]^{1/2}$$
$$d = \frac{1}{2}\left(\frac{B_2}{h^2} + 1\right) - B_1 \tag{10}$$
$$R_r = \frac{c}{c^2 + d^2} Z_0, \qquad X_r = \frac{-d}{c^2 + d^2} Z_0.$$

The similarity between this method and the first one will be immediately apparent to the reader. A short calculation will show that B_2 is proportional to h^2; consequently, B_2/h^2 does not contain h and (10) and (3) are exactly the same. The conditions for optimum accuracy will be the same for the two methods.

The specifications for the network for Method II are easily found to be given by:

$\lambda/8$ Network	$\lambda/4$ Network
$L_1 = hZ_0/\omega$	$L_1 = hZ_0/\omega$
$C_2 = 1/(1 + h)\omega Z_0$	$C_2' = 1/h\omega Z_0$
$= 0.2928/\omega^2 L_1$	$= 1/\omega^2 L_1 = 3.4142 C_2$
$Z_0 = 1/(1 + h)\omega C_2$	$Z_0' = hZ_0$

(11)

One quite satisfactory way to proceed is first to adjust the network for the $\lambda/4$ condition. With a given inductance L_1, this condition is reached by adjusting C_2' so that series resonance occurs in the circuit formed by connecting L_1 and C_2 in series at the working frequency. Another way of determining the proper value of C_2' is to connect an identical variable capacitance C_3 across the output and to vary C_2' and C_3 simultaneously until $V_1' = V_2'$. When this equality obtains, C_2' has its correct value. In practice, the two methods have always given very closely the same setting for C_2'. Having adjusted the network for the $\lambda/4$ condition, the $\lambda/8$ condition is immediately secured by changing the capacitance to the vew value $C_2 = 0.2928\ C_2'$.

The second method is perhaps generally to be preferred over the first one, because half as many inductances and condensers are required. However, if extended measurements are to be made in one frequency range, it is possible that the time expended in constructing the networks for Method I will be more than regained by the time saved in manipulation during the measurements. There is no choice on the basis of accuracy.

Other types of equivalent networks may be employed. A Π network has only one inductance, but it requires two calibrated variable condensers. An L network, i.e., a half T or half Π section, offers greater ease of construction than others, as it contains but one inductance and one capacitance. However, the proper lengths do not appear to be $\lambda/8$ and $\lambda/4$. This interesting case is being investigated at the present time.

There is a similarity between this equivalent network method of measuring impedances and the "three-voltmeter" method, of which it may be considered a generalization and extension. One of the disadvantages of the three-voltmeter method is the necessity of measuring voltage between two points *both* of which are above ground potential; this objection does not apply here. The first and second methods described above are special forms of a general method of measuring impedance by measuring voltage or current ratios at two terminal pairs of two arbitrary networks, as shown for cascaded networks *A* and *B* in Fig. 4. In the general problem, one would seek network structures *A* and *B* such that the unknown impedance would be found with the optimum accuracy.

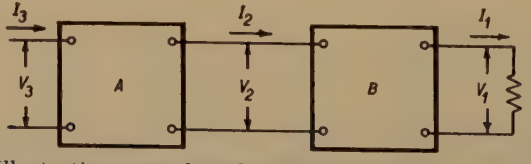

Fig. 4—Illustrating general method of measuring complex impedance with two arbitrary networks.

Measurement Considerations

Optimum Value for the Characteristic Impedance

In the preceding section it was shown how the equivalent network could be designed to have almost any value of Z_0. However, there is an optimum value that will give the greatest accuracy when measuring a given magnitude of impedance Z_r. In the following discussion, the impedance measuring methods based on voltage readings will be dis-

cussed in detail, although a similar discussion may be given for the current readings. Several special cases present themselves. As already pointed out, the following discussion of accuracy applies equally to Method I and to Method II.

Case $Z_r = R_r$. For the special case in which the unknown is a resistance R_r, the voltage ratios B_1 and B_2 are not independent. Introducing the notation

$$X = B_1(B_2 - B_1 + 1), \quad Y = \tfrac{1}{4}(B_2 - 1)^2, \quad c = \sqrt{X - Y} \qquad (12a)$$

we find from (3a)–(3) that $B_2 = 2B_1 - 1$ and hence

$$R_r = \frac{Z_0}{c} = \frac{Z_0}{\sqrt{X - Y}} = \frac{Z_0}{\sqrt{2B_1 - 1}} = \frac{Z_0}{\sqrt{B_2}} = \left|\frac{V_1}{V_3}\right| Z_0. \qquad (12b)$$

Obviously, the measurement of an impedance known to be purely resistive requires the determination of only one voltage ratio,[1] preferably B_2. The accuracy of the measurement depends on the relative magnitudes of R_r and of Z_0 and it is a maximum when they are equal. This follows from an inspection of any of the forms given in (12b). For example, the relation $Z_0/R_r = \sqrt{X - Y}$ from (12b) indicates that the ratio of the characteristic impedance to the terminal impedance is a function of $X - Y$ and hence only those values of Z_0/R_r can be found accurately for which the ratio X/Y is substantially larger than unity. That great accuracy occurs only for unknown resistances of the same magnitude as Z_0 may be seen from the curve of X/Y vs. R_r/Z_0 plotted in Fig. 5; similar curves are also plotted in this figure for capacitance and for inductance terminations.[7] It follows from these curves that it is impossible to measure inductance with high accuracy with this network, a matter to be discussed later. The conditions affecting the accuracy are even more strikingly displayed when X and Y are plotted as functions of R_r for a given constant characteristic impedance (a logarithmic scale is used so that the difference of the two curves will represent their quotients). When X and Y are almost equal, very small errors in either quantity will introduce enormous inaccuracies in $\sqrt{X - Y}$. Hence, in this representation the useful range of the apparatus is confined to the region where the two curves are widely separated in the horizontal direction. Such curves for the resistance termination are reproduced in Fig. 6. Maximum accuracy is seen to occur when $R_r = Z_0$; as R_r departs from this value, the curves draw together and the satisfactory performance of the device is rapidly impaired.

[7] The computations of these curves was made by R. H. Winters in connection with his Master's Thesis in electrical engineering, "Measurement of impedances at high frequencies," Massachusetts Institute of Technology, June, 1934.

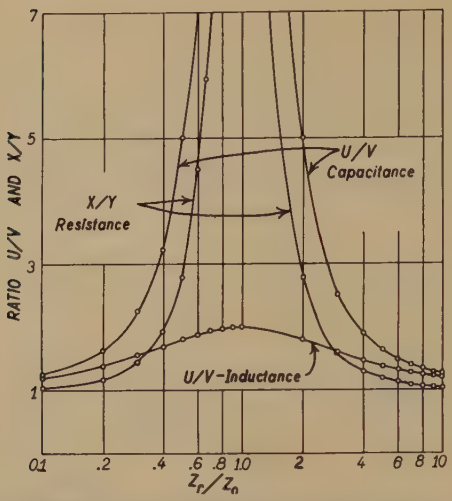

Fig. 5—Effect of the characteristic impedance Z_0 on the accuracy with which Z_r can be measured for three kinds of unknown impedances. Satisfactory accuracy is only secured for values of Z_r/Z_0 for which U/V or X/Y is considerably larger than unity.

Case $Z_r = -X_r$. When the unknown impedance is a capacitive reactance $-X_r$, a situation exists similar to that above. Introducing the notation

$$U = \tfrac{1}{2}(B_2 + 1), \quad V = B_1, \quad d = U - V \tag{13a}$$

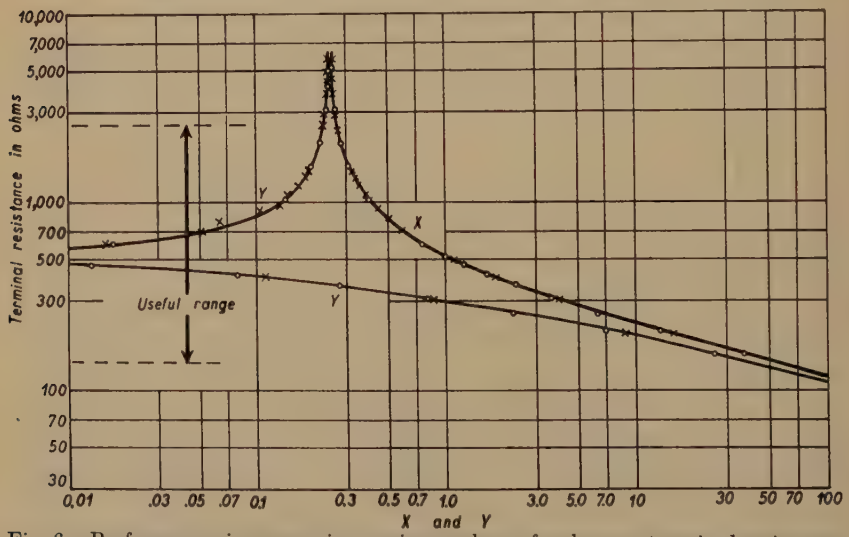

Fig. 6—Performance in measuring various values of unknown terminal resistance of a network having a characteristic impedance $Z_0 = 512$ ohms. Useful range based on a 1 per cent error in results. Maximum accuracy occurs for $R_r = Z_0$. Circles indicate computed values, crosses indicate actual measured values.

it may be found that $B_1^2 = \frac{1}{2}(1 - B_1^{1/2})^2$ and hence

$$X_r = -\frac{Z_0}{d} = -\frac{Z_0}{U - V} = -\frac{Z_0}{1 - \sqrt{2B_1}} = -\frac{Z_0}{\sqrt{B_2}} = -\left|\frac{V_1}{V_3}\right| Z_0. \tag{13b}$$

Here, we expect the accuracy to be poor in those ranges of X_r for which U is almost equal to V. Curves of U and of V as functions of X_r are reproduced in Fig. 7 (and as functions of Z_r/X_r in Fig. 5), and they

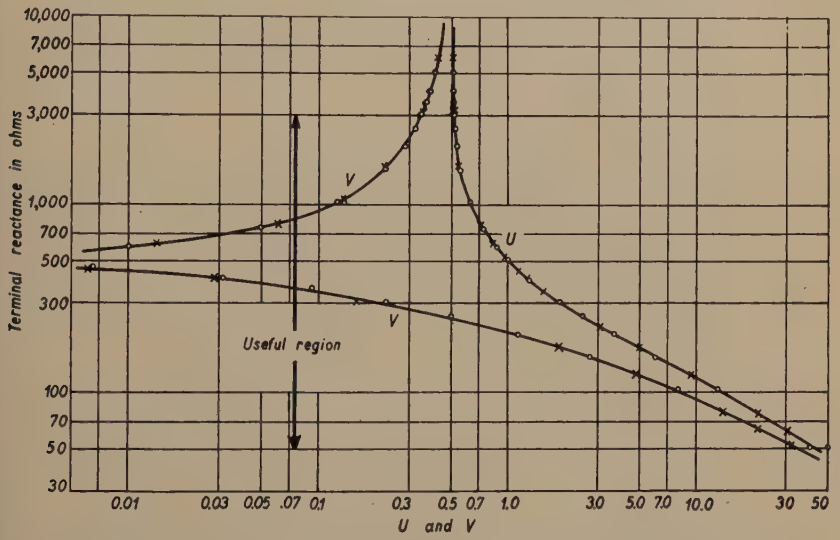

Fig. 7—Same as Fig. 6 except that curves are for an unknown terminal capacitive reactance.

display the same general characteristics as those of Fig. 6. Again, it is certain that the region of high accuracy is centered about the characteristic impedance.

Case $Z_r = +X_r$. When the unknown impedance is an inductive reactance $+X_r$ it may be shown that $\sqrt{B_2} = \sqrt{2B_1} - 1$, hence,

$$+X_r = -\frac{Z_0}{d} = -\frac{Z_0}{U - V} = \frac{Z_0}{-1 + \sqrt{2B_1}} = -\frac{Z_0}{\sqrt{B_2}} = \left|\frac{V_1}{V_3}\right| Z_0 \tag{13c}$$

and, as before, curves of U and of V must be examined to determine the conditions for best accuracy. These curves are shown in Figs. 8

and 5. They also possess the characteristic of drawing together as $+X_r$ departs in value from Z_0, although their shapes are different from the curves for R_r and for $-X_r$. As a result of their smaller relative separation, it is to be expected that an inductance may not in general be measured with the assumed networks to the same degree of accuracy as may a resistance or a capacitance. This was found experimentally to be the case.

Case $Z_r = R_r \pm jX_r$. In the general case in which the unknown impedance contains both resistance and reactance, no helpful simplifica-

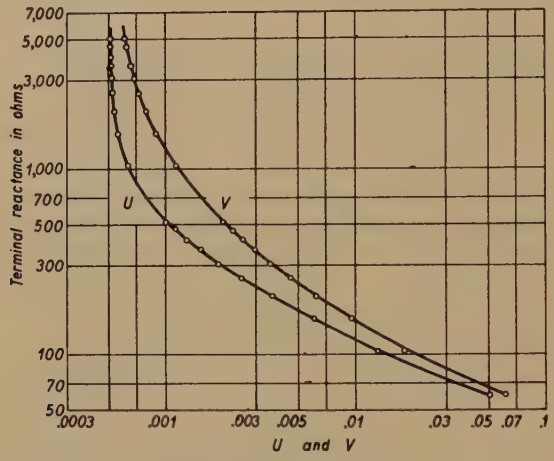

Fig. 8—Same as Fig. 6 except that curves are for an unknown terminal inductive reactance.

tions can be made and the complete expressions (3) must be used. The relative accuracy is still determined mainly by the accuracy with which c and d can be calculated, hence we again examine curves of X, Y and U, V for typical examples. Several curves of this nature are reproduced in Figs. 9 to 12, where R_r has been given different fixed values in each set of curves and where the reactive component has been taken as the independent variable. Two pairs of curves must now be considered. Accurate measurements of R_r and of X_r result only when *both* pairs of curves have a satisfactory separation. In each of the four cases, this separation limits the usefulness of a given measurement network to a range of impedances not too different in value from the characteristic impedance X_0 of the network. The useful range for a general complex impedance is, therefore, restricted to narrower limits than is that for pure resistance or reactance. In most of the Figs. 6 to 12, a region has been indicated as "useful range." This is the range of values of the unknown impedance for which the error of measurement is estimated

as less than 1.0 per cent when an error of ± 1 in the third place of c or d is made. A greater tolerance may considerably extend this useful range, and the above criterion is thought to be a comparatively severe one.

Thus, the best accuracy obtains when the network is designed to have a characteristic impedance equal in magnitude to the impedance to be measured. Based on the above definition, satisfactory accuracy obtains for the range of impedances from about $2Z_0$ to $Z_0/5$.

The relatively poor accuracy with which inductive impedance can

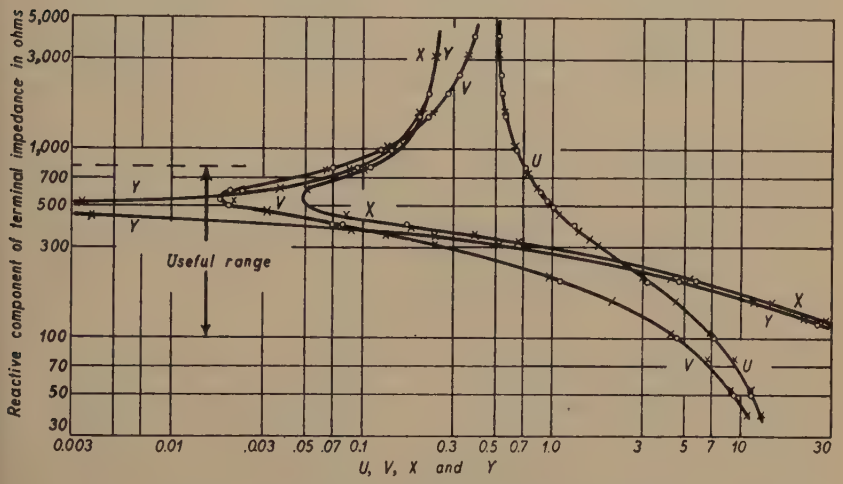

Fig. 9—Same as Fig. 6 except that curves are for an unknown terminal impedance $R_r - jX_r$; $R_r = 100$ ohms, $-X_r =$ variable.

be measured is directly connected with the fact that the voltage ratios were taken at the ends of a $\lambda/8$ and a $\lambda/4$ section. This difficulty is completely removed if two sections $3/8\lambda$ and $6/8\lambda$ long are used. Inductive impedances may then be measured with the same accuracy as that applying to the measurement of capacitive impedances when using the networks previously discussed. This illustrates the general fact that in designing impedance measuring networks, the absolute magnitude of the "unknown" *and* its complex nature must both be taken into account.

If a network has been designed to have optimum accuracy for capacitive impedances and one wishes to measure inductive impedance the inductive unknown $R_r + jX_r$ may be connected in series or in parallel with a known capacitance of sufficiently high magnitude to make the combination appear as $R_r' - jX_r'$. The measurement may then be carried out with a high degree of accuracy. The value of $R_r + jX_r$ is

easily computed from the results. This artifice makes it possible to measure accurately both inductive and capacitive impedances with the same network.

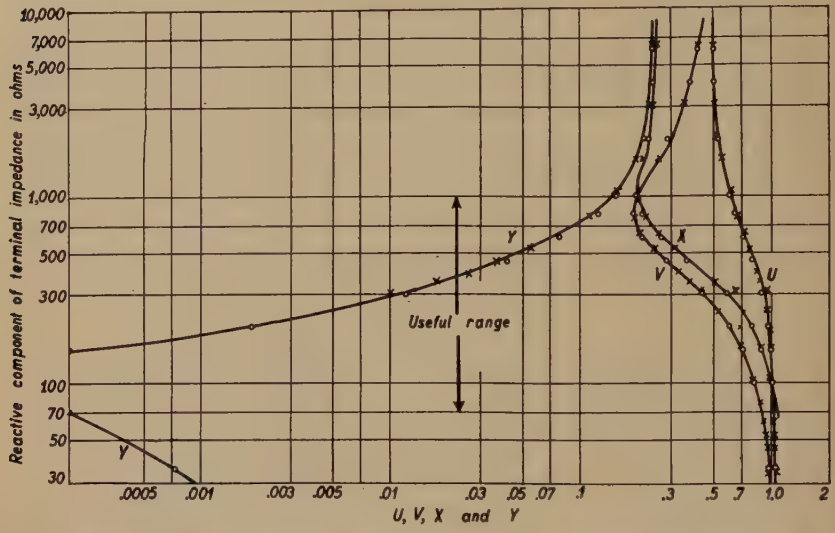

Fig. 10—Same as Fig. 6 except that curves are for an unknown terminal impedance $R_r - jX_r$; $R_r = 500$ ohms, $-X_r =$ variable.

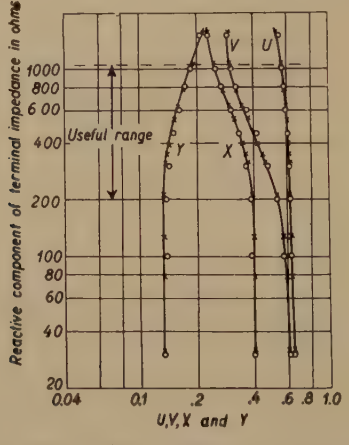

Fig. 11—Same as Fig. 6 except that curves are for an unknown terminal impedance $R_r + jX_r$ $R_r = 1000$ ohms, $+X_r =$ variable.

Except as noted above, the network section must possess an electrical length of $\lambda/8$ or of $\lambda/4$ at the frequency of measurement. With a given network this condition will obtain at one frequency only. Therefore, when measurements are to be made over a band of fre-

quencies, the network parameters must be readjusted for each frequency in the band. Several ways of doing this suggest themselves, but it is thought that changing the value of the capacitance C_2 is the most practicable method. In the actual network set-up, a calibrated variable condenser may be used for the element C_2. If L_1 is constant the associated values of C_2 and ω are those given by (7) and by (11). Changing C_2 changes the value of Z_0 for the network, but this may be determined easily as a function of the frequency or of the condenser capacitance by means of (8). Curves showing C_2 and Z_0 as functions of the frequency for one illustrative case are reproduced in Fig. 13. The value of Z_0 increases linearly with the frequency when the inductance L_1 is held constant and C_2 is varied. Therefore, the "useful range" of the network may be displaced to unwanted magnitudes of impedance. It may be returned to the desired location by changing the inductance L_1. The "useful range" of the network for a fixed frequency may also be shifted to the desired position by this means. When it is desired to extend either the frequency range or the impedance range of the network, a set of plug-in coils can be used.

Measurement Technique

Grounds and Shielding

One of the valuable features of the above-described method of impedance measurement is the common conductor connecting generator, network, voltmeter, and the unknown impedance. This conductor may be put at ground potential, and the voltages are then measured between this grounded conductor and the 0, $\lambda/8$, and $\lambda/4$ points. This allows the filament terminal of a vacuum tube voltmeter to remain at ground potential during the entire measurement. From the viewpoint of shielding, this arrangement is ideal. The use of current ratios instead of voltage ratios does not offer quite the same nice possibilities; this is also true of the networks employing ladder type structures.

Voltmeter Input Impedance

The voltmeter must be connected directly across the network; therefore, the minimum impedance that this meter may have without appreciably affecting the measurement must be known or its effect must be determined experimentally. The latter may be carried out by alternately connecting and disconnecting a high impedance in series with the meter. If the insertion of the extra impedance does not change the voltage readings the meter is suitable. If the generator supplying the network has an impedance $Z_g \ll Z_0$, the maximum allowable meter input capacitance C_m is given by

$$C_m = \frac{\gamma}{\omega \cdot |Z_r| \cdot 100}, \tag{14}$$

where γ is the tolerable error in per cent in the voltage ratio V_3/V_1, Fig. 1. The maximum allowable meter capacitance is thus inversely proportional to frequency and to terminal impedance Z_r. Assuming $\gamma = 1$ per cent, representative values have been computed and are shown in Table I, where f_{kc} indicates frequency in kilocycles. Obviously ordinary vacuum tube apparatus may be used directly except for very high values of f_{kc} and Z_r. In interpreting this table, one should bear in mind the fact that the input impedance to a vacuum tube voltmeter may generally be increased many times by connecting a very high resistance, say one-half to twenty megohms, in series with the lead to the grid. On this basis, the values given in the table are entirely too pessimistic. Actually, measurements have been made on a line at a wavelength of twelve meters with a simple type of voltmeter that did not noticeably affect the line conditions.

TABLE I

C_m IN $\mu\mu$f FOR DIFFERENT $|Z_r|$

f_{kc}	$Z_r = 10\omega$	100ω	500ω	$1{,}000\omega$	$10{,}000\omega$
1	160,000	16,000	3,200	1,600	160
10	16,000	1,600	320	160	16
100	1,600	160	32	16	1.6
1,000	160	16	3.2	1.6	0.16
10,000	16	1.6	0.32	0.16	0.016

Voltmeter Indications

The three voltages V_1, V_2, V_3 may produce meter deflections from zero to maximum. Generally, the smaller voltages cannot be read with the same accuracy as can the larger ones. The same voltmeter should be used for all readings, as only one calibration is required and as deviations between meters are eliminated. The following scheme for using the same voltmeter has been employed with success. When one of the voltages, say V_2, is at the lower end of the meter scale, the voltage applied to the network is increased by a known fraction k sufficiently large to allow an accurate reading $V_2' = kV_2$ to be read, and the correct value $V_2 = V_2'/k$ is used in the calculations. The factor k can be determined by using the same meter at one of the other network terminals where the voltage is large enough to allow accurate readings, or a current meter in the input circuit may also be used. This method of taking low voltage readings obviates difficulties associated with the use of several different instruments and it extends the range of impedances that can be measured with a given network.

Experimental Results

The methods of measuring impedance described herein have been investigated experimentally in the frequency range of 50 to 1500 kilocycles. The results have been quite satisfactory for values of impedance that do not differ from the characteristic impedance by a factor of more than about 5 or 1/5, and they are sufficiently accurate for many purposes over a much greater range. The conclusions drawn from the analytical study were all found to hold in practice. The author favors the second method described with a single T network, because this arrangement is simple to construct and to manipulate, but each com-

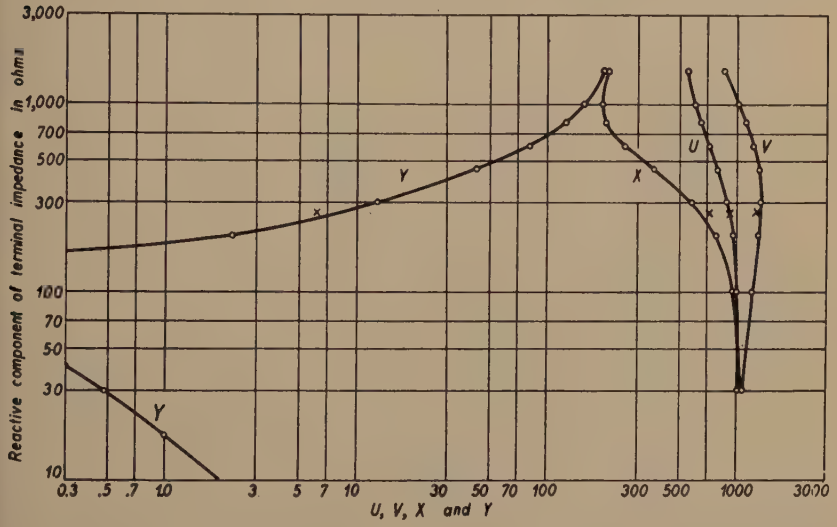

Fig. 12—Same as Fig. 6 except that curves are for an unknown terminal impedance R_r+jX_r; $R_r=500$ ohms, $+X_r=$variable.

bination has some particular feature. In the broadcast band, small plug-in coils in copper shields and a 750-micromicrofarad standard variable condenser have performed very well. At lower frequencies, larger coils without shielding and a larger condenser were used with excellent results.

Actual data will be discussed only as to its agreement with calculated values and as regards the conditions for optimum accuracy. For this purpose, results obtained at 50 kilocycles with Method I are chosen, because stray effects were at a minimum and the rated values of comparison impedances were to be relied on. Two equivalent T sections were used[8] having the following constants:

$L_1 = 0.674$ mh $\qquad f = 50{,}000$ cps

$C_2 = 4400\ \mu\mu$f $\qquad Z_0 = 512$ ohms.

The common lead was grounded, coils and condensers were widely spaced, and no further shielding was employed. The characteristic impedance was found by actual measurement to be 512 ohms. Calculations based on Sommerfeld's expression for the high-frequency resistance of coils showed that the coil resistance was entirely negligible compared to its reactance, as required by the underlying assumptions of the measurement theory. The vacuum tube voltmeter had no observable effect on voltage distribution when connected across the network.

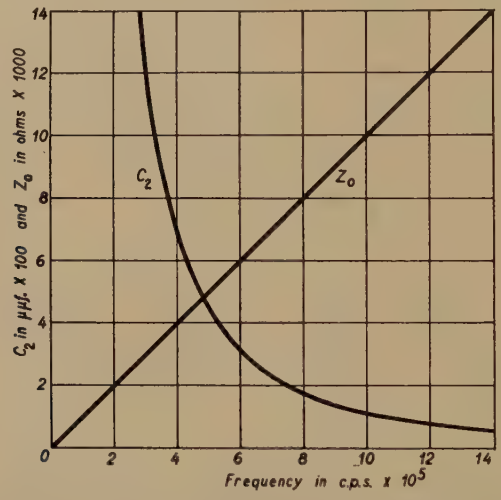

Fig. 13—Associated values of C_2 and Z_0 for different frequencies in the broadcast band and for $L_1 = 0.1305$ millihenry.

A series of measurements on impedances of various kinds were made and some of the results are reproduced here. First, values of X, Y, U, V obtained from actual measurements were compared with calculated values. The small crosses in Figs. 6 to 12 denote experimentally obtained points; the theoretical values are given by the small circles. The agreement is thought to be remarkably good for measurements on an experimental set-up at 50 kilocycles, and it demonstrates that the theory holds to within the precision of the meter readings.

---

[8]The experimental work at 50 kilocycles was largely carried out by R. H. Winters,[7] to whom the author wishes to express his gratitude. The assistance of N. S. Kornetz in making measurements of broadcast frequencies is also gratefully acknowledged.

Consequently, previous conclusions concerning the accuracy and the useful impedance range must manifest themselves in the values of impedance computed from the voltage ratios. That these conclusions were verified in the experiments may be seen from the data of Table II, which were typical of the measurements. These data follow the expected trend and they show decisively that satisfactory accuracy is only obtained when the unknown impedance is of the same order of magnitude as the network characteristic impedance. Similar results were obtained at frequencies in the broadcast band.

TABLE II

MEASUREMENT NETWORK $Z_0 = 512$ ohms: FREQUENCY = 50,000 cps.

Resistance			Reactance (capacitive)		
Rated value ohms	Measured value ohms	Deviation per cent	Rated value ohms	Measured value ohms	Deviation per cent
4,000	3,160	21.00			
1,500	1,427	4.90			
785	800	1.88			
401	400	0.25			
200	200	0.00			
20.2	20	1.00			
			54,900	20,600	62.50
			6,100	5,925	2.90
			1,061	1,074	1.20
			636.6	642	0.85
			106.1	101.5	4.30
			53.1	44.7	15.80
500	410	19.5	3,182	2,400	25.0
500	532	3.3	1,061	1,600	9.5
500	491	1.6	530.5	507.5	4.3
500	497.5	0.5	212.3	210.2	1.0
500	497	0.6	77.5	79.56	2.5
500	498	0.4	34.0	35.4	4.0

CONCLUSION

The method of measuring the complex value of an impedance with networks simulating lines appears to be well suited to the frequency range from about 50 kilocycles up to several thousand kilocycles. Above this range, an actual line is preferable. The requirement for optimum accuracy is that the characteristic impedance of the network should equal the impedance of the unknown, but the range of impedances that can be measured with a given network is quite wide. In constructing the network, only the capacitance of an adjustable condenser and the frequency of the applied voltage need be known accurately; these two quantities are the reference standards. This is an advantage, because capacitance and frequency may be quite well known at radio frequencies. The presence of a common conductor that may be grounded, the measurement of potential above this grounded conductor, and the use of voltage ratios, rather than voltage magnitudes,

are also desirable features. In operation, the network method is particularly stable and precise. The author does not, however, present the method as a cure-all for the high-frequency impedance measurement problem. For example, it is not well adapted to the measurement of very small impedances (less than ten ohms) or of a very small reactance (or resistance) in series with a very large resistance (or reactance). Other criticisms may be made, but it is believed that the method possesses a sufficient number of superior features to make it useful in many practical problems.

BOOKS RECEIVED

Twenty-Fifth Anniversary Year Book of the Radio Club of America. Published by the Radio Club of America, 11 West 42nd Street, New York City. 85 pages. Price $1.00.

Approximately one half of the book is devoted to a history of the Radio Club of America prepared by George E. Burghard and is illustrated with pictures of individuals, equipment, and clippings portraying the history of the organization and some of its members from about 1910 on.

The balance of the book is devoted to an index of papers published by the Club, photographs of its past officers, a list of its present members, and its constitution.

Directory of Organizations in the Engineering Profession. Published jointly by American Engineering Council, 744 Jackson Place, N. W., Washington, D. C.; The Engineering Foundation, 29 West 39th Street, New York City; and Engineers Council for Professional Development, 29 West 39th Street, New York City. Available from any of the joint publishers at 50 cents per copy. 53 pages.

The history, organization and operation of six joint bodies in engineering having activities of national scope are given. Data on headquarters, managing officials, meetings, membership and qualifications, publications, principal activities, and awards are given for national associations, institutes, and societies, and for a number of state and local bodies.

SOS to the Rescue, by Karl Baarslag. Published by the Oxford University Press, 114 Fifth Avenue, New York City. 304 pages. Price $2.50.

The author of this book as a marine radio operator was able not only to consult the official records of various countries but had the advantage of discussing a number of maritime disasters about which he writes with the radio operators who participated in the events. It is devoted to such disasters as those which befell the Republic, Titanic, Empress of Ireland, Antinoe, Vestris, Morro Castle and a number of lesser known catastrophes. It pleads for a more strict set of requirements for American merchant marine radio communications as a protection for life at sea.

Internationale Sprachnormung in der Technik (International Language Standardization in Engineering with Special Reference to Electrical Engineering), by E. Wüster. Published by VDI-Verlag, Berlin, Germany, in 1931. 431 pages. Price RM 20.

BOOKLETS, CATALOGS, AND PAMPHLETS RECEIVED

Copies of the publications listed on this page may be obtained without charge by addressing the publishers.

DeJur-Amsco Corporation of 95 Morton Street, New York City, has issued Bulletin 36 on variable condensers and No. 37 on remote control devices.

Public address amplifiers and accessory equipment are described in a booklet issued by Morlen Electric Company of 100 Fifth Avenue, New York City.

A. H. Ross and Company, Glenside, Pa., have issued a leaflet on their Model 4-C short-wave superheterodyne receiver.

Littelfuse products are described in a booklet issued by Littelfuse Laboratories, 4507 Ravenswood Avenue, Chicago, Ill.

International Resistance Company, 2100 Arch Street, Philadelphia, has issued a leaflet on its resistance indicator, a calibrated variable resistor.

The Insuline Corporation of America of 25 Park Place, New York City, has issued booklets on their conversion resistovolts for converting a battery receiver to air-cell operation, their auto radio accessories, and a general Catalog No. 185 covering an extensive line of radio parts and accessories.

Bulletin No. 270 of the Rubicon Company, 29 North 6th Street, Philadelphia, describes precision potentiometers for portable and laboratory use.

Folder No. 11 of the American Instrument Company, 776 Girard Street, N. W., Washington, D. C., covers constant temperature apparatus, piezo-electric crystals, relays and measuring instruments.

Bulletin 4001 of the Leeds and Northrup Company, 4900 Stenton Avenue, Philadelphia, describes three-lead null type electrical-resistance thermometers designed for air-conditioning systems.

Catalog H of the General Radio Company, 30 State Street, Cambridge, Mass., lists component parts, measuring devices, oscillators, amplifiers, and accessory equipment.

Low power factor wattmeters are described in leaflet Volume 1, No. 3, issued by Sensitive Research Instrument Corporation of 4545 Bronx Boulevard, New York.

Tubing by Summerill is the title of a catalog issued by Summerill Tubing Company of Bridgeport, Pa., which describes and gives engineering data on numerous types of metal tubing.

Ward Leonard Electric Company of Mount Vernon, N. Y. circular 507A describes adjustohm resistors having a sliding band for adjustment and wire-wound fixed resistors. Circular 507C covers transmitter control relay equipment and 507D vitrohom voltage dividers as replacement units for various broadcast receivers.

A report on "The 6F7 Used as an Amplifier and Second Detector" by J. R. Nelson, is issued by the Raytheon Production Corporation of Newton, Mass.

RCA Radiotron of Harrison, N. J., has issued Application Note No. 47 on the use of the 954 as a vacuum tube voltmeter. Note No. 46 will be issued later. Data booklets are available on the 802 radio-frequency power amplifier pentode, the 954 acorn type detector and amplifier pentode, and on the 955 acorn type detector, amplifier, and oscillator triode.

CONTRIBUTORS TO THIS ISSUE

Barrow, W. L.: See PROCEEDINGS for February, 1935.

Brainerd, John Grist: Born 1904. Police reporter, *Philadelphia North American*, 1923–1925. Instructor and assistant professor, Moore School of Electrical Engineering, University of Pennsylvania, 1925 to date. Received B.S. degree, University of Pennsylvania, 1925; Sc.D. degree, 1934. Associate member, Institute of Radio Engineers, 1933.

Judson, E. B.: Born December 3, 1898, at Washington, D. C. Naval radio service, 1917–1919; U. S. Naval Radio Research Laboratory, 1919–1923; assistant to Dr. L. W. Austin, radio transmission research laboratory, Bureau of Standards, 1923–1932; wave propagation group, Bureau of Standards, 1932 to date. Associate member, Institute of Radio Engineers, 1926.

Kirby, S. S.: Born October 27, 1893, at Gandy, Nebraska. Received A.B. degree, College of Emporia, 1917; M.A. degree, University of Kansas, 1921. Signal Corps, U. S. Army, A.E.F., 1918–1919. High school teacher, 1919–1921; professor of physics, Friends University, Wichita, Kansas, 1921–1926; assistant physicist, Bureau of Standards, 1926–1930; associate physicist, Bureau of Standards, 1930 to date. Associate member, Institute of Radio Engineers, 1927.

Kozanowski, Henry N.: Born August 15, 1907, at Buffalo, New York. Received B.S. degree, University of Buffalo, 1927; M.A. degree, 1929; Ph.D degree in physics, University of Michigan, 1930. Graduate teaching assistantship, University of Buffalo, 1927–1928. Research assistant, University of Michigan, 1929–1930; research assistant, power tube section, Westinghouse Electric and Manufacturing Company, 1930 to date. Member, American Physical Society. Associate Member, Institute of Radio Engineers, 1934.

Lapham, E. G.: Born September 26, 1902, at Gladstone, Michigan. Received A.B. degree in physics, University of Oregon, 1926. Graduate assistant, University of Oregon, 1927; highway research, U. S. Bureau of Public Roads, 1928–1929; Bureau of Standards, 1929 to date. Associate member, Institute of Radio Engineers, 1931.

Mouromtseff, Ilia Emmanuel: Born December, 1881, at St. Petersburg, Russia. Received M.A. degree, Engineering Academy, St. Petersburg, 1906; Diploma-Ingenieur degree, Institute of Technology, Darmstadt, Germany, 1910. Radio laboratory, Russian Signal Corps, 1911. Member, technical staff, Westinghouse Electric and Manufacturing Company, 1923 to date. Associate Member, Institute of Radio Engineers, 1934.

Noyes, Atherton, Jr.: Born September 27, 1904, at Colorado Springs, Colorado. Received A.B. degree, Harvard University, 1926; A.M. degree, 1928; S.M. degree, 1929; Sc.D. degree, 1934. Research and development work, Boonton Research Corporation, 1929–1931. Research assistant to Professor G. W. Pierce, Harvard University, 1931 to date. Nonmember, Institute of Radio Engineers.

Polkinghorn, F. A.: Born July 23, 1897, at Holbrook, Massachusetts. Received B.S. degree in electrical engineering, University of California, 1922. U. S. Naval Radio Laboratory, Mare Island Navy Yard, 1922–1924; A-P Radio Laboratories, San Francisco, 1924–1925; engineer, Pacific Telephone and Telegraph Company, 1925–1927; member, technical staff, Bell Telephone Laboratories, 1927 to date. Engaged primarily in design of high-frequency receiving and test equipment. Associate Member, Institute of Radio Engineers, 1925.

Schlaack, N. F.: Born June 4, 1901, at Birmingham, Michigan. Received B.S. degree in electrical engineering, University of Michigan, 1925. Member, technical staff, Bell Telephone Laboratories, 1925 to date. Engaged primarily in development of short- and ultra-short-wave transmitting equipment. Associate member, Institute of Radio Engineers, 1925.

Schumacher, Eric W.: Born June 26, 1906, at Nürnberg, Germany. Educated at University of Erlangen, Germany. Foreign department, C. Conradty, Nürnberg; president, Noris Carbon Company, distributors for C. Conradty in the United States, Canada, and South America. Nonmember, Institute of Radio Engineers.